Doctoraatsproefschrift nr. 902 aan de faculteit Bio-ingenieurswetenschappen van de K.U.Leuven

PLANT PECTIN METHYLESTERASE AND ITS INHIBITOR:

A QUANTITATIVE INTERACTION STUDY IN A FOOD PROCESSING CONTEXT

Ruben JOLIE

Promotor:
Prof. M. Hendrickx, K.U.Leuven

Leden van de examencommissie:
Prof. R. Schoonheydt, K.U.Leuven, voorzitter
Prof. C. Michiels, K.U.Leuven
Prof. C. Courtin, K.U.Leuven
Prof. K. Heremans, K.U.Leuven
Prof. A. Gils, K.U.Leuven
Prof. K. Dewettinck, UGent

Proefschrift voorgedragen
tot het behalen van de
graad van Doctor in de
Bio-ingenieurswetenschappen

Juni 2010

ISBN 978-90-8826-142-8
Wettelijk depot D/2010/11.109/20

VOORWOORD

De voorbije doctoraatsjaren waren enorm boeiend en leerrijk, maar liepen bij momenten langs hobbelige wegen. De PME-inhibitor, centraal in mijn onderzoek, toonde zich vaak geen gewillig onderzoeksobject en heeft me dan ook geregeld op de proef gesteld. Gelukkig kon ik, ook tijdens die moeilijkere periodes, rekenen op een hele reeks mensen om me heen, die er elk op hun manier toe hebben bijgedragen dat ik sta waar ik nu sta en dit boekje uiteindelijk is geworden wat het is. Al die mensen wil ik erg graag één voor één bedanken.

Mijn grootste dank gaat uit naar mijn promotor en hoofd van het Laboratorium voor Levensmiddelentechnologie, Prof. Marc Hendrickx. Marc, ik ben je niet alleen dankbaar voor de kans om het doctoraat te starten en in de loop ervan allerhande ervaringen, ook buitenlandse, op te doen, maar vooral ook omdat je al die tijd bijna onvoorwaardelijk achter me stond met hulp en goeie raad, en mijn (vele) twijfels wegnam of relativeerde. Je was een uitstekende leermeester voor me. Je vertrouwen heeft me steeds doen doorbijten en daar ben ik nu enorm blij om. Daarnaast ook heel veel dank aan Prof. Ann Van Loey, voor haar interesse, steun, hulp, raad, verbeterwerk en enthousiasme.

Ook bovenaan mijn lijstje staat Dr. Thomas Duvetter. Thomas, *maestro*, jouw bijdrage de voorbije jaren is nauwelijks te overschatten. Steeds was je mijn eerste klankbord en stond je klaar met praktische hulp. Bovenal was je echter mijn *mental coach*, een rol die je met glans vervulde, in het labo en samen op de fiets. Onze 'zakelijke' samenwerking stopt samen met dit doctoraat, maar ik hoop dat je altijd een beetje mijn *mental coach* en ideale fietspartner zal blijven…
Heel erg belangrijk de laatste jaren waren Dr. Philippe Verlinde (Phille, ook jij stond er áltijd voor me, en dan nog vooral toen het echt nodig was) en Dr. Sandy Van Buggenhout (Sandy, bedankt voor alle waardevolle hulp, verbeterwerk en relativerende babbels aan de microscoop).

Ook buiten de deuren van ons labo zijn er, binnen onze universiteit, de voorbije jaren vele helpende handen geweest. Daarbij oprechte dank aan Prof. Paul Declerck, Prof. Ann Gils, Griet Compernolle en de andere medewerkers van het

Laboratorium voor Farmaceutische Biologie voor de uitstekende assistentie en fijne samenwerking in het kader van de interactie-analyses op de Biacore, Dr. Elke Clynen van de Onderzoeksgroep Functionele Genomics en Proteomics voor de MALDI-TOF MS analyses, en Prof. Karel Heremans en Dr. Filip Meersman voor de leerrijke discussies omtrent proteïnedenaturatie.

Ik dank het FWO Vlaanderen dat mij door middel van een aspirantenmandaat gedurende vier jaar financieel heeft gesteund, alsook het Onderzoeksfonds van de K.U.Leuven. De leden van de examencommissie wil ik van harte bedanken voor hun interesse in en het constructief becommentariëren van mijn doctoraatswerk.

Misschien wel de hoofdreden waarom ik met een heel goed gevoel terugkijk op de voorbije jaren aan het Labo voor Levensmiddelentechnologie wordt gevormd door de volledige groep collega's, ex-collega's en eindwerkstudenten. Ik heb al die jaren genoten van de uitmuntende werksfeer en teamgeest tijdens de werkuren en van de talloze ontspanningsactiviteiten erbuiten (laboweekends, 3D-avonden, labo-ontbijten, -lunches en -dinertjes,…). Een bijzonder woordje van dank aan:

- Lut, Katrien, Katrijn, Heidi, Margot, Klara, José, Eef, Eef(je) en Bart, voor jullie deskundigheid bij het administratieve en technische werk;
- Thesisstudenten Annick en Ken, voor de toffe samenwerking en jullie bijdrage tot het experimentele werk, duidelijk aanwezig in dit boekje;
- Mijn bureaugenootjes in 'de 01.16', voor de ideale mix van motiverende werkijver en momenten van verstrooiing tussendoor;
- Het IDO-KP team, voor de leuke, vlotte samenwerking en al jullie hulp binnen *ons* onderzoeksproject;
- Het labo-squashteam en onze labosportploeg 'The Pressure Rangers', voor de inspannende en onvergetelijke sportprestaties;
- Ilse en de andere leden van 'The Singing Can', die me mijn plezier in samen-muziek-maken deden herontdekken en het maandaggevoel speels verdreven;
- Dr. Sila, to show me the way to LFT, your everlasting laugh and friendship;
- De *poepkes* onder de collega's (Lien, Liesbeth, Philippe, Tara en Thomas) en *die-van-hen*, voor alle fantastische momenten samen, binnen en buiten de labomuren. Onze vriendschap reikt zonder twijfel voorbij de grenzen van dit doctoraat!

Onvoorwaardelijke steun heb ik ook altijd gekregen van mijn ouders, grootouders, schoonmama, (schoon)zussen en (schoon)broers, (schoon)familie en vrienden. Bedankt allemaal, voor de ontspannende momenten, bemoedigende woorden, oprechte interesse en hulp. Ik ben ontzettend blij en dankbaar voor zoveel prachtige mensen rondom mij!

Ten slotte, een heel warme dankjewel aan 'Dr. Ans De Roeck'. Ansje, in woorden valt moeilijk te vatten wat je de voorbije jaren voor me betekend hebt. Als een perfect team hebben we ons door ons doctoraat geworsteld. Jij was altijd mijn grootste steun en toeverlaat, altijd mijn vurigste supporter. Jouw geloof in en liefde voor mij hebben een immens verschil gemaakt, en zullen dat steeds blijven doen…

Mei 2010,

Ruben

SAMENVATTING

Pectin methylesterase (PME) is endogeen aanwezig in groenten en fruit en beïnvloedt, door zijn werking op pectine, de structurele kwaliteit van de rauwe producten en van afgeleide levensmiddelen. Vaak treden nadelige effecten op. Het gebruik van een specifieke PME-inhibitor (PMEI), die een inactief complex vormt met plantaardig PME, werd geopperd om ongewenste PME-activiteit in bepaalde plantgebaseerde levensmiddelen af te remmen (bv. met het oog op troebelstabiele sappen). Daarnaast zou deze PMEI hypothetisch kunnen worden gebruikt voor de ontwikkeling van een PME-detectiemethode, gebruik makend van een gemerkte PMEI-afgeleide. Binnen deze context beoogde het voorliggende werk een verbeterd inzicht in de PME-PMEI binding, zoals beïnvloed door product- en procesparameters, en een *proof-of-principle* van PMEI als moleculaire probe.

PMEs uit verscheidene plantenbronnen en PMEI uit kiwi's werden opgezuiverd via affiniteitschromatografie. De zuiverheid van de extracten werd bevestigd door middel van gelelektroforese en MALDI-TOF massaspectrometrie. Daaropvolgend werd de interactie tussen plantaardig PME en kiwi-PMEI bestudeerd aan de hand van drie methodologisch verschillende benaderingen. Naast de gangbare enzymactiviteit/-inhibitiemetingen werden complexvormingsexperimenten via gelfiltratie en interactie-analyses op basis van een *surface plasmon resonance* biosensor uitgevoerd. Op de biosensor werden strategieën uitgewerkt voor immobilisatie van PME (via directe aminokoppeling) evenals PMEI (via binding aan streptavidine na biotinylatie van PMEI). Slechts het gebruik van deze drie complementaire methoden leidde tot een volledig, geïntegreerd beeld van de PME-PMEI binding, met een gewenste graad van mechanistisch inzicht.

Aan de ene kant werden de bovenstaande methoden aangewend om het effect van intrinsieke factoren met relevantie in levensmiddelenmatrices, met name pH en zoutconcentratie, op de PME-PMEI interactie na te gaan. Beiden vertoonden een uitgesproken invloed. De mate van enzyminhibitie en/of de sterkte van binding (in termen van K_D) waren hoog in het pH-domein van 5 tot 7 en bij lage NaCl-concentraties (0 - 0.25 M), daar waar hogere pH-waarden en [NaCl] de interactie verzwakten, met nauwelijks binding bij pH ≥ 8 en [NaCl] van ca. 1.0 M.

Aan de andere kant werd het effect van de extrinsieke factoren temperatuur en druk, van belang bij levensmiddelenconservering, op de interactie tussen PME en PMEI onderzocht, met focus op de individuele interactiepartners (met name PME en PMEI) en op het PME-PMEI complex in zijn geheel.
Het effect van denaturatie van PMEI, geïnduceerd door hoge temperatuur (55 - 95 °C) of hoge druk (500 - 800 MPa, 25 °C), op zijn interactie met plantaardig PME werd geanalyseerd door de residuele inhibitiecapaciteit na behandeling te meten en de parameters van de inactivatiekinetiek te schatten. Een zekere fractie van de inhibitiecapaciteit werd behouden, zelfs na lange procestijd (in tegenstelling tot de PME-activiteit onder dezelfde condities). Bij lage pH-waarden (ca. pH 4) was de invloed van hoge druk op de inhibitiecapaciteit slechts minimaal.
SPR-gebaseerde interactie-analyse met geïmmobiliseerd PMEI evenals gelfiltratie-chromatografie werden gehanteerd om de PME-PMEI interactie te bestuderen na (partiële) denaturatie van wortel-PME, geïnduceerd door temperatuur (50 - 60 °C) of druk (800 MPa, 25 °C). Beide methoden wezen uit dat de PME-PMEI binding sterk geassocieerd is met PME-inactivatie: binding beperkt zich tot de actieve (i.e., niet-geïnactiveerde) PME-subpopulatie, terwijl PMEI geen complex aangaat met de gedenatureerde enzymfractie.
Om het gedrag van het PME-PMEI complex bij verhoogde temperatuur- of drukniveaus te onderzoeken werd de productvorming (i.e. methanol) in een mengsel van PME, PMEI en pectine gevolgd in functie van de behandelingstijd. De verkregen resultaten suggereerden dat het complex niet dissocieert bij toepassing van hitte ($T \leq 65$ °C) en relatief milde druk ($p < 400$ MPa bij 25 °C), daar waar blootstelling aan hogere drukniveaus dissociatie van het complex veroorzaakt. Deze initiële experimenten werden aangevuld met HPSEC-analyses van equimolaire PME-PMEI mengsels na behandeling bij verschillende intensiteiten. De eerdere observaties werden bevestigd. Bij verhoogde temperatuur (55 - 65 °C) bleven enzym en inhibitor verenigd en denatureerden ze als één geheel. Hoge-druk behandeling (800 MPa, 25 °C) daarentegen leidde tot een dissociatie van enzym en inhibitor, gevolgd door graduele inactivatie van PME en PMEI en hereniging van de niet-geïnactiveerde partners bij decompressie. PMEI vertoonde uitgesproken pH-afhankelijke inactivatiekarakteristieken en was opvallend drukweerstandig bij lage pH-waarden (ca. pH 4).

In de zoektocht naar een moleculaire probe voor *in situ* detectie van plantaardig PME in model- of levensmiddelensystemen werd PMEI gebiotinyleerd en het gebiotinyleerde PMEI (bPMEI) uitvoerig gekarakteriseerd. De bPMEI behield de capaciteit tot complexvorming met PME en won het vermogen om avidine te binden. De PMEI-gebaseerde probe werd succesvol getest en zijn veelzijdigheid aangetoond in *dot-blot* bindingsassays (met natieve en gedenatureerde PMEs) en weefselprints van verscheidene plantenorganen (bv. wortel, broccolistam en tomaat). In overeenstemming met eerdere resultaten herkende de PMEI-probe enkel het niet-geïnactiveerde PME.

De resultaten verzameld in dit werk onderschrijven de geopperde toepassing van PMEI in PME-inhibitie en -detectie. Tegelijkertijd schetsen ze de mogelijkheden en definiëren ze de grenzen voor toepassing. Toekomstig onderzoek is echter vereist om de bevindingen te vertalen naar reële levensmiddelensystemen en het inherente potentieel van de PME-inhibitor ten volle te benutten.

ABSTRACT

Pectin methylesterase (PME) is endogenously present in fruits and vegetables and impacts, through its action on pectin, on the structural quality of the raw materials or derived food products. Often, undesired effects occur. The use of a specific proteinaceous PME inhibitor (PMEI), forming an inactive complex with all plant PMEs tested, has been proposed for inhibition of unwanted PME activity in particular plant-based food applications (e.g., cloud-stable juices). Moreover, this PMEI can hypothetically be employed in the development of a PME detection technique using a labelled PMEI derivative. Within this context, the current work aimed at an enhanced insight in the PME-PMEI binding event, as affected by product and process parameters, and at a proof-of-principle of PMEI as a molecular probe.

PMEs from various plant sources and PMEI from ripe kiwi fruits were purified through affinity chromatography. Extract purity was confirmed by gel electrophoresis and MALDI-TOF mass spectrometry. Subsequently, the plant PME - kiwi PMEI interaction was explored by means of three methodologically different approaches. Besides the more common enzyme activity/inhibition assays, complex formation experiments by analytical size exclusion chromatography and interaction analyses using a surface plasmon resonance biosensor method were conducted. On the biosensor, immobilisation strategies for both PME (via direct amine coupling) and PMEI (via capture by streptavidin after protein biotinylation) to the chip surface were implemented. Only the use of these three complementary methods allowed for a complete, integrated picture of the PME-PMEI binding, with a desired extent of mechanistic insight.

On the one hand, the above methods were applied to examine the effect of intrinsic factors with relevance in food matrices, notably pH and salt concentration, on the PME-PMEI interaction. Both parameters exhibited a marked influence. The extent of enzyme inhibition and/or the strength of binding (in terms of K_D) were high in the pH range from 5 to 7 and at low NaCl concentrations (0 - 0.25 M), whereas increasing pH and [NaCl] weakened the interaction, with hardly any binding at pH ≥ 8 and [NaCl] of ca. 1.0 M.

On the other hand, the effect of extrinsic process parameters, namely high temperature and high pressure, on the interaction between plant PME and kiwi PMEI was investigated, with focus on the individual interaction partners (i.e., PME and PMEI) as well as on the PME-PMEI complex as a whole.
The effect of a high-temperature- (55 - 95 °C) or high-pressure- (500 - 800 MPa, 25 °C) induced denaturation of kiwi PMEI on its interaction with plant PME was analysed by measuring residual inhibitory capacity (towards carrot PME) after treatment and estimating inactivation kinetic parameters. Even upon prolonged thermal or pressure processing, a certain fraction of the PMEI inhibitory capacity was conserved (contrary to the PME activity under the same conditions). In fact, the inhibition capacity was only minimally affected by high pressure at low pH values (ca. pH 4).
SPR-based interaction analysis with immobilised PMEI and size exclusion chromatography were applied to study the PME-PMEI interaction ensuing (partial) denaturation of carrot PME induced by temperature (50 - 60 °C) or pressure (800 MPa, 25 °C). Both strategies revealed that the PME-PMEI binding is highly associated with PME inactivation: binding was restricted to the active (i.e., non-inactivated) PME subpopulation, whereas PMEI did not engage a complex with the denatured enzyme fraction.
To examine the behaviour of the PME-PMEI complex at elevated temperature or pressure levels, product formation (i.e., methanol) in a mixture of PME, PMEI and pectin as a function of treatment time was followed. The results obtained suggested the complex not to dissociate upon the application of heat ($T \leq 65$ °C) and relatively mild pressure ($p < 400$ MPa at 25 °C), whereas exposure to higher pressure levels caused the complex to separate. These initial experiments were complemented with HPSEC analyses of equimolar PME-PMEI mixtures after treatment at various intensities. The earlier observations were confirmed. At elevated temperature (55 - 65 °C), enzyme and inhibitor remained united and denatured as a single entity. High-pressure treatment (800 MPa, 25 °C), conversely, induced dissociation of enzyme and inhibitor, followed by gradual inactivation of PME and PMEI and subsequent reunion of the non-inactivated partners upon decompression. PMEI showed distinct pH-dependent inactivation characteristics, being strikingly baroresistant at low pH values (ca. pH 4).

Finally, in the quest of obtaining a molecular probe for *in situ* detection of plant PME in model or food systems, PMEI was biotinylated and the biotinylated PMEI (bPMEI) extensively characterised. The bPMEI retained its complex forming capacity towards PME and gained the ability to strongly bind an avidin species. The PMEI-based probe was successfully tested and its versatility demonstrated in dot-blot binding assays (with native and denatured PMEs) and tissue prints of various plant organs (i.e., carrot root, broccoli stem and tomato fruit). In agreement with the earlier results, the PMEI probe only recognised the non-inactivated PME.

The whole of the data collected in this thesis endorses the putative application of PMEI in PME inhibition and detection. In the mean time, the results highlight the opportunities and define the application boundaries. However, further research will be needed to translate the findings to real food matrices and to fully exploit the inherent potential of the PME inhibitor.

TABLE OF CONTENTS

LIST OF NOTATIONS

LIST OF ABBREVIATIONS

A.	*Aspergillus*
AtPMEI	*Arabidopsis thaliana* PMEI
BCA	Bicinchoninic acid
bPMEI	Biotinylated PMEI
CNBr	Cyanogen bromide
Corr R^2	Corrected R^2 (correlation coefficient)
DM	Degree of methyl-esterification
E.	*Erwinia*
ExA-FITC	ExtrAvidin®-Fluorescein isothiocyanate
FTIR	Fourier transform infrared
GalA	Galacturonic acid
HG	Homogalacturonan
HM	High-methoxylated
HPSEC	High-performance size exclusion chromatography
IEF	Isoelectric focusing
LM	Low-methoxylated
MALDI-TOF	Matrix-assisted laser desorption/ionisation time-of-flight
MES	2-(*N*-morpholino)ethanesulfonic acid
MS	Mass spectrometry
NHS	*N*-hydroxysuccinimide
PBS	Phosphate-buffered saline
PG	Polygalacturonase
PGIP	Polygalacturonase inhibiting protein
PL	Pectate lyase
PME	Pectin methylesterase
PMEI	Pectin methylesterase inhibitor

PNL	Pectin lyase
PVPP	Polyvinylpolypyrrolidone
RG-I	Rhamnogalacturonan I
RG-II	Rhamnogalacturonan II
RU	Resonance unit
SDS-PAGE	Sodium dodecyl sulphate polyacrylamide gel electrophoresis
SPR	Surface plasmon resonance
Tris	Tris(hydroxymethyl)aminomethane
U	Unit (of PME activity)
UI	Unit of inhibition (of PMEI)

LIST OF SYMBOLS

A	Activity (at treatment time t) of enzyme or inhibitor
A_0	Initial activity (at time $t = 0$)
A_L	Activity of labile fraction
A_S	Activity of stable fraction
A_∞	Non-zero residual activity (after prolonged treatment)
A_1	Activity of first enzyme/inhibitor form
A_2	Activity of second (intermediate) enzyme/inhibitor form
E_a	Activation energy (J/mol)
k	Inactivation rate constant (min^{-1})
k_L	Inactivation rate constant of labile fraction (min^{-1})
k_{ref}	Inactivation rate constant at T_{ref} or p_{ref} (min^{-1})
k_S	Inactivation rate constant of stable fraction (min^{-1})
k_1	Inactivation rate constant of first inactivation step (min^{-1})
k_2	Inactication rate constant of second inactivation step (min^{-1})
k_a	Association rate constant ($M^{-1}\cdot s^{-1}$)
k_d	Dissocation rate constant (s^{-1})
K_D	Dissociation equilibrium constant (M)
p	Pressure (MPa)
p_{ref}	Reference pressure (MPa)
pI	Isoelectric pH
R_T or R_p	Universal gas constant (8.314 J/mol·K or cm^3·MPa/mol·K)
R^2	Correlation coefficient
t	Treatment time (min)
T	Temperature (°C or K)
T_{ref}	Reference temperature (°C or K)
V_a	Activation volume (cm^3/mol)
V_0	Reaction rate constant (µmol methanol/(mL·min))

GENERAL INTRODUCTION

Pectin methylesterase (PME) is one of the key enzymes in fruit and vegetable processing. Through its action on pectin, a major plant cell well polysaccharide, plant PME alters pectin's fine structure in terms of degree and pattern of methoxylation, thus affecting pectin's physicochemical and functional properties, in raw fruit and vegetable material as well as in derived food products. From a food technological point of view, PME can impact desirably or deleteriously on the quality of plant-based foods, mainly with regard to structure. For instance, demethoxylated pectin is prone to enzymatic depolymerisation by polygalacturonase, inducing texture or viscosity loss (Van Buren, 1979). However, demethoxylation of pectin reduces its susceptibility to chemical β-eliminative depolymerisation that can occur during thermal processing and is associated with heat-induced softening of fruits and vegetables (Keijbets and Pilnik, 1974). In addition, pectin with a reduced degree of methyl-esterification can cross-link via divalent ion bridges to form intermolecular networks, promoting gel formation (Van Buren, 1979), but also compromising cloud stability in fruit and vegetable juices (Versteeg *et al.*, 1980).

Consequently, PME activity control is a major point of interest in order to meet specific quality targets for plant-based food products. Depending on the intention with the product at hand, PME stimulation or inactivation can be pursued. In this context, traditional thermal and 'novel' high hydrostatic pressure processing have been shown to be valuable tools to rigorously tailor PME-induced pectin conversions and, hence, to control pectin-related functional features of plant-derived foods in terms of texture, rheology and cloud stability (Van Buggenhout *et al.*, 2009). Yet, it should be noted that processing can also bring about undesirable organoleptic and nutritional quality changes, and should often preferably be minimised.

The discovery of a proteinaceous PME inhibitor (PMEI) in kiwi fruit, forming an inactive 1:1 complex with plant PME (Balestrieri *et al.*, 1990), has added a new dimension to endogenous PME activity control. Relying on the strong PME-PMEI interaction, kiwi PMEI may be exploited as a technological adjuvant for inhibition of undesired PME activity in food applications remaining after (mild) processing,

through pre- or post-processing addition of the inhibitor, e.g., to obtain cloud-stable juices. Thus, less harsh preservation treatments, compared to those needed to inactivate all PME, may be applied, resulting in better flavour and nutrient retention. Recent cloning of the cDNA of kiwi PMEI and its expression in the yeast *Pichia pastoris* encourages a widespread application (Mei *et al.*, 2007). In addition, the discovery of this PMEI opens perspectives for the development of an innovative (microscopic) technique using labelled PMEI to localise endogenous PME *in situ* and, hence, to ameliorate the insight in the relationship between enzymatic pectin conversions and allied (macroscopic) functional properties (such as firmness and viscosity), both in model systems and in structured, real food matrices. Information on how food processing can possibly change these locations, e.g., as a result of enzyme inactivation or tissue damage, may further improve the understanding.
An indispensable prerequisite for efficient application of PMEI, in either PME inhibition or PME detection, is a profound knowledge of the PME-PMEI interaction, as influenced by both relevant intrinsic product factors (such as pH and ionic strength) and extrinsic process factors (such as high temperature and high pressure). However, this knowledge is lacking to date.

The objective of the current work is twofold. On the one hand, an improved (quantitative) insight in the interaction between plant PME and kiwi PMEI in a food processing context is pursued. Hereto, different methodological approaches are employed. On the other hand, a proof-of-principle of the application of kiwi PMEI for detection of endogenous PME in plant-based food systems is aimed at.

A schematic outline of the present thesis is shown in **Figure 1**.
Chapter 1 entails a literature review, providing a detailed and up-to-date introduction on relevant chemical/biological and food technological aspects concerning pectin (Section 1.1), PME (Section 1.2), PMEI (Section 1.3) and the effect of processing on proteins and enzymes (Section 1.4), extensively illustrating the problem addressed in this thesis and sketching the broader framework.
In the experimental part, two major subparts can be distinguished. In the first subpart, three different and complementary experimental strategies to monitor the interaction between plant PME and kiwi PMEI are examined. These include enzyme activity/inhibition measurements (**Chapter 2**), interaction analysis based on surface plasmon resonance (**Chapter 3**) and complex formation through size exclusion chromatography (**Chapter 4**). In all chapters, the effects of product factors (pH and NaCl concentration) and/or processing factors (high temperature and high pressure) are analysed, both on the individual interaction partners (i.e., PME and PMEI) and on the enzyme-inhibitor complex as a whole. Throughout the study, self-purified enzyme (mainly carrot PME, as a representative plant PME) and inhibitor solutions are used. Wherever possible and relevant, a quantitative and mechanistic approach is followed. Results of these chapters should allow a theoretical evaluation of the feasibility of PME inhibition through PME addition (in combination with processing), and a definition of application boundaries.
In the second experimental subpart (**Chapter 5**), building on the insights gained in the previous chapters, an attempt is made to bridge the gap to one of the application of PMEI. More precisely, the potential of PMEI as a molecular probe for detection of plant PME *in situ* is critically assessed, also in the context of food

processing. Hereto, a labelled PMEI derivative is constructed and its binding properties tested in dot-blot and tissue-print assays.

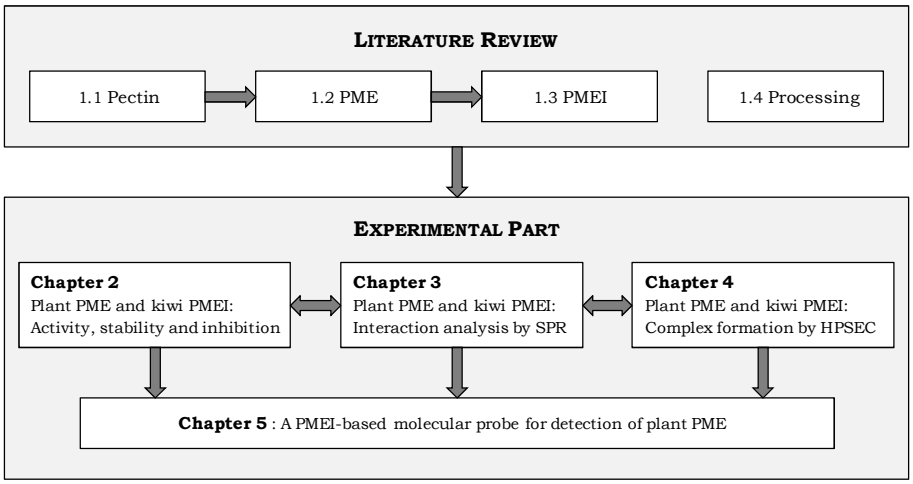

Figure 1. Schematic outline of the present thesis.

1

LITERATURE REVIEW

Pectin, one of the main components of the plant cell wall, contributes to many quality attributes of plant-based foods, chiefly in relation to texture. Pectin methylesterase (PME) catalyses the demethoxylation of pectin. Through pectin remodelling, the enzyme can have both beneficial and detrimental effects on food quality. Activity control is therefore often pursued. In this context, the proteinaceous PME inhibitor (PMEI) and (thermal and high-pressure) processing are particularly relevant.
In this first chapter, a literature review is presented. In four sections, some main aspects concerning pectin, PME, PMEI and the effect of processing on proteins and enzymes are introduced. In all sections, basic chemical and biological information is complemented with the food technological relevance. Finally, based on the conclusions of the literature review, the scope of this work is defined.

1.1 PECTIN

Pectin is a polysaccharide present in the cell wall of all higher plants, contributing to tissue integrity and rigidity. As such, it plays an important role during ripening, storage and processing of plant raw materials for foods. It is also extracted from suitable plant sources and widely used in food industry because of its gelling, stabilising and thickening properties. Recently, pectin has gained interest as a functional food ingredient because of possible health-promoting effects.

1.1.1 Pectin structure

1.1.1.1 Constituent polymers

Pectin is one of the most complex macromolecules in nature. The term “pectin” refers to a class of closely associated polysaccharides that are rich in galacturonic acid (GalA). However, it can be composed of as many as 17 different monosaccharides and contain more than 20 different linkages (Ridley *et al.*,

2001; Voragen *et al.*, 2009). Over the years, several pectin structural elements have been described and all pectins are believed to essentially contain the same repeating elements, although the amount and chemical fine structure of these elements vary (Schols and Voragen, 1996; Voragen *et al.*, 2009). Generally, three pectic polymers are recognised: homogalacturonan (HG), rhamnogalacturonan I (RG-I) and rhamnogalacturonan II (RG-II). Besides, other substituted galacturonans have been described, such as xylogalacturonan and apiogalacturonan (Ridley *et al.*, 2001; Willats *et al.*, 2001a; Coenen *et al.*, 2007; Mohnen, 2008).

HG is a linear homopolymer of 1,4-linked α-D-GalA. The backbone has an estimated length of around 100 GalA residues, although shorter regions of HG have been detected (Thibault *et al.*, 1993; Mohnen, 2008; Wolf *et al.*, 2009). HG is partially methyl-esterified at the C-6 carboxyl and, depending on the plant source, may be O-acetylated at C-2 or C-3 (Ridley *et al.*, 2001; Mohnen, 2008). HG is considered the most abundant pectic polysaccharide in plant cell walls, accounting for greater than 60% of the total pectin amount (Caffall and Mohnen, 2009). HG in general and its methyl-esterification (degree and pattern) in particular have gained a lot of attention in pectin research since they are assumed to strongly determine the functional properties of pectin (Willats *et al.*, 2006; Voragen *et al.*, 2009).

RG-I is a family of polymers that contain a backbone of the repeating disaccharide [→4)-α-D-GalA-(1→2)-α-L-Rha-(1→], of which up to 80% of the rhamnose residues can be substituted at C-4 with neutral and acidic sugar side chains (Albersheim *et al.*, 1996; Ridley *et al.*, 2001). These side chains are mainly composed of galactosyl and/or arabinosyl residues and range from a single unit to polymeric linear or branched substitutions, such as (arabino)galactan and arabinan (Willats *et al.*, 2001a; Vincken *et al.*, 2003; Mohnen, 2008). Diversity in the number and nature of side chains results in RG-I being a complex and variable polysaccharide (Ridley *et al.*, 2001). Acetylation is possible on the GalA residues. However, it is not yet clear whether methyl-esterification occurs as well (Voragen *et al.*, 2009).

Despite its name, RG-II is not structurally related to RG-I, unless for its branched nature. It has a HG backbone of around nine GalA residues and is substituted by four hetero-oligomeric side chains with known and consistent composition and length (conserved throughout the plant kingdom) (Ridley *et al.*, 2001; Voragen *et al.*, 2009). Along with widely occurring monosaccharides (such as GalA, Glu, Rha, Gal, Ara), also some peculiar sugar residues, such as aceric acid, 3-deoxy-lyxo-2-heptulosaric acid (DHA) and 3-deoxy-D-*manno*-2-octulosonic acid (KDO) have been identified (Willats *et al.*, 2001a; Ovodov, 2009; Voragen *et al.*, 2009).

1.1.1.2 Macromolecular organisation

Although the chemical composition and structure of the constituent polymers of pectin are largely known, there is no consensus as to how these structural elements are combined into a macromolecular structure. It is generally assumed that the pectic polysaccharides are covalently linked to each other (Ridley *et al.*, 2001; Coenen *et al.*, 2007). For long, it was widely accepted that HG, RG-I and RG-II form a continuous backbone, forming an extended chain with alternating

smooth (mainly HG) and hairy (RG-I, RG-II and side chains) regions (Willats *et al.*, 2001a) (**Figure 1.1A**). However, an alternative structure has been proposed more recently, in which HG, like arabinan and galactan, is considered a long side chain of RG-I (Vincken *et al.*, 2003) (**Figure 1.1B**). No conclusive evidence confirming or rejecting either of the models has been presented since, but the currently available information tends to support the conventional model (Coenen *et al.*, 2007; Mohnen, 2008).

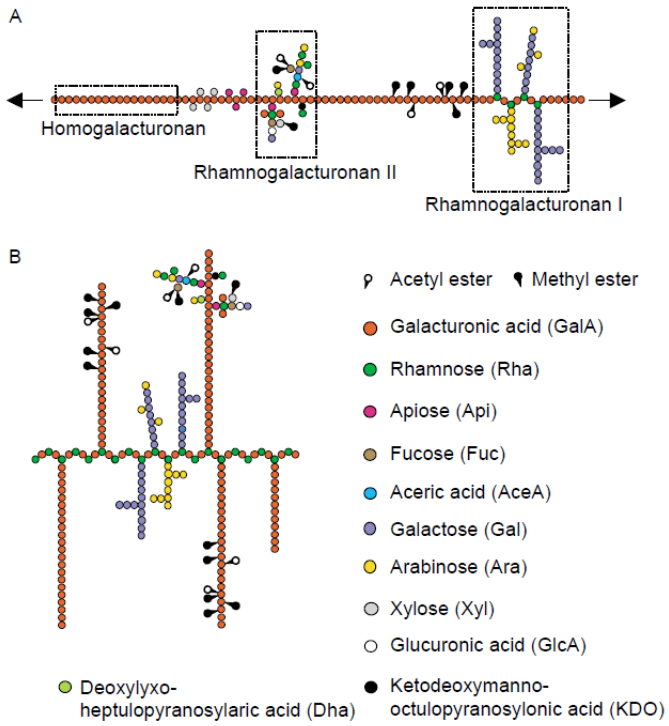

Figure 1.1. Schematic representation of the chemical structure of pectin according to (A) the conventional model and (B) the alternative model proposed by Vincken *et al.* (2003). The polymers shown here are intended only to illustrate some of the major domains found in most pectins rather than definitive structures (Willats *et al.*, 2006).

1.1.1.3 Network-formation through cross-linking

Pectin macromolecules can assemble in much larger networks, e.g., in the plant cell wall (cf. next section). Different types of pectin cross-links have been described so far.

Negatively charged, nonmethoxylated GalA residues in the HG domain can ionically interact with calcium ions. Blocks of 7 - 20 free GalA residues are reported to be required to build a stable linkage between chains (Vincken *et al.*, 2003; Voragen *et al.*, 2009). According to this principle, calcium-pectate gels can be made (cf. Section 1.1.3.1). In a second type of cross-linking, dimerisation of RG-II through a 1:2 borate-diol ester linkage between the apiosyl residues of two

RG-II monomers occurs. As RG-II is covalently linked to HG, RG-II dimer formation is postulated to be a major contributor to the formation of a three-dimensional pectic network within the plant cell wall (Ishii and Matsunaga, 2001; Mohnen, 2008). Furthermore, it was suggested that uronyl ester linkages can be formed between the carboxyl group of a GalA residue in HG and a hydroxyl group of another glycosyl residue. Given the abundance of methyl-esterified HG in cell walls, these molecules hold an enormous potential for cross-linking (Brown and Fry, 1993; Voragen *et al.*, 2009). Specifically for *Chenopodiaceae* (e.g., sugar beet and spinach), cross-linking of neutral sugar pectic side chains, esterified with ferulic or coumaric acid, via oxidative coupling has been reported (Ridley *et al.*, 2001; Ralet *et al.*, 2005).

1.1.1.4 Pectin in the plant cell wall

The pectin network is a major component of the plant cell wall, the highly sophisticated macromolecular structure surrounding the plasma membrane and protecting the plant cell. The cell wall consists of three types of layers: middle lamella, primary cell wall and secondary cell wall. The middle lamella is the earliest formed layer and shared by two adjacent cells. A secondary wall may be laid down at the onset of differentiation, after cell elongation has ceased, but is limited to certain specialised cells (Brett and Waldron, 1996; Caffall and Mohnen, 2009). In edible plants, the primary cell wall often is of most interest since secondary walls are virtually absent from mature fruits (Van Buren, 1979).

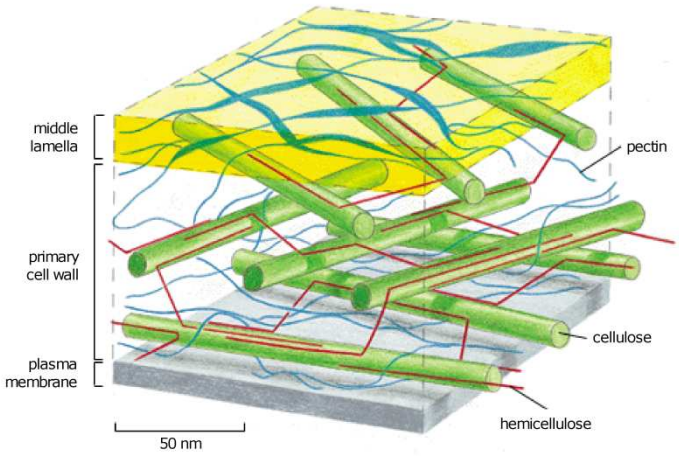

Figure 1.2. A simplified, schematic representation of the cell wall of higher plants (adapted from McCann and Roberts, 1996)

Besides pectin, two other major categories of plant cell wall polysaccharides are distinguished: cellulose (i.e., linear chains of β-(1→4)-linked D-glucose units) and hemicellulose (i.e., heterogeneous polymers such as xyloglucans, xylans and mannans). Most models describe the cell wall in general terms as a network of long, rigid and inextensible cellulosic microfibrils embedded in a cementing matrix of non-cellulosic polysaccharides (pectins and hemicelluloses), proteins

(enzymes and structural proteins), (often) phenolics (lignin and others), lower molar mass solutes and water (Van Buren, 1979; Waldron *et al.*, 2003; Brummell, 2006) (**Figure 1.2**). However, no model presently explains all of the measured physical properties, and many questions remain unsolved. For instance, it is not clear to what extent ionic and covalent cross-links are being formed between the different components (Van Buren, 1979; McCann and Roberts, 1996; Brett and Waldron, 1996; Mort, 2002; Waldron *et al.*, 2003; Vicente *et al.*, 2007; Mohnen, 2008).

The relative composition of the cell wall varies spatially, from plasma membrane to middle lamella. Furthermore, the precise ratio of components differs phylogenetically between plant taxa, between the tissues of a given plant and temporarily during the development of a given cell (Fry, 2004; Brummell, 2006; Caffall and Mohnen, 2009). In general, pectin is present in the primary cell wall and the middle lamella. It accounts for about one-third of the cell wall polymeric content of the primary wall of dicotyledonous plants (Thakur *et al.*, 1997; Brummell, 2006), whereas grasses contain lower amounts of pectin (2 - 10%) and fruit cell walls are often pectin-enriched (Brummell, 2006; Voragen *et al.*, 2009). The middle lamella, considered to be an extension of the matrix material of the primary cell wall lacking the cellulose fibrils, predominantly contains pectin (Van Buren, 1979; Jarvis *et al.*, 2003).

Localisation and visualisation of the varying distribution of the pectic components over the different cell-wall layers in the intact cell-wall architecture has been made possible by the development of a number of monoclonal antibodies recognising defined structural features of pectin, backbone as well as side chain domains (Jauneau *et al.*, 1998; Willats *et al.*, 2000; Willats *et al.*, 2006). Most extensively studied and used are the HG-directed antibodies. JIM5, JIM7, LM7 and PAM1 all bind HG but have different specificities with regard to degree and pattern of methyl-esterification (VandenBosch *et al.*, 1989; Knox *et al.*, 1990; Willats *et al.*, 2001a; Clausen *et al.*, 2003). 2F4 binds specifically to HG that is cross-linked via calcium (Liners *et al.*, 1989). These tools have indicated that the methyl-esterification of HG is highly varied in relation to cell development: the wall around a single cell can contain discrete microdomains, each accumulating a particular type of HG (Willats *et al.*, 2001b; Vincken *et al.*, 2003; Verhertbruggen *et al.*, 2009). It is believed that the use of antibody tools for *in situ* analysis of cell-wall polymers will bring major progress in cell-wall biology and in understanding the functional significance of development-specific or cell-type-specific wall configurations of polymers (Knox, 2008).

Pectin's functionality to a plant is quite diverse, although not defined precisely. First, pectin plays a key role in the formation of higher plant cell walls, contributing to the mechanical strength of the wall and to the adhesion between cells. It is involved in complex physiological processes like cell growth and cell differentiation and, as such, determines the integrity and rigidity of plant tissue. Second, pectin influences various cell-wall properties such as porosity, surface charge, pH and ion balance and, therefore, is of importance to the ion transport in the cell wall, the permeability of the walls for enzymes and the water-holding capacity. Furthermore, pectin oligosaccharides are known to act as signalling molecules, both as elicitors during pathogen attack or wounding and as hormone-like compounds during plant development (Van Buren, 1979; Thakur *et*

al., 1997; Willats *et al.*, 2001a; Mohnen, 2008; Wolf *et al.*, 2009; Voragen *et al.*, 2009).

1.1.2 Pectin conversions

Pectin can undergo numerous enzymatic as well as non-enzymatic conversion reactions, modifying its fine structure. The overview given in this section is restricted to the well-known conversion reactions occurring at the linear HG chain, reactions that are believed to govern many of pectin's functional properties, both in plants and in foods. A schematic summary is given in **Figure 1.3**.

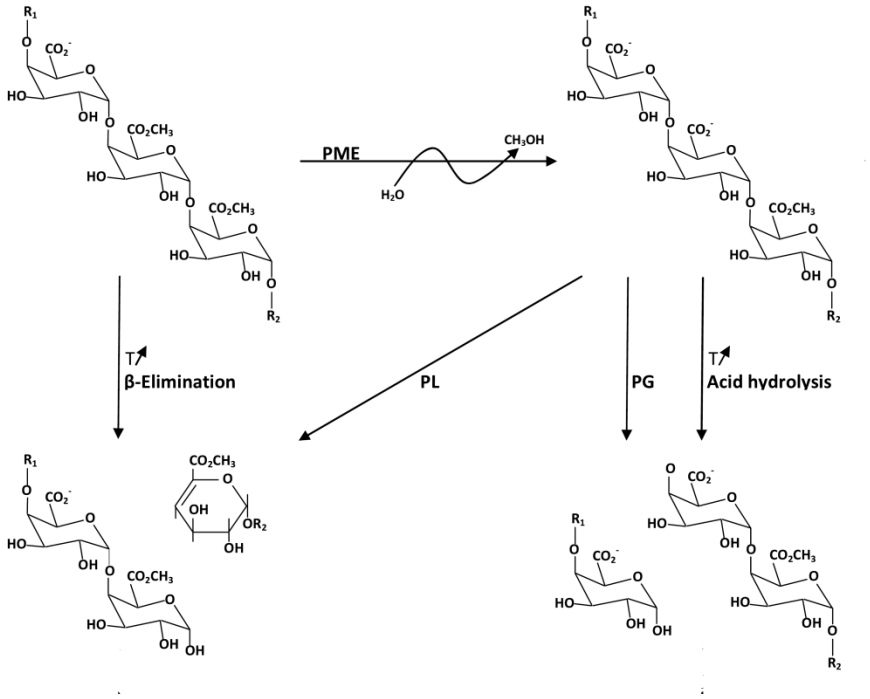

Figure 1.3. Schematic overview of enzymatic and non-enzymatic conversion reactions occurring at the HG chain of pectin: PME = pectin methylesterase, PG = polygalacturonase, PL = pectate lyase, T↗ = temperature increase, R1/R2 = initial/ terminal fragment of the pectin polymer (adapted from Van Buggenhout *et al.*, 2009).

1.1.2.1 Non-enzymatic conversions

Pectin generally shows a good stability around pH 3 - 4, the pK_a range of its carboxyl groups. However, under selected conditions of pH and temperature, pectin demethoxylation or depolymerisation can occur (Rolin, 2002).

Methyl-esters at C-6 of GalA residues can be hydrolysed under alkaline or near-neutral conditions (Van Buren, 1979). This chemical demethoxylation is a random process, resulting in a statistical distribution of free and methoxylated GalA residues on the HG chain (Van Buren, 1979; Limberg *et al.*, 2000). The

saponification reaction is accelerated at higher temperatures (Renard and Thibault, 1996; De Roeck *et al.*, 2009) and, since saponification is initiated by hydroxyl ions, with increasing pH (Renard and Thibault, 1996). Moreover, the rate of saponification is proportional to the amount of esters remaining, so decreasing as the reaction proceeds (Renard and Thibault, 1996).
When heating pectin at neutral or alkaline pH, β-eliminative depolymerisation can take place. The hydrogen at C-5 of GalA is removed by a hydroxyl ion, leading to an unstable, intermediary anion. This anion is stabilised by eliminative cleavage of the glycosidic linkage in the β-position, resulting in the formation of an unsaturated bond between C-4 and C-5 at the nonreducing end (Albersheim *et al.*, 1960; Kiss, 1974). A prerequisite is the presence of a methyl-ester group at C-6, rendering H-5 sufficiently acidic to be removed by an alkali. Consequently, pectin with a high degree of methoxylation (DM) has an increased susceptibility towards β-elimination (Albersheim *et al.*, 1960; BeMiller and Kumari, 1972; Keijbets and Pilnik, 1974; Sajjaanantakul *et al.*, 1989). Chemical demethoxylation, proceeding under the same temperature and pH conditions and affecting the DM, will influence the β-elimination (Kravtchenko *et al.*, 1992; De Roeck *et al.*, 2009). Since hydroxyl ions initiate the reaction, the reaction rate increases with increasing pH (Kravtchenko *et al.*, 1992; Krall and McFeeters, 1998; Sila *et al.*, 2006). B-elimination is also stimulated in presence of cations (Keijbets and Pilnik, 1974) and accelerated with increasing temperature (Sila *et al.*, 2006; De Roeck *et al.*, 2009).
A second mechanism leading to pectin depolymerisation during heating is the acid-catalysed hydrolytic splitting of glycosidic bonds (pH < 3). The reaction proceeds through an initial protonation of the glycosidic oxygen, followed by a rate-limiting formation of a cyclic oxocarbenium ion leading to rearrangements resulting in the breakage of the disaccharide linkage (Van Buren, 1979). Pectin with low DM hydrolyses faster, and the rate of hydrolysis increases with decreasing pH, addition of NaCl and increasing temperature (Krall and McFeeters, 1998).

1.1.2.2 Enzymatic conversions

A wide range of enzymes can synergistically modify and degrade pectin. They are collectively named pectinases and can be of both microbial and plant origin (Tucker and Seymour, 2002). In HG, the enzymes involved can be either esterases or depolymerases. The depolymerising enzymes comprise hydrolases and lyases.
Pectin methylesterases (PME, E.C. 3.1.1.11) catalyse the specific demethoxylation of HG at the O-6 of GalA, releasing methanol and protons and creating dissociable carboxyl groups on the pectin chain. A more elaborate discussion on this enzyme will follow in Section 1.2.
Pectin acetylesterases (PAE, EC 3.1.1.6) remove acetyl groups from O-2 and/or O-3 of GalA residues in the HG part. So far, their presence is only demonstrated in a limited number of plant species and micro-organisms, but it is likely that they are more widespread (Tucker and Seymour, 2002; Benen *et al.*, 2003a; Bonnin *et al.*, 2008).
Polygalacturonases (PG) cleave the α-1,4-D linkages between two adjacent GalA residues in the HG domain of pectin by acid/base-assisted hydrolysis. Whereas

endo-PGs (EC 3.2.1.15) hydrolyse the polymer substrate randomly (resulting in a fast decrease in molar mass of pectin), the exo-PGs are confined to cleave off GalA monomers (EC 3.2.1.67) or digalacturonides (EC 3.2.1.82) from the nonreducing end of a chain (Benen and Visser, 2003b). The exact substrate requirement for PG action is still subject to debate, but it is generally acknowledged that the enzyme will cleave only between demethoxylated GalA residues (Tucker and Seymour, 2002). Consequently, PG shows increasing activity with decreasing DM, e.g., caused by action of PME (Rexova-Benkova and Markovic, 1976; Benen and Visser, 2003b). PG has been found in some fungi, bacteria, yeasts and many higher plants (Tucker and Seymour, 2002; Duvetter *et al.*, 2009). It is considered a key enzyme in the degradation of plant cell walls upon phytopathogenic attack, and many plants have evolved a resistance mechanism relying on PG-inhibiting proteins (PGIP). These PGIPs are extracellular glycoproteins, found in virtually all tissues and organs of all plants investigated, and belong to a family of leucine-rich repeat proteins that are specialised in the recognition of non-self molecules (Protsenko *et al.*, 2008). PGIPs are active against microbial PGs, but do not interact with plant-derived PGs (Federici *et al.*, 2001; Juge, 2006).

Pectate lyases (PL) catalyse the cleavage of α-1,4-D galacturonosidic linkages in HG via a β-elimination reaction mechanism, resulting in the formation of a double bond between C-4 and C-5 at the newly formed nonreducing end (Rexova-Benkova and Markovic, 1976; Benen and Visser, 2003a). They can be endo- (E.C. 4.2.2.2) or exo-acting (E.C. 4.2.2.9) and require calcium ions for catalysis. For many PLs, highest specific activity was recorded using pectins of moderate DM (20 - 50%) instead of pectin with 0% DM (Benen and Visser, 2003a). Initially, it was thought that PLs were secreted only by plant pathogens, their action resulting in the maceration of plant tissues. However, putative pectate lyases have been identified in plants through cDNA sequencing of plant tissue specific cDNA libraries (Marin-Rodriguez *et al.*, 2002; Benen and Visser, 2003a; Vicente *et al.*, 2007).

Pectin lyases (PNL, EC 4.2.2.10) perform the same reaction as the pectate lyases but this class of enzymes requires the galacturonic acid residues adjacent to the scissile bond to be methyl-esterified. Hence, the specific activity increases with increasing DM (Benen and Visser, 2003a). Currently, only endo-acting PNLs are known. Pectin lyases have so far only been identified in and isolated from micro-organisms (Benen and Visser, 2003a; Yadav *et al.*, 2009)

1.1.3 Relevance of pectin in the food industry

From a food technological point of view, pectin is particularly important. On the one hand, extracted pectin is widely used in the food industry as an ingredient/additive, mainly relying on its gelling capacity. On the other hand, endogenous pectin is related to many quality attributes of fresh and processed plant-based foods, in particular to texture. Moreover, health-promoting effects, such as anti-cancer activities and lowering cholesterol and serum glucose levels (Yamada, 1996), have been ascribed to pectin.

1.1.3.1 Pectin as food additive

Extracted pectin (EU code: E440) is widely used as a functional food ingredient and is listed among the ingredients of innumerable food products (Willats *et al.*, 2006). Addition of pectin is often based on its gelling properties. A pectin gel is formed when portions of HG are cross-linked to form a three-dimensional network in which water and solutes are trapped (Thakur *et al.*, 1997; Thibault and Ralet, 2003). Basically, two mechanisms of pectin gelation are distinguished, depending on the pectin's DM.

In high-methoxylated (HM) pectins (DM > 50%), junction zones are formed by association of HG chains through hydrogen bridges between carboxylic acid groups and hydrophobic forces between methoxyl groups. Their gelation requires an acidic medium (pH < 3.5), reducing carboxylic dissociation and electrostatic chain repulsion, and a high soluble solid content (> 55%), e.g., due to sugars, creating conditions of low water activity and promoting chain-chain interactions (Thibault and Ralet, 2003; Endress *et al.*, 2006).

Low-methoxylated (LM) pectins (DM < 50%) form gels in the presence of divalent ions (i.e., calcium for food purposes). Gelation is due to the formation of junction zones between HG regions of different pectin chains through calcium bridges between dissociated carboxyl groups, often described by the "egg-box" model. In addition to electrostatic interactions, van der Waals interactions and hydrogen bonds are probably involved as well (Braccini and Perez, 2001; Thibault and Ralet, 2003). To achieve LM pectin gelation, the pH range required is broader than for HM pectins and sugar addition is not necessary (Thibault and Ralet, 2003; Endress *et al.*, 2006).

Pectin is used in a variety of foods as gelling agent, thickener, texturiser, emulsifier and stabiliser (Thakur *et al.*, 1997). HM pectins are applied as a gelling agent in sweetened fruit products such as jams, jellies and marmalades. As LM pectins do not require sugars for gelation, they are used in the low-calorie surrogates. Furthermore, pectin is employed in the production of fruit juices, confectionary products and bakery fillings. Another major use of pectin is for the stabilisation of acidified milk drinks and yoghurts, since pectins react with caseins to prevent coagulation at acidic pH. In recent years, pectin has been used as a fat or sugar replacer in low-calorie foods to create a desired mouthfeel (Thakur *et al.*, 1997; Thibault and Ralet, 2003; Willats *et al.*, 2006; Endress *et al.*, 2006).

Although most plant tissues contain pectin, commercial production is limited to a few sources. Currently, citrus peel and apple pomace, both by-products of the juice industry, are the major sources of extracted pectin. Other potentially valuable sources (e.g., sugar beet) remain largely unused because of certain structural features, adversely affecting their functionality, e.g., gelling capacity (May, 1990; Thakur *et al.*, 1997; Rolin, 2002; Thibault and Ralet, 2003; Willats *et al.*, 2006).

1.1.3.2 Pectin in relation to texture of plant-based foods

Texture of fruits, vegetables and derived products is a major quality attribute and determinant of consumer acceptance and preference (Szczesniak, 1971). Texture is a subjective parameter described as "the sensory and functional manifestation

of the structural, mechanical and surface properties of foods detected through the senses of vision, hearing, touch and kinesthetics", the latter being the sensation of presence, movement and position as resulting from nerve-ending stimulation (Szczesniak, 2002). Texture is an extremely complex, multi-parameter attribute and the physiological basis for texture of fruits and vegetables is complicated. Besides turgor pressure, structural characteristics of the cell-wall polymers, in particular of pectin, are believed to play a central role, since changes in pectin content, composition and fine structure occur during events that modulate texture, such as fruit ripening and thermal processing (Waldron *et al.*, 2003; Jarvis *et al.*, 2003; Sila *et al.*, 2009).

Ripening of fruits is a complex, often fruit-specific, process that generally involves tissue softening (Brummell, 2006). Many questions on the exact mechanisms remain unsolved, but it is well documented that during ripening a variety of enzyme-catalysed reactions takes place converting cell-wall pectin: pectin depolymerisation (and related solubilisation) by PG and PL, demethoxylation of the pectin backbone by PME (stimulating PG and PL activity), and enzymatic degradation of arabinan and galactan side chains. All these reactions are thought to change cell-wall mechanical strength and to weaken cell-cell adhesion, inducing softening (Brownleader *et al.*, 1999; Waldron *et al.*, 2003; Jarvis *et al.*, 2003; Brummell, 2006; Vicente *et al.*, 2007).

Thermal processing of fruits and vegetables often results in a loss of firmness. This softening is caused partly by the disruption of the plasmalemma and the concomitant loss of turgor (Greve *et al.*, 1994), but the most significant softening is a result of an increase in the ease of cell separation (Van Buren, 1979; Ng and Waldron, 1997). The latter has been generally attributed to the β-eliminative depolymerisation and solubilisation of pectic polysaccharides involved in cell-cell adhesion (BeMiller and Kumari, 1972; Keijbets and Pilnik, 1974). Softening of acidic fruit tissues upon heating can possibly be ascribed to acid hydrolysis of cell-wall polysaccharides (Krall and McFeeters, 1998; Waldron *et al.*, 2003).

Due to the depolymerisation and solubilisation of pectin at the intercellular connections during fruit ripening or thermal treatment, tissue failure characteristics evolve from cell rupture to cell separation (Waldron *et al.*, 1997; Waldron *et al.*, 2003; Sila *et al.*, 2007b; Van Buggenhout *et al.*, 2009). Cell separation here refers to failure of the tissue through the middle lamella/ intercellular joints, in other words: minimal cell breakage and release of cell contents. As a result, overripe and heated fruits and vegetables lose their juicy and crispy character (Waldron *et al.*, 2003; Van Buggenhout *et al.*, 2009).

To control textural changes and to pursue texture improvement of plant-based food products, pectin structural changes can be tailored *in situ* using specific processes ("pectin engineering"). Both enzymatic and non-enzymatic reactions can be influenced purposively (Waldron *et al.*, 2003; Van Buggenhout *et al.*, 2009). The most convenient way to direct pectin changes during processing is to control the enzymatic pectin conversions (mainly PME and PG) by inactivating the undesired enzymes or boosting the activity of the functionally important ones (e.g. in Duvetter *et al.*, 2009). To illustrate: one of the major techniques to enhance firmness of heat-treated fruits and vegetables is to strengthen the middle lamella matrix. This can be achieved by a controlled demethoxylation of

pectin by PME to stimulate the formation of salt-bridges between divalent cations and free carboxyl groups of the pectic chains (Van Buggenhout *et al.*, 2009).
The specific role of PME in a food technological context will be discussed in more detail in Section 1.2.5.

1.2 PECTIN METHYLESTERASE

Pectin methylesterase (PME, E.C. 3.1.1.11, CAZy class 8 of carbohydrate esterases (Cantarel *et al.*, 2009)) is an enzyme of either plant or microbial origin that catalyses the specific hydrolysis of the methyl-ester bond at C-6 of a GalA residue in the linear HG domain of pectin, thus altering the degree and pattern of methyl-esterification and releasing methanol and protons. The demethoxylation reaction is depicted in **Figure 1.4**. Through modification of its fine structure, PME affects pectin's functional properties, both in the plant cell wall and in pectin-containing food products. Consequently, the enzyme is of high interest for plant biologists as well as for food technologists.

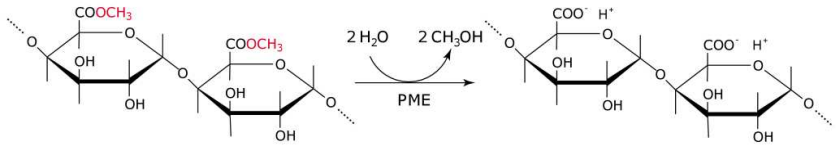

Figure 1.4. Demethoxylation reaction of pectin catalysed by PME (adapted from Micheli, 2001).

1.2.1 PME occurrence, properties and polymorphism

1.2.1.1 Occurrence and localisation

PMEs are ubiquitous enzymes (Pelloux *et al.*, 2007). They have been identified in all higher plants examined – in their fruits, leaves, stems as well as roots (Rexova-Benkova and Markovic, 1976; Markovic *et al.*, 2002; Benen *et al.*, 2003a). Plant PMEs are mainly associated with the cell wall by ionic interactions, and hence released on treatment with high ionic strength solutions or shifting the pH towards the alkaline region (Rexova-Benkova and Markovic, 1976; Bordenave, 1996). However, some soluble forms have been detected as well (Bordenave, 1996; Benen *et al.*, 2003a; Ciardiello *et al.*, 2004). Attempts have been made to visualise PMEs *in situ* at the plant tissular and ultrastructural level using polyclonal antibodies raised against flax PME in immunofluorescence and immunogold microscopy. The results indicated a heterogeneous distribution of PME and a colocalisation of PME with acidic pectins, but could not confirm whether the PMEs are directly attached to the pectins or only situated in their neighbourhood (Quentin *et al.*, 1997; Morvan *et al.*, 1998).
PMEs are also produced by phytopathogenic bacteria and fungi (Rexova-Benkova and Markovic, 1976; Markovic and Janecek, 2004) and by symbiotic micro-organisms during their interactions with plants (Lievens *et al.*, 2002). Finally, PME has been found in a few yeasts (Benen *et al.*, 2002).

1.2.1.2 Physicochemical properties

PMEs are medium-sized enzymes with a molar mass in the range of 25 to 54 kDa. They are active as monomers (Bordenave, 1996; Benen *et al.*, 2003a). Like many other cell-wall proteins (e.g., PG, PL), PMEs from eukaryotic origin may be glycosylated by attachment of glycans to the protein via the nitrogen of Asn (N-linked) or the oxygen of Ser or Thr (O-linked) (Bordenave, 1996; Warren *et al.*, 2002; Benen *et al.*, 2003a). However, only few glycosylated plant PMEs are actually reported (Ciardiello *et al.*, 2008).

The isoelectric pH (pI) of PME varies from as low as 3.1 for a fungal PME to 11 for a tomato PME (Benen *et al.*, 2003a). Most purified plant PMEs present neutral or alkaline pIs, explaining their tight association with the slightly acidic cell wall (Bordenave, 1996). Only a few studies have revealed the presence of acidic plant PMEs (Bordenave and Goldberg, 1993; Ding *et al.*, 2002). It was suggested, however, that some failure to detect acidic PMEs in plants may be related to the experimental conditions used for protein extraction, often including a step discarding the soluble plant tissue content (and, possibly, the weakly bound acidic PMEs) (Micheli, 2001). In contrast to plant PMEs, microbial PMEs often present more acidic pIs, although exceptions have been reported (Bordenave, 1996).

PMEs, especially those of plants, appear to be very sensitive to the ionic environment. For plant PMEs, cations are essential for enzymatic activity (Rexova-Benkova and Markovic, 1976; Moustacas *et al.*, 1991; Bordenave, 1996). Their activity increases with salt concentration up to an optimal concentration above which activity usually decreases (Nari *et al.*, 1991), with the optimal concentration depending on the nature of the cation (Micheli, 2001). It has been proposed that positive charges would interact with the free negatively charged carboxyl groups that are formed upon enzyme action and would otherwise trap the enzyme (since most plant PMEs have alkaline pIs, and are therefore positively charged even at slightly basic pHs). Monovalent cations would compete with cationic proteins for fixation on pectins, thus allowing enzyme liberation (Bordenave, 1996; Benen *et al.*, 2003a). The effect of divalent ions seems more complex, possibly due to ionic cross-link formation (Bordenave, 1996).

PMEs are also closely regulated by pH. The pH stability depends on the source of the enzyme, and the range for all PMEs stretches from pH 1 to pH 10 (Benen *et al.*, 2003a). The optimal pH of different PMEs is likely to vary substantially, as suspected from their wide pI ranges (Pelloux *et al.*, 2007). The most common alkaline plant PMEs may be poorly active at acidic pH values due to strong interactions between the positively charged enzyme and the free carboxyl groups of HG, the product of the enzymatic action. At basic pHs, alkaline PMEs might be released from their substrate because of electrostatic repulsion between free carboxyl groups and the negatively charged enzyme (Nari *et al.*, 1991).

1.2.1.3 Polymorphism

In many plants, multiple isoforms of PME are found both at the expression and genetic level. This large variety of PME isoforms is more pronounced in dicotyledonous than monocotyledonous species, and is not present in micro-organisms (Bordenave, 1996; Benen *et al.*, 2003a; Pelloux *et al.*, 2007). PME

isoforms are encoded by a large multigene family in all plant species analysed. For instance, analysis of the *Arabidopsis thaliana* genome has revealed 66 genes encoding (putative) PMEs (Wolf *et al.*, 2009).
PME isoforms all catalyse the same reaction (Micheli, 2001). However, they differ in pI (alkaline, neutral or acidic), molar mass, degree of glycosylation and/or catalytic properties (Bordenave, 1996; Benen *et al.*, 2003a; Bosch and Hepler, 2005). For instance, different pH optima and demethoxylation action patterns (cf. Section 1.2.3.2) have been demonstrated (Catoire *et al.*, 1998; Goldberg *et al.*, 2001; Markovic and Janecek, 2004).
Relative proportions of PME isoforms may vary greatly according to the developmental stage and the organ considered (Bordenave, 1996). Some isoforms are constitutively expressed throughout the plant tissues (Gaffe *et al.*, 1994; Giovane *et al.*, 1994; Micheli, 2001), whereas others are specific for one tissue and/or precise developmental stage, e.g., fruit ripening, microsporogenesis, germination, or stem elongation (Bordenave, 1996; Micheli *et al.*, 2000; Markovic and Janecek, 2004). Furthermore, PME isoforms can have stress-specific expression patterns, depending on environmental changes (Pelloux *et al.*, 2007).
Overall, the large number of PME isoforms in plants is likely to reflect the diversity of their role in the modification of the cell wall in various aspects of plant development (cf. Section 1.2.4) (Wolf *et al.*, 2009). Differential expression of PME isoforms, both spatially and temporarily, is believed to be a major mechanism in plants to regulate the endogenous PME activity (Bosch and Hepler, 2005).

1.2.2 PME structure

1.2.2.1 Primary structure

A high number of plant and microbial PMEs have already been sequenced, either by means of protein sequencing or sequencing of the PME genes (Markovic and Jornvall, 1986; Laurent *et al.*, 1993; Markovic *et al.*, 2002). Although strictly homologous, the enzymes appear to be quite divergent, with overall residue identity versus carrot PME ranging from ~85% (for some plant PMEs) to 20 - 30% (for some microbial PMEs) (Markovic and Jornvall, 1992; Jenkins *et al.*, 2001; Markovic *et al.*, 2002; Pelloux *et al.*, 2007) (cf. http://www.cazy.org/CE8.html and http://services.uniprot.org, 2010).
Comparison of amino acid sequences of more than 100 plant and microbial PMEs, both experimentally confirmed and putative enzymes, has shown that all PMEs contain five segments of high sequence similarity (representing the signature patterns characteristic for PME), six strictly conserved residues (three Gly residues, one Asp, one Arg and one Trp), and several highly conserved aromatic residues, which have all been shown to be functionally important (Markovic and Janecek, 2004; Pelloux *et al.*, 2007). Yet, significant differences between plant, fungal and bacterial PMEs were demonstrated, especially in terms of His, Cys and aromatic residues (Markovic and Janecek, 2004).
Also with regard to disulfide bridges, differences between various PMEs have been reported. For instance, the presence of two intrachain disulfide bridges was described for the main tomato PME (Markovic and Jornvall, 1992; D'Avino *et al.*, 2003), although refuted by Di Matteo *et al.* (2005). One disulfide bridge was

detected in the bacterial PME of *Erwinia chrysanthemi* (Jenkins *et al.*, 2001), whereas no disulfide bridges are thought to exist in carrot PME (Johansson *et al.*, 2002).
Based on the alignment of sequences of 70 representative PMEs, an evolutionary tree was build. The tree supports the division of PMEs into several phylogenetic clades: one fungal clade, one bacterial clade and eight plant clades (Markovic and Janecek, 2004).
It should be noted that the majority of *pme* genes in higher plants encode so-called *pre-pro*-proteins, in which the mature, active part of the protein is preceded by an N-terminal extension of variable length. This *pre-pro*-extension is presumed to be cleaved off before or during secretion to the apoplasm, where only the catalytic part is found (Micheli, 2001; Bosch and Hepler, 2005; Pelloux *et al.*, 2007). The *pre*-region (or signal peptide) is required for protein targeting to the endoplasmic reticulum (Micheli, 2001; Dorokhov *et al.*, 2006). The exact function of the *pro*-region is still under discussion, but an autoinhibitory activity towards the mature part (to prevent premature demethoxylation), a role as intramolecular chaperone for protein folding, or a role in targeting PMEs towards the cell wall have been hypothesised (Micheli, 2001; Bosch *et al.*, 2005; Dorokhov *et al.*, 2006). A classification of PMEs has been created, based on the absence (group 1) and presence (group 2) of the *pro*-domain (Pelloux *et al.*, 2007; Wolf *et al.*, 2009). PME proteins of bacteria and fungi do not contain any *pro*-region (Markovic and Janecek, 2004).

1.2.2.2 Three-dimensional structure

To date, the three-dimensional structure of the bacterial PME of *E. chysanthemi* (Jenkins *et al.*, 2001) and of the plant PMEs of carrot (Johansson *et al.*, 2002) and tomato (D'Avino *et al.*, 2003; Di Matteo *et al.*, 2005) have been elucidated.
All three enzymes show a high similarity in the overall folding topology, characterised by a right-handed parallel β-helix structure consisting of three parallel β-sheets (PB1, PB2 and PB3) with interconnecting loops (T1, T2 and T3) protruding from the helix core and forming the substrate-binding cleft (shown for carrot PME in **Figure 1.5A** and **1.5B**). The space inside the β-helix structure is essentially hydrophobic. The pectin binding site is situated in a long shallow cleft across the molecule, formed by the external loops. The central part of this cleft is lined by several aromatic residues, as is characteristic for carbohydrate binding sites. A pectin molecule in roughly 2_1-helix configuration (with the carboxymethyl groups pointing in different directions in successive carbohydrate residues) can be accommodated in this cleft (**Figure 1.5C**).
The putative active site (depicted for carrot PME in **Figure 1.6**) is located in the crevice (on the PB3 sheet) and contains several conserved amino acid residues: two Asp, two Glu and one Arg (Jenkins *et al.*, 2001; Johansson *et al.*, 2002; D'Avino *et al.*, 2003; Di Matteo *et al.*, 2005).
Superposition of the known PME structures of carrot, tomato and *E. chrysanthemi* (**Figure 1.7**) confirms the similarity of the overall folding topologies. Concurrently, it also reveals one major difference between the plant PMEs and the bacterial PME from *E. chysanthemi*, namely the shape of the substrate cleft, which has higher walls in the bacterial PME due to much longer loops (D'Avino *et al.*, 2003; Di Matteo *et al.*, 2005).

Remarkably, the 3D structure of PME differs from that of most esterases, having been found to adopt the common α/β hydrolase fold and to contain a catalytic Ser-His-Asp catalytic triad (Pickersgill and Jenkins, 2003). Instead, PME appears to be a carboxylate hydrolase with two Asp residues at the active site (Jenkins *et al.*, 2001), and possesses a folding topology similar to that found for other pectinases, such as PG (Pickersgill *et al.*, 1998), PL (Lietzke *et al.*, 1996) and PNL (Vitali *et al.*, 1998). The conservation of this unique topology among these enzymes strongly suggests that a complete set of different pectinases have evolved from the same ancestral gene (Benen *et al.*, 2003a).

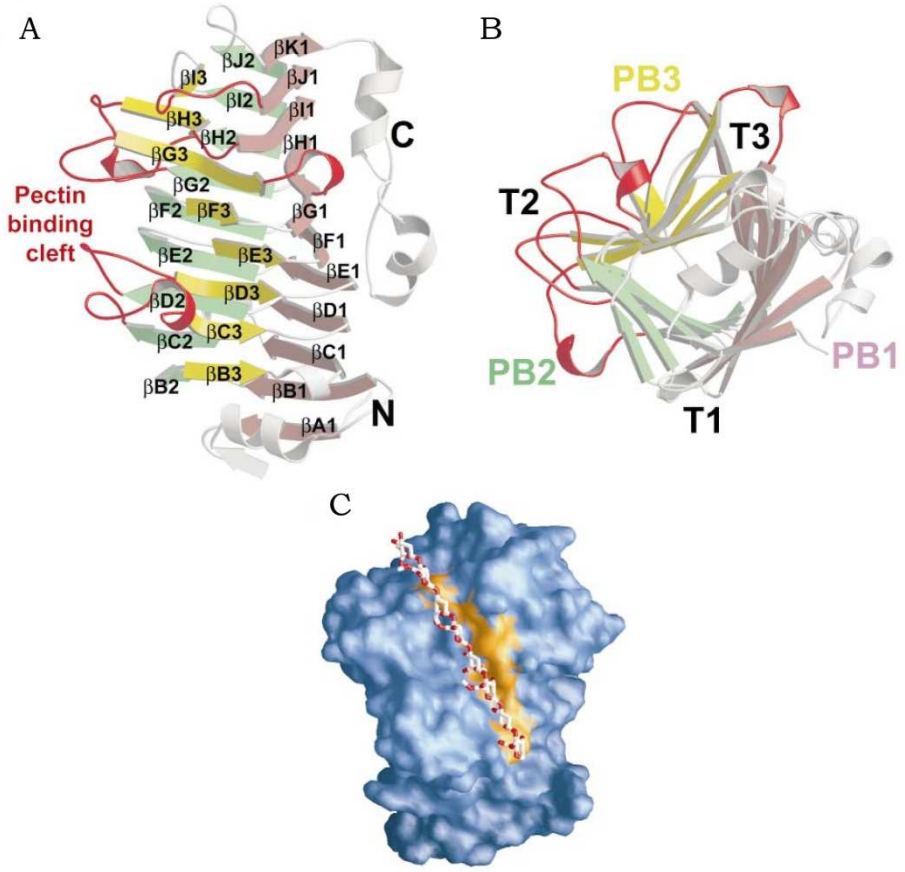

Figure 1.5. The structure of carrot PME (Johansson *et al.*, 2002). (A) The β-helix structure consisting of three parallel β-sheets PB1, PB2 and PB3 (coloured brown, green and yellow, respectively). Strands are numbered from βA1 to βK1 for sheet PB1, βB2 to βJ2 for sheet PB2 and βB3 to βI3 for sheet PB3. Loops forming the pectin binding cleft are in red; parts not participating in the β-sheets are in white. (B) View of the structure rotated 90° around the *x*-axis, looking down from the N-terminal side. Colouring is the same as above. The location of PB1, PB2 and PB3 as well as the loops (T1, T2 and T3) between the sheets are indicated. (C) Surface representation of the pectin binding cleft. Loops from T2 and T3 form the walls of a cleft running across the molecule. Aromatic residues (in orange) are lining the cleft. A pectin molecule is modelled in approximately 2_1-helix conformation.

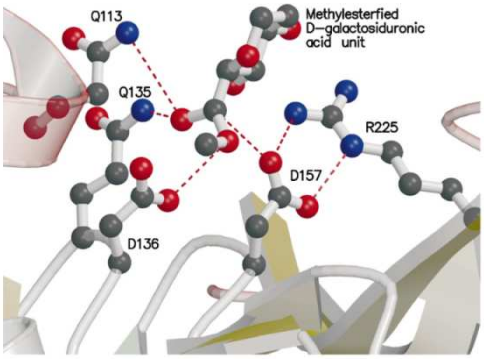

Figure 1.6. The active site of carrot PME (Johansson *et al.*, 2002). The substrate, a methyl-esterified D-GalA unit, is modelled in the active site. The five catalytically important residues (Gln113, Gln135, Asp136, Asp157 and Arg225) are depicted.

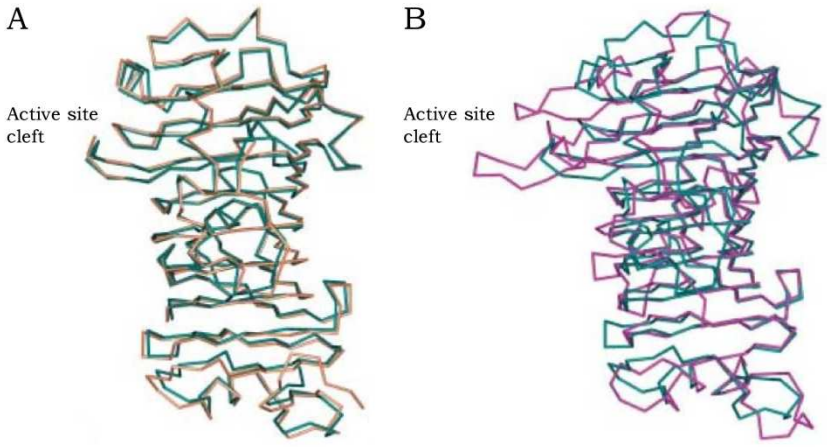

Figure 1.7. Comparison of the known 3D structures of PME (adapted from Di Matteo *et al.*, 2005). (A) Overlay of tomato (green) and carrot (orange) PME. Structures are almost completely superimposable. (B) Overlay of tomato (green) and *E. chrysanthemi* (violet) PME. Although the β-helices are completely superimposable, main differences are located in the length of the loops protruding out from the β-helix in proximity of the putative active site cleft.

1.2.3 PME catalytic activity

1.2.3.1 Reaction mechanism

PME catalyses the specific hydrolysis of the methyl-ester bond at C-6 of a GalA residue in pectin, thus forming a dissociable carboxyl function on the pectin chain and releasing methanol. Free carboxyl groups in the vicinity of the active site appear to be required for PME action (Bordenave, 1996).

Based on the structure of the catalytic site of (carrot) PME (**Figure 1.6**), Johansson *et al.* (2002) proposed a mechanism of PME action, which was later confirmed by Di Matteo *et al.* (2005). Asp157, stabilised by a hydrogen bond to

Arg225, performs a nucleophilic attack on the ester bond of the carboxymethyl group of HG. In analogy with other hydrolytic mechanisms, a tetrahedral, negatively charged intermediate is formed, that is stabilised by an anion hole formed by the two conserved glutamine side chains (Gln113 and Gln135). Subsequently, Asp136 likely acts as a proton donor in the cleavage step where methanol is released. The active site is restored via extraction of a proton from an incoming water molecule by the resulting carboxylate group of Asp136, cleaving the covalent bond between the substrate and Asp157. By its interaction with the aromatic rings, the HG chain is held in place within the substrate cleft, awaiting the next demethoxylation step.
In an alternative mechanism suggested by Jenkins *et al.* (2001), an active site Asp is thought to be responsible for the deprotonation of a catalytic water molecule, rather than a direct nucleophile attack by an Asp residue.

1.2.3.2 Mode of action

While non-enzymatic demethoxylation is a random process (cf. Section 1.1.2.1), enzymatic demethoxylation by PME proceeds through a more ordered mechanism. To date, the mode of action (or action pattern) of PME on HG remains controversial (Wolf *et al.*, 2009). It is generally believed that PMEs with an alkaline pI (like most plant PMEs) remove methyl-esters in a processive block-wise fashion, creating long contiguous stretches of de-esterified GalA residues on the pectin, whereas acidic PMEs (like many microbial PMEs and few plant PMEs) demethoxylate pectin more randomly, resulting in a rather random distribution of the de-esterified GalA units (Markovic and Kohn, 1984; Limberg *et al.*, 2000; Ralet *et al.*, 2001; Duvetter *et al.*, 2006b). However, this picture is simplified, as it is believed that other factors, such as pH, initial DM and pattern of methoxylation (PM) of the pectin, can influence the mode of action: the action pattern of some isoforms has been shown to be pH-dependent, and, at a given pH, some isoforms are more effective than others on highly methyl-esterified pectins (Catoire *et al.*, 1998; Denès *et al.*, 2000b; Goldberg *et al.*, 2001; Kim *et al.*, 2005).
Since not only the amount but also the distribution of methyl-esters (i.e., the PM) determines pectin's functional properties, both in the plant cell wall and in certain food products (e.g., susceptibility towards enzymatic depolymerisation by PG or PL, and capacity of calcium-pectin gel formation) (Willats *et al.*, 2001a; Willats *et al.*, 2001b), the mode of action of PME has been of interest to both plant scientists and food technologists.

1.2.3.3 Inhibition

Several compounds, both proteinaceous and non-proteinaceous, have been reported to exert an inhibitory effect on PME. Besides end-product inhibition (by polygalacturonic acid) and a number of general inhibiting substances, such as iodine, detergents (e.g., SDS), tannin, sugars (e.g., sucrose and glucose) and glycerol (Rexova-Benkova and Markovic, 1976; Benen *et al.*, 2003a), several specific PME inhibitors from various plant sources have been described. An overview is given in **Table 1.1**. The proteinaceous PME inhibitor (PMEI) found in kiwi fruit (and, to a minor extent, the related PMEIs encoded by *Arabidopsis*

thaliana and *Capsicum annuum* genes) will be discussed more elaborately in Section 1.3.

Table 1.1. Overview of the specific PME inhibitors described in various plant sources.

Source	Nature	Reference
Kiwi fruit (*Actinidia deliciosa*)	Protein (~16.3 kDa)	Balestrieri *et al.* (1990)
Potato tuber (*Solanum tuberosum*)	Side-branched uronic acid (~200 kDa)	McMillan and Perombelon (1995)
Jelly fig achenes (*Ficus awkeotsang*)	Small polypeptides (~3.5 - 4.5 kDa)	Jiang *et al.* (2002)
Rubbery banana (*Musa sapientum*)	Not defined	Wu *et al.* (2002)
Arabidopsis *(Arabidopsis thaliana)*	Protein (related to kiwi PMEI)	Wolf *et al.* (2003)
Pepper leaves (*Capsicum annuum*)	Protein (related to kiwi PMEI)	An *et al.* (2008)
Green tea (*Camellia sinensis*)	Catechins	Lewis *et al.* (2008)

1.2.4 PME role *in vivo*

As a major component of the plant cell wall, pectin contributes to the mechanical strength of the wall and to adhesion between cells (cf. Section 1.1.1.4). Endogenous plant PMEs are involved in the metabolism of the cell-wall pectin and, hence, take part in important physiological processes associated with both vegetative and reproductive plant development (Pelloux *et al.*, 2007; Wolf *et al.*, 2009), including cell-wall extension and stiffening, cellular adhesion and separation, fruit ripening, wood development, stem elongation, leaf growth, microsporogenesis, pollen formation, pollen tube growth and seed germination (Tieman and Handa, 1994; Wen *et al.*, 1999; Micheli, 2001; Bosch *et al.*, 2005; Pelloux *et al.*, 2007). In addition, plant PMEs are associated with plant defence responses upon biotic or abiotic stresses, either directly through interaction with virulence factors (e.g., binding of PME to movement proteins of some viruses), or indirectly via the products of the reactions they catalyse (methanol, protons and oligogalacturonides) (Dorokhov *et al.*, 1999; Ridley *et al.*, 2001; Pelloux *et al.*, 2007).

Many of the *in vivo* roles of plant PMEs are thought to rely on some basic principles. Through demethoxylation, pectins can aggregate into calcium-linked gel structures, increasing wall firmness and influencing porosity (Willats *et al.*, 2001b). On the other hand, the action of PME makes pectins more susceptible to depolymerisation by PGs and PLs, contributing to softening of the cell wall (Brummell and Harpster, 2001; Wakabayashi *et al.*, 2003). Moreover, PME action produces protons and, hence, results in a local decrease of the cell-wall pH. It has been proposed that this acidification could reduce the PME activity (at least of a set of PME isoforms), while activating other cell-wall enzymes (such as PG

and PL), thus loosening the cell wall and facilitating a growth pulse (Moustacas *et al.*, 1991; Bordenave, 1996; Bosch and Hepler, 2005).
Considering the wide range of biological functions of plant PMEs, it is not surprising that plants have developed a complex regulatory network to carefully orchestrate PME activity in order to fine-tune properties of the pectin network. The precise nature of the control mechanism *in vivo* is still poorly understood, but it is believed to entail differential expression, both temporarily and spatially, of various isoforms (cf. Section 1.2.1.3), plant hormones (such as auxins, abscisic acid and gibberellic acid) (Micheli, 2001), environmental conditions (e.g., subtle changes of cell-wall local pH), and PME inhibition (cf. Section 1.2.3.3) (Giovane *et al.*, 2004; Bosch and Hepler, 2005; Wolf *et al.*, 2009).
The role of the PMEs produced by plant pathogenic micro-organisms (fungi and bacteria) during plant infection seems obvious: PME activity facilitates pectin degradation by the concomitantly secreted depolymerising enzymes PG and PL, thus causing a synergistic break-down of the cell-wall barrier (Bordenave, 1996; Jayani *et al.*, 2005).

1.2.5 Relevance of PME in the food industry

PME is one of the key enzymes in the context of fruit and vegetable processing. On the one hand, endogenously present plant PME can positively or negatively affect structural quality of plant-based foods (cloud stability, viscosity, texture). On the other hand, PME, together with other pectinases, finds (actual or potential) applications as an exogenous processing aid.

1.2.5.1 PME in relation to cloud stability

It is well-established that endogenous plant PME compromises cloud stability of many fruit and vegetable juices, e.g., from citrus, apple, carrot and tomato (Krop and Pilnik, 1974; Versteeg *et al.*, 1980; Sims *et al.*, 1993; Laratta *et al.*, 1995; Beveridge, 2002). Although cloud or turbidity loss is a rather complex phenomenon of which the mechanism is not yet fully understood, the exact features differing for different plant sources, the role played by PME is clear (Croak and Corredig, 2006). By its action, blocks of free carboxylic acids on adjacent pectin molecules are formed, which can be cross-linked by endogenous divalent cations (mostly calcium), increasing the apparent molar mass of aggregates, reducing their solubility and leading to juice cloud precipitation (Krop and Pilnik, 1974; Baker and Cameron, 1999). Cloud loss is considered a serious quality defect of juices, determining consumer acceptance, not only because of the appearance (i.e., phase separation), but also since sensory properties such as colour, flavour, and texture (i.e., mouthfeel), associated with the cloud particles, are reduced (Baker and Bruemmer, 1972; Klavons *et al.*, 1994; Baker and Cameron, 1999; Ackerley *et al.*, 2002).
Cloud stabilisation is traditionally accomplished by heating the juice to inactivate PME. However, severe conditions (even above those required to control microbial growth) are often required, affecting nutritional and organoleptic properties of the juice (Eagerman and Rouse, 1976; Versteeg *et al.*, 1980; Denès *et al.*, 2000a; Ludikhuyze *et al.*, 2003). Alternative methods have been proposed, such as PME inactivation by high hydrostatic pressure processing (Ogawa *et al.*, 1990; Ly-

Nguyen *et al.*, 2002), PME inhibition by frozen storage or by addition of a specific PME inhibitor (cf. Section 1.3) (Castaldo *et al.*, 1991), or degradation of the PME substrate using PG or PL (Baker and Bruemmer, 1972).

1.2.5.2 PME in relation to texture of plant-based foods

Pectin's structural characteristics, besides other factors, are believed to play an important role in the texture of fruits and vegetables (cf. Section 1.1.3.2). Consequently, the action of PME on pectin affects the textural quality of plant-derived food products, either favourably or deleteriously, depending on the product at hand. Different underlying mechanisms can be distinguished.

First, demethoxylated pectin becomes a substrate for PGs (and PLs), enzymes that catalyse the depolymerisation of the pectin chain, inducing loss of textural integrity of tissue systems (Van Buren, 1979), also thought to occur during fruit ripening (Waldron *et al.*, 2003; Brummell, 2006). This pectin fragmentation may also cause a viscosity or consistency loss in, for instance, pastes and purées of plant sources with high levels of endogenous PG (e.g., tomato) (Lopez *et al.*, 1997; Crelier *et al.*, 2001).

Second, pectin with a low degree of methyl-esterification can cross-link via divalent ion bridges to form intermolecular networks, promoting gel formation (Van Buren, 1979). In intact plant tissues, cell-wall reinforcement and, hence, an increase in firmness will take place. This strengthening effect is often deliberately pursued through controlled stimulation of endogenous PME activity, e.g., by means of a mild temperature or hydrostatic pressure pretreatment, prior to the actual conservation process (Ng and Waldron, 1997; Sila *et al.*, 2004; Van Buggenhout *et al.*, 2009). Supplementing these pretreatments by calcium soaking further increases the firmness improvement (Sila *et al.*, 2004). In cases where a (thermal) pretreatment would activate detrimental enzymes or where only low amounts of endogenous PME are present, application of exogenous PME (e.g., through infusion) can be performed (Duvetter *et al.*, 2005a; Van Buggenhout *et al.*, 2009). Formation of calcium-pectin cross-links may also improve or preserve the viscosity of liquid plant-based products (Porretta, 1996).

Third, demethoxylation of pectin reduces its sensitivity to chemical β-eliminative depolymerisation, occurring during heating and associated with heat-induced softening of many fruits and vegetables (Keijbets and Pilnik, 1974; Van Buren, 1979; Sajjaanantakul *et al.*, 1989). Thus, a reduction in DM by PME stimulation through pretreatment has a second texture-conserving effect, reducing the vulnerability to thermal softening.

1.2.5.3 Exogenous PME

The largest industrial application of exogenous PME and other pectinases as processing aids is in the fruit juice industry. Mostly, pectinases derived from food-grade fungi (*Aspergillus niger* and *A. aculeatus*) are used. On the one hand, extraction yields can be increased and extraction times reduced by enzymatic degradation of the pectin (e.g., by a combination of PME and PG), reducing viscosity and improving the subsequent mechanical separation of juice and pulp particles by pressing, sieving or centrifugation. An additional advantage is often a better extraction of pigments and aroma. On the other hand, pectinases are useful for juice clarification, either by the stimulated formation of a removable

precipitate (e.g., through addition of PME and calcium, forming insoluble calcium-pectin complexes according to the principle outlined in Section 1.2.5.1), or by combined enzymatic breakdown of the pectins to lower the viscosity and to enhance mechanical removal of the suspended matter (mostly by filtration). Obviously, the concrete enzyme treatment depends on the plant source and on the intended type of juice (e.g., cloudy versus clear juice). Additionally, PME and other pectinases are employed in related processes, such as the production of wine, cider, fruit concentrates and jams, and liquefaction, where a complete degradation of the cell wall is aimed at (Alkorta *et al.*, 1998; Kashyap *et al.*, 2001; Benen *et al.*, 2003b; Sorensen *et al.*, 2004; Jayani *et al.*, 2005).
As mentioned in the previous section, exogenous PME may be applied in texture engineering of thermally processed intact fruits and vegetables, e.g., via enzyme infusion.
PMEs can also be useful for the commercial production of tailor-made pectins for specific applications. As sketched in Section 1.1.3.1, pectin is often used as food additive, mainly because of its gelling properties. However, its functionality is highly dependent on the degree and pattern of methoxylation (e.g., LM versus HM pectins), which can be modified by PMEs with specific modes of action (Savary *et al.*, 2003; Benen *et al.*, 2003a).
Finally, pectinases, among which PME, are used for numerous other applications, also outside the food industry, e.g., in textile processing, retting and degumming of fiber crops, pectic waste water treatment (e.g., from the citrus-processing industry), paper making, animal feed production, coffee and tea fermentation, and oil extraction (Kashyap *et al.*, 2001; Jayani *et al.*, 2005).

1.3 PECTIN METHYLESTERASE INHIBITOR

Over the years, several compounds have been identified that exert an inhibitory activity on PME (cf. Section 1.2.3.3). The best described PME inhibitor (PMEI) so far is the proteinaceous inhibitor discovered in kiwi fruit by Balestrieri *et al.* (1990). More recently, database searches indicated that homologous sequences are present in a number of other plants as well (cf. http://services.uniprot.org, 2010).
Due to its capacity to inhibit the action of plant PME, PMEI probably plays an important physiological role in PME regulation in plants. For the same reason, PMEI possesses several potential applications in a food technological context.

1.3.1 PMEI occurrence

PMEI was originally discovered in green kiwi fruit (*Actinidia deliciosa*) (Balestrieri *et al.*, 1990). Active PMEI was only found in the fully mature stage, whereas it was undetectable in the unripe fruit (Balestrieri *et al.*, 1990; Giovane *et al.*, 1995). Later, it was confirmed that the relative expression levels of the PMEI genes in kiwi fruit increase with the progression of fruit maturation (Irifune *et al.*, 2004). Unlike PME, PMEI is not tightly bound to cell walls and can be extracted easily from the fruits at low ionic strength (Balestrieri *et al.*, 1990; Camardella *et al.*, 2000). Remarkably, PMEI appears as one of the highest represented proteins in the aqueous extract from the fruit (Balestrieri *et al.*, 1990).

Attempts to detect PMEI in fruits from several other plant species were unsuccessful (Scognamiglio *et al.*, 2003; Bellincampi *et al.*, 2004), possibly due to a tight binding to its own PME, thus escaping biochemical detection (Giovane *et al.*, 2004). However, PMEI genes encoding functional proteins were identified in *Arabidopsis thaliana* (Wolf *et al.*, 2003; Raiola *et al.*, 2004) and pepper (*Capsicum annuum*) (An *et al.*, 2008), and their expression demonstrated (Wolf *et al.*, 2003; Pina *et al.*, 2005; An *et al.*, 2008). These findings led authors to suggest that the protein may be ubiquitously expressed in higher plants (Camardella *et al.*, 2003; Giovane *et al.*, 2004; Röckel *et al.*, 2008; Wolf *et al.*, 2009).

1.3.2 PMEI structure

1.3.2.1 Primary structure and homology

The primary structure of kiwi PMEI was determined by direct protein analysis (Camardella *et al.*, 2000). The total sequence (**Figure 1.8**) consists of a single polypeptide chain, comprising 152 -predominantly acidic- amino acid residues, yielding a molar mass of 16277 Da and an acidic pI (reported estimates ranging from <3.5 to 4.8) (Balestrieri *et al.*, 1990; Marquis and Bucheli, 1994; Camardella *et al.*, 2000; Camardella *et al.*, 2003; Ly-Nguyen *et al.*, 2004; Ciardiello *et al.*, 2008). It contains five Cys residues, four of which are connected by two disulfide bridges (first to second and third to fourth), believed to play a considerable role in the maintenance of the protein structure. The fifth Cys residue has a free thiol group. Neither Met nor Trp residues are present (Camardella *et al.*, 2000).

E N H L I S E I **C** P K T R N P S L **C** L Q A L E S D P R S A S K D L K G L G Q F S
(20) (40)

I D I A Q A S A K Q T S K I I A S L T N Q A T D P K L K G R Y E T **C** S E N Y A D
(60) (80)

A I D S L G Q A K Q F L T S G D Y N S L N I Y A S A A F D G A G T **C** E D S F E G
(100) (120)

P P N I P T Q L H Q A D L K L E D L **C** D I V L V I S N L L P G S
(140) (152)

Figure 1.8. Amino-acid sequence of PMEI from kiwi fruit (adapted from Camardella *et al.*, 2000). The five Cys residues are represented in bold; those involved in disulfide bonds are underlined.

The protein shows (micro)heterogeneities at the N-terminus (part of the polypeptide chains has an additional Ala residue) and at five positions along the amino acid sequence (Ala/Ser56, Tyr/Phe78, Ser/Asn117, Asn/Asp123 and Val/Ile142). The detection of different amino acid residues at well-defined positions along the polypeptide chain can be attributed to the presence of multiple PMEI isoforms in the kiwi fruit, whereas the presence of two forms, having or lacking the initial Ala residue, can be ascribed to an incomplete processing of the protein (Camardella *et al.*, 2000; Mattei *et al.*, 2002; Giovane *et al.*, 2004). The latter finding points towards the probable existence of a signal sequence, which is cleaved off by a proteolytic agent during the maturation of the protein, and is in line with the observation that PMEI is synthesised as an inactive precursor of higher molar mass, subsequently transformed into the active protein during the fruit ripening process (Giovane *et al.*, 1995).

Considering that PMEI interacts with PME, which is localised in the cell wall, it is probable that a signal sequence is required to direct the protein towards its final cellular localisation (Camardella *et al.*, 2000).
More recently, several full-length cDNAs encoding kiwi PMEI isoforms were isolated from a kiwi fruit cDNA library (Irifune *et al.*, 2004; Mei *et al.*, 2007), confirming the above mentioned amino acid sequence, including some of the micro-heterogeneities. This finding indicates that there exists a family of genes coding multiple isoforms of PMEI in kiwi fruit. The complete coding sequences of the entire cDNAs show an N-terminal extension of 32 amino acid residues, due to the presence of a signal peptide required for the extracellular targeting of the protein, as predicted earlier (Giovane *et al.*, 2004; Irifune *et al.*, 2004).
A comprehensive database search revealed sequence homology of PMEI with plant invertase inhibitors (INHs). INHs are apoplasmic and vacuolar proteins of about the same size as PMEI that specifically inhibit plant invertases, enzymes playing central roles in the sucrose metabolism in higher plants. The overall amino acid residue identity is low, ranging between 25 - 30%, but PMEI and INHs share the same pattern of four Cys residues, involved in disulfide bridges. Both inhibitors have exclusive target specificity (Camardella *et al.*, 2000; Scognamiglio *et al.*, 2003; Camardella *et al.*, 2003; Bellincampi *et al.*, 2004; Rausch and Greiner, 2004).
In addition, the kiwi PMEI sequence shows significant similarity with the N-terminal non-catalytic *pro*-region of many plant PMEs (cf. Section 1.2.2.1). Again, the four Cys residues engaged in disulfide bridges are conserved. The observed similarity is in favour of the hypothesis that the *pro*-peptide has an autoinhibitory function towards its own (premature) PME, as suggested earlier (Micheli, 2001). It is conceivable that, in certain plants, a genome rearrangement during evolution has produced the physical separation of the inhibitory domain initially linked to the catalytic domain, leading to a separate *pmei* gen (like it is the case in kiwi fruit) and a distinct protein with PME inhibitory activity (Camardella *et al.*, 2003; Bellincampi *et al.*, 2004; Giovane *et al.*, 2004; Wolf *et al.*, 2009).
Furthermore, database search identified a large family of *Arabidopsis thaliana* sequences closely related to the kiwi PMEI sequence (Pelloux *et al.*, 2007). Two sequences were already shown to encode functional PMEIs, named AtPMEI-1 and AtPMEI-2 (Wolf *et al.*, 2003; Raiola *et al.*, 2004). Both proteins (of 151 and 148 amino acid residues, respectively) share about 38% identity at the amino acid level with kiwi PMEI, and, like the latter, show an N-terminal signal peptide and five conserved Cys residues, the first four of which engaged in disulfide bridges (Raiola *et al.*, 2004). Only very low expression of both isoforms was found in most *Arabidopsis* tissues, except for the flowers and the pollen (Wolf *et al.*, 2003; Pina *et al.*, 2005).
On the basis of amino acid sequence similarity and Cys residue conservation, a large protein family, including kiwi PMEI, INHs and other related proteins, has been identified, all showing the same structural motive (Giovane *et al.*, 2004).

1.3.2.2 Three-dimensional structure

The three-dimensional structure of kiwi PMEI was determined at 1.9 Å resolution, using a synthetic gene constructed on the basis of the amino acid

sequence of PMEI (cf. previous section) and expressed in *Pichia pastoris* (Di Matteo *et al.*, 2005). The structure is represented in **Figure 1.9**.
As already indicated by circular dichroism measurements (Camardella *et al.*, 2000; Scognamiglio *et al.*, 2003), kiwi PMEI is almost all helical. It folds in an up-and-down four helical bundle in which the helices (α1, α2, α3 and α4) align in an antiparallel manner. The interior of the bundle is stabilised by hydrophobic interactions and by a disulphide bridge, connecting helices α2 and α3. The N-terminal region, composed of three short and distorted helices (αa, αb and αc), extends outside the central domain and lines roughly parallel to the plane defined by the helices α1 and α4. A disulphide bridge connects αa and αb (Di Matteo *et al.*, 2005).

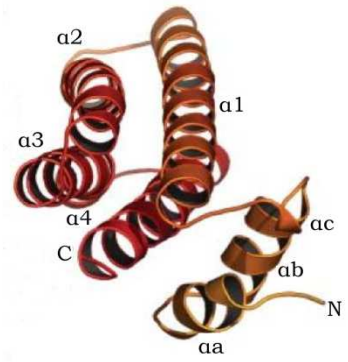

Figure 1.9. Three-dimensional structure of kiwi fruit PMEI (adjusted from Di Matteo *et al.*, 2005). The α-helices of the four-helix bundle are indicated as α1 to α4, whereas the helices of the N-terminal region are named αa, αb and αc.

The topology of kiwi PMEI is quite similar to the one of *Arabidopsis* PMEI (AtPMEI), elucidated by Hothorn *et al.* (2004), at least in the bundle. Significant differences are located in the N-terminal extension. The N-terminal region of kiwi PMEI folds back and packs with the bundle through hydrophobic interaction, whereas the N-terminal extension of AtPMEI packs against the bundle of another molecule, resembling a molecular handshake of the two extensions and forming a PMEI dimer. The different topology of the two inhibitors is probably due to the presence of different residues at the same position (Hothorn *et al.*, 2004; Di Matteo *et al.*, 2005).

1.3.3 PMEI inhibitory capacity

1.3.3.1 Specificity

The PME inhibitor from kiwi fruit is specific for PME. It is not active towards other (poly)saccharide-degrading enzymes, such as PG, amylase and invertase (Balestrieri *et al.*, 1990; Camardella *et al.*, 2000). Kiwi PMEI inhibits successfully the activity of a wide range of plant PMEs (e.g., orange, apple, tomato, kiwi, kaki, potato, apricot, banana, cucumber, strawberry, flax) (Balestrieri *et al.*, 1990; Giovane *et al.*, 1995; Ly-Nguyen *et al.*, 2004; Ciardiello *et al.*, 2004; Dedeurwaerder *et al.*, 2009), whereas it is ineffective against all microbial PMEs

assayed so far, fungal as well as bacterial (D'Avino *et al.*, 2003; Giovane *et al.*, 2004; Duvetter *et al.*, 2005b). Notably, kiwi PMEI had no effect on the activity of a plant PME recently purified from *Arabidopsis thaliana* (Dedeurwaerder *et al.*, 2009).
A similar specificity (i.e., active against various plant PMEs but insensitive to microbial PMEs and invertase) was observed for the two recombinant *Arabidopsis* PMEIs (Wolf *et al.*, 2003; Raiola *et al.*, 2004).

1.3.3.2 Mode of action of the inhibitor

Inhibition of PME by PMEI occurs through the formation of an inactive stoichiometric 1:1 complex between enzyme and inhibitor. The interaction is noncovalent and reversible (e.g., by means of high salt and high pH conditions) (Balestrieri *et al.*, 1990; Giovane *et al.*, 1995). The stability of the complex is strongly influenced by pH, the actual effect differing for PMEs from different plant sources (Balestrieri *et al.*, 1990; Marquis and Bucheli, 1994; Mattei *et al.*, 2002; Ly-Nguyen *et al.*, 2004; Ciardiello *et al.*, 2004).
Di Matteo *et al.* (2005) elucidated the three-dimensional structure of the complex between kiwi PMEI and the most abundant PME isoform from tomato fruit (at 1.9 Å resolution) (**Figure 1.10**). PME and PMEI form a complex in which the inhibitor covers the shallow cleft of the enzyme where the putative active site is located (cf. Section 1.2.2.2), an observation that confirms the earlier indications based on fluorescence-quenching experiments (D'Avino *et al.*, 2003). The four-helix bundle of PMEI packs roughly perpendicular to the parallel β-helix of PME by interacting with three (α2, α3 and α4) out of four helices of the bundle in proximity of the putative active site. Contrary to what was proposed for AtPMEI (Hothorn *et al.*, 2004), the N-terminal region of kiwi PMEI is only poorly involved in the formation of the complex and may play a role in the structural stability of the inhibitor (Di Matteo *et al.*, 2005). Neither PME nor PMEI undergo dramatic conformational changes upon complex formation (Camardella *et al.*, 2003; Di Matteo *et al.*, 2005).

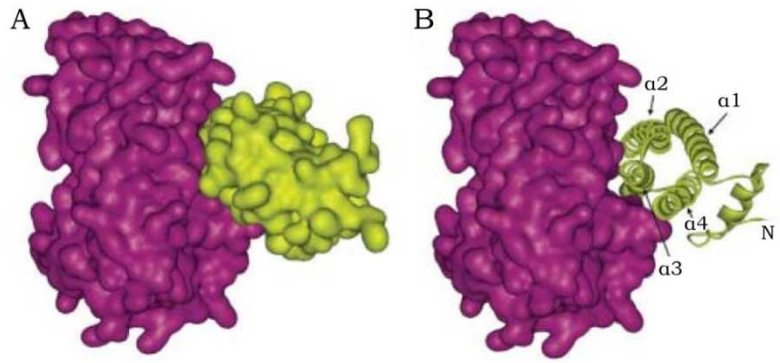

Figure 1.10. Three-dimensional structure of the complex between (tomato) PME and kiwi PMEI (according to Di Matteo *et al.*, 2005). (A) Representation of the molecular surface of the enzyme (violet) and the inhibitor (green) in the complex; (B) Same view as in A, showing the molecular surface of PME and a ribbon diagram of PMEI. The α-helices α2, α3 and α4 of the inhibitor fit into the substrate binding cleft of the enzyme.

The protein-protein interface is fairly large (buried surface of 2208 Å^2), compared to the average interface area reported for noncovalent protein complexes (1600 ± 400 Å^2) (Lo Conte *et al.*, 1999), and displays a high polar character. No extended zones of hydrophobic interactions are present, whereas more than half of the buried surface arises from polar and charged atoms. Such a polar character of the interface is typical of non-obligate complexes formed by soluble proteins, which need to expose a hydrophilic surface in their uncomplexed form (Jones and Thornton, 1996). The formation of the complex is mediated by a high number of direct and water-mediated H-bonds. Fifty residues (23 on PME and 27 on PMEI) establish molecular contacts. Twenty-two of these are engaged in H-bonds and four form salt bridges. Residues of PME forming contacts are mostly located in the proximity of the putative pectin binding site. The catalytically important residues (two Asp, two Glu and one Arg) do not establish contacts with the inhibitor, while three aromatic residues responsible for substrate binding interact with PMEI (Di Matteo *et al.*, 2005).
Based on the structure, a mode of action of the inhibitor on PME can be inferred. On the one hand, PMEI covers the active site cleft preventing the access of the substrate, while on the other hand, it impedes the interactions that are necessary for binding the substrate to the enzyme (Di Matteo *et al.*, 2005).
Modelling of the interaction between kiwi PMEI and kiwi PME showed that the binding site is the same as reported for tomato PME. However, a few substitutions in the amino acid sequence of kiwi PME provide additional salt interactions, connecting the external loops of PME to the inhibitor (Ciardiello *et al.*, 2008). This result suggests that the structure described for the PMEI - tomato PME complex is quite representative, but specific features can be expected for different PME sources. Meanwhile, it indicates that different structural features among plant PMEs (e.g., related to the ionisation state of specific groups) may explain different affinities or pH dependences of complex formation.
The structure of the PME-PMEI complex provides a possible explanation for the lack of inhibition of PMEI on non-plant PMEs. In the bacterial PME from *E. crysanthemi*, the putative binding site cleft is much deeper than in plant-derived PMEs. It is conceivable that the external loops of the bacterial enzyme (cf. Section 1.2.2.2) create a steric hindrance that prevents the interaction with the inhibitor (D'Avino *et al.*, 2003; Di Matteo *et al.*, 2005). On the other hand, the amino acid sequence alignment of PMEs from tomato, carrot and the fungus *A. aculeatus* reveals that almost all of the residues important for the interaction of tomato PME with the inhibitor are conserved in plant PMEs but not in the fungal enzyme (Di Matteo *et al.*, 2005). Moreover, the lack of inhibition of the atypical plant PME from *Arabidopsis* by kiwi PMEI is possibly due to a β-strand outside the core structure of PME, matching the position of the external loop found in *E. chrysanthemi* PME (Dedeurwaerder *et al.*, 2009).

1.3.4 PMEI role *in vivo*

The role of PMEI in plants is not yet fully clarified. In contrast to other inhibitors of cell-wall degrading enzymes that inhibit microbial enzymes (e.g., PGIP), PMEI is specific to plant PMEs. It is therefore conceivable that its physiological role lies in the modulation of the endogenous PME activity during plant growth and

development (for the *in vivo* role of PME, see Section 1.2.4) (Mattei *et al.*, 2002; Bellincampi *et al.*, 2004; Juge, 2006). However, a role in plant defence against pathogen infection cannot be excluded. On the one hand, PME is reported to be involved in the systemic spread of certain viruses through the plant, acting as a cell-wall receptor of the virus movement protein. Consequently, PMEI might hamper virus propagation by forming PME-PMEI complexes. On the other hand, it is widely accepted that highly methyl-esterified pectins are less susceptible to the action of PG and PL. By inhibiting the endogenous PME and maintaining the pectin in a high-methoxylated form, PMEI might indirectly play a role in plant defence against pathogen attack by limiting the action of microbial pectin-degrading enzymes (Bellincampi *et al.*, 2004; Juge, 2006; Lionetti *et al.*, 2007). The latter hypothesis was clearly demonstrated by means of transgenic plants with overexpressed PMEI, showing a decreased PME activity, an increased pectin DM and a higher resistance to fungal infection (Lionetti *et al.*, 2007).
Since functional PMEIs were recently identified in several species, including *Arabidopsis*, and their expression demonstrated (mainly in flowers and pollen), PMEIs are assumed to provide an effective post-translational control mechanism of PME. However, so far, studies actually describing the precise role of their interplay with PMEs in plant development are scarce (Wolf *et al.*, 2009). Some recent studies on pollen tube suggest that, presumably, the specific co-regulation and interaction of given PME and PMEI isoforms are of the utmost importance in controlling the DM of pectins, thus modifying cell-wall mechanical properties during growth (Juge, 2006; Röckel *et al.*, 2008; Peaucelle *et al.*, 2008).

1.3.5 Relevance of PMEI in the food industry

Based on the strong interaction between PMEI and plant PMEs, several potential applications of the PME inhibitor have been proposed to date.
First of all, PMEI could be employed as a technological adjuvant in processes where the control of endogenous plant PME activity is critical. As outlined in Section 1.2.5, PME is responsible for a number of commercially deleterious effects on plant-based foods, such as cloud loss in fruit and vegetable juices and consistency loss in, e.g., pastes and purées. The addition of PMEI was proposed to inhibit undesirable PME and to allow a less harsh thermal treatment (in comparison with the one needed to inactivate all PME) for pasteurisation, resulting in better flavour and nutrient retention (Balestrieri *et al.*, 1991; Castaldo *et al.*, 1991). Additionally, PME inhibitors may be useful in processes such as fruit maceration (i.e., the process to obtain a suspension of intact cells) and juice clarification, where a controlled degradation of pectin is aimed at (Sorensen *et al.*, 2004). The recent cloning of the cDNA of kiwi PMEI and its expression in the yeast *Pichia pastoris* resulted in a functional recombinant PMEI and may allow large scale industrial use (Mei *et al.*, 2007).
The high affinity of the inhibitor for plant PME also enabled the development of an affinity chromatography method on resin-bound PMEI, that can be exploited for preparative purification of plant PMEs (Giovane *et al.*, 1995; Denès *et al.*, 2000a; Ly-Nguyen *et al.*, 2002) or to concentrate and detect low amounts of residual PME activity present in fruit and vegetable products (Castaldo *et al.*, 1996; Giovane *et al.*, 1996; Castaldo *et al.*, 1997).

Finally, PMEI may have an application in the bioconversion of plant biomass to ethanol (biofuel) or other industrial products. By overexpression of a PMEI *in planta*, modified plants with a reduced content of demethoxylated HG (and a reduced potential for calcium-pectate cross-linking) can be obtained, exhibiting an increased efficiency of enzymatic saccharification, thus reducing the need for thermochemical pretreatments of the plant cell walls (Lionetti *et al.*, 2010). Already earlier, Irifuni *et al.* (2004) pointed to the broad potential of producing genetically modified crops containing PMEI genes to inactivate endogenous PME.

1.4 EFFECT OF PROCESSING ON PROTEINS AND ENZYMES

1.4.1 Preservation processing of plant-based foods

Plant-based foods are subjected to preservation processes in order to eliminate, inactivate or reduce micro-organisms and enzymes (including PME) that would, upon storage, cause deterioration of the food or endanger the health of the consumers. Traditionally, thermal processing is the most commonly applied preservation technology since it allows efficient inactivation of both pathogenic and spoilage micro-organisms and quality-related enzymes. Unfortunately, high-temperature treatments (blanching, pasteurisation and sterilisation) often entail undesirable organoleptic and nutritional quality changes (e.g., texture, flavour, colour, vitamins). To achieve a good balance between food quality and food safety (i.e., the 'minimal processing' concept), there is a need to optimise conventional (thermal) processing techniques on the one hand and to implement alternative, novel processing technologies on the other hand. The latter include, among others, pulsed electric field (PEF), irradiation, high-intensity light pulse and high hydrostatic pressure (HHP) processing (San Martin *et al.*, 2002; Ludikhuyze *et al.*, 2003; Oey *et al.*, 2008a).

HHP processing possesses several advantages as food preservation process. In general terms, it allows inactivation of vegetative bacteria, yeasts and moulds (Hoover *et al.*, 1989; Patterson, 2005; Considine *et al.*, 2008) as well as food-spoiling enzymes (Cheftel, 1992; Hendrickx *et al.*, 1998; Ludikhuyze *et al.*, 2003) at moderate temperatures, while food quality attributes such as colour, flavour, texture and nutritional values are retained to a large extent, partly due to a limited effect of HHP on covalent bonds (Oey *et al.*, 2008a; Oey *et al.*, 2008b). Additionally, the pressure application process is independent of the size and geometry of the product due to the isostatic rule, according to which pressure is transmitted in a uniform and instantaneous manner throughout the whole sample (Cheftel, 1992; San Martin *et al.*, 2002). Today, several HHP pasteurised products are commercially available on the market (e.g., guacamole, fruit juices, salsa, poultry and meat products) (Considine *et al.*, 2008). To cope with the extreme pressure resistance of bacterial spores and certain enzymes, HHP treatment in combination with elevated temperatures has been proposed and is currently under study. A more pronounced effect on quality attributes can be expected (Matser *et al.*, 2004; Oey *et al.*, 2008b).

As outlined above, processing of plant-based foods often aims at the inactivation of endogenous enzymes with detrimental effects on food quality. Sometimes, however, enzymes are beneficial, and a stimulation of their activity during

processing is pursued. In either case, knowledge on enzyme stability and activity under the relevant processing conditions is required. Given the scope of the current work, focus in the next sections will be on the effect of the processing parameters temperature and pressure on proteins and enzymes in general and on PME in particular.

1.4.2 General aspects of protein structure and stability

Proteins are delicate structures, maintained by interactions within the protein chain (determined by the amino acid sequence) and by interactions with the surrounding solvent, being noncovalent forces such as hydrogen bonds, hydrophobic, ionic and van der Waals interactions (Jaenicke, 1991; Balny, 2004). Enzymes are a special class of globular proteins in which biological/biocatalytic activity arises from an active site, brought together by the three-dimensional configuration of the molecule.

Proteins exert only marginal stability, in a narrow physical-chemical zone (Pace, 1990). Changes in environmental factors, such as pH, solvent composition (e.g., chemicals such as urea), temperature and pressure, can perturb the subtle balance between the forces stabilising the folded conformation of the native protein, and can therefore lead to changes on one of the structural levels (Masson, 1992; Balny, 2004). In enzymes, even small conformational changes in the active site can lead to changes in substrate specificity or a total loss of enzyme catalytic activity (Tsou, 1986).

Given the low stability of proteins (and enzymes) in solution, the native state will only exist within a particular pressure-temperature (p,T) domain under given solvent conditions. This can be represented in a p,T phase diagram (**Figure 1.11**), typically elliptic for proteins. Within the elliptic contour, the protein is in the native conformation, whereas outside the contour the protein is denatured (Hawley, 1971; Smeller, 2002; Meersman *et al.*, 2006). Both high temperature and high pressure, when exceeding the limits of the diagram, can induce protein denaturation/enzyme inactivation, although substantially different mechanisms will be followed (as outlined in the following sections).

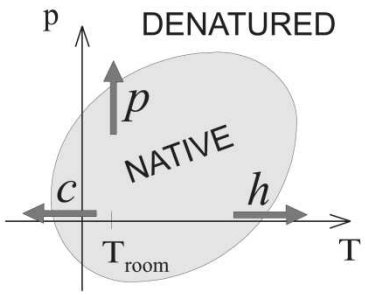

Figure 1.11. Schematic representation of the elliptic pressure-temperature phase diagram of proteins (according to Smeller, 2002). Denaturation can be accomplished by pressure (p), heat (h) and cold (c).

The crucial role of water in the stability of proteins is very clear from the experimental fact that dry proteins cannot be denatured by temperature or pressure: the elliptic diagram can only be observed for proteins in solution. The *p,T* stability will also be strongly affected by solution conditions (such as pH, urea etc), changing the size and position of the ellipse (Smeller, 2002; Meersman *et al.*, 2006).

1.4.3 Effect of high temperature on proteins and enzymes

1.4.3.1 Effect of high temperature on protein structure

The effect of an elevated temperature on the protein structure is complex. In general terms, noncovalent forces stabilising the native protein structure, notably hydrogen bonds, ionic and van der Waals interactions, diminish upon temperature increase. As a result, the protein unfolds (i.e., acquires a less ordered conformation), partly loosing secondary and tertiary structure. Multimeric proteins may be dissociated into the individual subunits. The (partial) unfolding of the protein is considered the universal first step in protein thermoinactivation and is mostly reversible. The subsequent events, however, are highly specific for individual proteins and often bring about irreversibility. They entail covalent and noncovalent modifications (Lumry and Eyring, 1954; Mozhaev and Martinek, 1982; Klibanov, 1983).

Changes in covalent bonding, and hence changes in the primary structure of the protein, occur at extreme temperatures (e.g., 100 °C), where chemical reactions involving amino acids of the protein as well as other molecules, such as nucleotides, sugars, lipids and metal ions, become significant. Examples of such reactions are inter- and intramolecular thiol-disulfide exchange, oxidation of Cys (sulfhydryl group) or Trp (indole ring) residues, deamidation of Asn and/or Gln residues, hydrolysis of peptide bonds at Asp residues, and reactions caused by the nucleophilic character of ε-amino groups of Lys and terminal α-amino groups (Klibanov, 1983; Ahern and Klibanov, 1985; Mozhaev *et al.*, 1988; Ludikhuyze *et al.*, 2003).

Besides, thermally unfolded protein molecules can undergo two types of noncovalent transformations: polymolecular (aggregation) and monomolecular (formation of incorrect structures). Upon unfolding, hydrophobic regions of the protein molecule, which heretofore were located in the interior, become exposed to the solution. Since this exposure is thermodynamically unfavourable, several unfolded molecules will reduce the free energy of the system by interacting with each other, the hydrophobic spots being the site of contact. Such interactions will result in protein aggregation (or coagulation). In dilute protein solutions, aggregation is rather unlikely and unfolded molecules can refold intramolecularly into new structures, differing from the native conformation. Kinetically or thermodynamically stable, incorrect structures are formed, that can even remain after cooling (Mozhaev and Martinek, 1982; Klibanov, 1983; Ahern and Klibanov, 1985; Mahler *et al.*, 2009).

1.4.3.2 Effect of high temperature on enzyme activity

Temperature affects the rate of an enzyme-catalysed reaction. According to the Arrhenius equation, enzyme-catalysed reactions (like chemical reactions) accelerate with increasing temperature, by increasing the fraction of collisions between molecules with sufficient energy (i.e., the activation energy) (Stauffer, 1989; Daniel *et al.*, 2001). However, the proteinaceous nature of enzymes lends them a limited thermal stability. Above a certain temperature, enzyme inactivation will take place, reversibly or irreversibly, due to local or global conformational changes (cf. previous section) that disrupt the enzyme's active site and render catalytic turnover impossible (Klibanov, 1983; Tsou, 1986).

1.4.3.3 Effect of high temperature on PME

Pectin demethoxylation by PME, like other enzyme-catalysed reactions, is enhanced by increasing temperature until a point is reached where the rate of inactivation dominates catalytic activity. Reported optimal temperatures for PME activity vary between 45 and 55 °C, depending on the enzyme source and environment. Above these temperatures, enzyme denaturation interferes (Duvetter *et al.*, 2009).

Thermal stability of PME is well documented, mainly from inactivation kinetic studies. Each PME type is characterised by a certain temperature stability window, varying for different sources of PME and different isoforms of the same source. Generally, PMEs are rather thermolabile, inactivating readily at temperatures below 70 °C (Duvetter *et al.*, 2009). However, thermostable forms occur as well and often cause technological problems (e.g., cloud loss) (Versteeg *et al.*, 1980; Cameron *et al.*, 1998; Corredig and Wicker, 2002). Additionally, thermal stability is dependent on environmental factors, such as pH, ionic strength, additives (e.g., sugars and/or polyols), and degree of purity (e.g., PME in real food systems is less vulnerable to thermal inactivation as compared to the purified form) (Balogh *et al.*, 2004; Plaza *et al.*, 2008; Duvetter *et al.*, 2009).

1.4.4 Effect of high pressure on proteins and enzymes

1.4.4.1 Effect of high pressure on protein structure

The effect of pressure on proteins is a complex phenomenon, resulting from the summation of numerous elementary contributions and depending on the structural characteristics of the protein, the pressure range studied and other external conditions, such as pH, temperature and solvent composition (Masson, 1992; Ludikhuyze *et al.*, 2003). Basically, the response of a system to the application of pressure is governed by the principle of Le Châtelier, which states that processes accompanied by a volume decrease ($\Delta V < 0$) are enhanced by a pressure increase, and vice versa (Heremans, 1982; Balny *et al.*, 2002). According to this principle, pressurisation will result in the formation or disruption of (intra- and intermolecular) interactions, conformational changes of the polypeptide backbone (i.e., the loss of void volume/cavities arising from packing defects in the completely folded protein) and solvation changes of solvent-exposed groups (Masson, 1992; Silva *et al.*, 2001; Meersman *et al.*, 2006). The relative magnitude of the individual contributions to the volume changes in protein

conformational equilibria has not yet been eludicated, and is still matter of debate (e.g., with regard to the volume change accompanying the exposure of hydrophobic residues) (Silva *et al.*, 2001; Boonyaratanakornkit *et al.*, 2002).
Pressure (at ambient temperature) does hardly affect covalent bonding (except for oxidation of sulfhydryl groups and thiol-disulfide interchange reaction), so the protein primary structure is rather pressure-insensitive (to a few GPa) (Cheftel, 1992; Heremans, 1993; Silva *et al.*, 2001; Ludikhuyze *et al.*, 2003; Balny, 2004). However, pressure can induce oligomer dissociation (protein quaternary structure) and protein unfolding and denaturation (protein secondary and tertiary structure).
Dissociation of oligomeric proteins into individual subunits, held together by noncovalent bonds, occurs at relatively low pressures (< 200 MPa) and is mostly accompanied with negative volume changes, possibly as a result of the weakening of hydrophobic and/or electrostatic interactions. The solvent-exposure of protein surfaces, which formerly interacted with each other, results in binding of water molecules, causing a volume decrease in the system. After pressure release, the reverse transition may be shown, but hysteresis phenomena ('conformational drift') are often observed. At higher pressures, unfolding and/or aggregation of the dissociated subunits may take place (Cheftel, 1992; Balny and Masson, 1993; Silva and Weber, 1993; Boonyaratanakornkit *et al.*, 2002; Ludikhuyze *et al.*, 2003; Balny, 2004).
Pressure denaturation of (monomeric) proteins occurs at comparatively high pressure levels (> 400 MPa) and is considered to be initiated by forcing water into the interior of the protein matrix, leading to conformational transitions and resulting in unfolding (Suzuki, 1960; Silva and Weber, 1993; Balny *et al.*, 2002; Knorr *et al.*, 2006; Meersman *et al.*, 2006). Contrary to thermal unfolding, the pressure-induced unfolded state often remains considerably structured ('partial unfolding') (Masson, 1992; Balny and Masson, 1993; Knorr *et al.*, 2006). Loss of tertiary structure is predominantly ascribed to disruption of hydrophobic and electrostatic interactions. The large hydration changes accompanying these structural modifications (i.e., ordering of solvent molecules around newly exposed polar and non-polar groups) are assumed to be the major source of volume reduction associated with pressure denaturation (Masson, 1992; Gross and Jaenicke, 1994; Balny *et al.*, 1997; Silva *et al.*, 2001; Ludikhuyze *et al.*, 2003; Balny, 2004), although not all authors agree with the contribution of hydrophobic interactions (Heremans, 1993; Silva *et al.*, 2001; Boonyaratanakornkit *et al.*, 2002). Denaturation affecting the tertiary structure sometimes involves intermediate states, such as the molten globule state, leading to multiple denatured forms (Balny, 2004). Changes in secondary structure, maintained by hydrogen bonds (having small positive or negative ΔV upon formation), occur only at very high pressure levels (usually > 700 MPa) and mostly cause irreversible protein denaturation. B-domains seem to be even more pressure-stable than α-helical structures (Balny and Masson, 1993; Gross and Jaenicke, 1994). Besides, irreversibility of pressure-induced protein denaturation can be brought about by chemical modifications (e.g., thiol oxidation) or by aggregate formation. The latter can occur when localised unfolding unmasks buried groups that are able to interact intermolecularly with other newly exposed

residues, and sometimes takes place only after pressure release (Cheftel, 1992; Masson, 1992; Hendrickx *et al.*, 1998).
A second principle governing pressure denaturation, next to Le Châtelier's principle, is that of microscopic ordering, which states that an increase in pressure at constant temperature leads to an ordering of molecules, resulting in a decrease of entropy of the system. A temperature rise, conversely, leads to disordering. Therefore, the effects of pressure and temperature on proteins are often antagonistic: at elevated temperature, pressure stabilizes the protein, while at low temperature, pressure denaturation occurs at lower pressures (Balny *et al.*, 1997; Boonyaratanakornkit *et al.*, 2002; Balny, 2004). Increased thermostability at elevated pressures is especially the case if the temperature-induced denatured state is less compressed than the native state (i.e., if thermal unfolding is associated with a positive ΔV) (Knorr *et al.*, 2006). The antagonistic effect of temperature and pressure is also visualised by the elliptic shape of the phase diagram of protein denaturation, but the molecular origin is not well understood (Balny, 2004; Meersman *et al.*, 2006). An important role of (the physical properties of) water, however, is beyond questioning (Meersman *et al.*, 2008).

1.4.4.2 Effect of high pressure on enzyme activity

The effect of high pressure on enzymes may be twofold. On the one hand, as enzymes are proteins, pressurisation (at room temperature) may bring reversible or irreversible, partial or complete enzyme inactivation due to structural changes in the overall protein structure or at/near the active site (as described above). Obviously, the pressure range of inactivation depends on the type of enzyme, pH, medium composition, temperature, etc. Available studies on heat- and pressure-induced enzyme inactivation have made clear that there is no systematic correlation between the stability of an enzyme towards heat and elevated pressure (Aertsen *et al.*, 2009).
On the other hand, pressure may also exert an influence on the catalytic activity of the enzyme (at comparatively lower pressure levels). Enzyme activation or inhibition can occur due to conformational changes of the protein structure, changes in the enzyme-substrate interaction, or effects on the catalytic reaction itself (Balny and Masson, 1993; Heremans, 1993). Again, the principle of Le Châtelier is involved, stating that pressure favours the reduction of the volume of a system. For instance, pressure will hamper reactions with a positive volume change upon substrate binding to the active site, and will direct/accelerate reactions having a negative reaction/activation volume (Cheftel, 1992; Boonyaratanakornkit *et al.*, 2002; Aertsen *et al.*, 2009). High pressure can also alter the substrate specificity of an enzyme (e.g., if the conversion of one substrate gives rise to a product with a smaller volume) or enhance the sensitivity of macromolecular substrates to enzymatic action (e.g., protein and starch after pressure-induced unfolding or gelatinisation) (Cheftel, 1992; Balny, 2004; Knorr *et al.*, 2006; Aertsen *et al.*, 2009). Moreover, in particular cases, enzyme activation can arise from pressure-induced decompartmentalisation, with pressure damaging membranes and facilitating enzyme-substrate contact (Cheftel, 1992; Hendrickx *et al.*, 1998). Finally, it is relevant to mention that, given that the rate of an enzyme-catalysed conversion reaction is often limited by

the thermosensitivity of the corresponding enzyme, it is conceivable that superimposing pressure-induced thermostabilisation of the enzyme (as discussed in the previous section) with an accelerated substrate conversion at increased temperatures could lead to a new optimum reaction condition with regard to an improved overall reaction rate (Mozhaev *et al.*, 1996; Aertsen *et al.*, 2009).

1.4.4.3 Effect of high pressure on PME

A high number of (kinetic) studies on PME stability demonstrate that most PMEs are rather barotolerant. However, the actual pressure stability of a particular PME (at room temperature) can vary considerably, ranging from moderately pressure-sensitive (> 600 MPa, e.g., carrot PME) to extremely pressure-stable (> 1 GPa, e.g., tomato and *A. aculeatus* PME). Even within one species, PME isoforms can show significant differences in pressure-stability (Ly-Nguyen *et al.*, 2003; Plaza *et al.*, 2007; Sila *et al.*, 2007a; Duvetter *et al.*, 2009).
For several PMEs, the substrate conversion rate has been demonstrated to increase at elevated pressures up to a certain pressure level (e.g., for carrot, orange, pepper, tomato and *A. aculeatus* PMEs) (Sila *et al.*, 2007a; Duvetter *et al.*, 2009). In addition, moderate pressure levels (up to ca. 400 MPa) have been shown to retard thermal inactivation of several PMEs studied, an antagonistic effect also reflected by the elliptic shape of isorate contour plots in the *p,T* domain. Consequently, the optimal temperature for PME action can shift to higher temperatures at pressure levels beyond atmospheric pressure (Verlent *et al.*, 2004; Duvetter *et al.*, 2009).

1.5 CONCLUSIONS AND SCOPE OF THIS WORK

In conclusion, it can be stated that endogenous PME can have favourable as well as detrimental effects on the structural quality of plant-derived foods. For instance, PME is associated with cloud and consistency loss occurring in fruit and vegetable juices and pastes. Both positive and negative effects are based on the PME-catalysed demethoxylation of pectin, altering the amount and distribution of methyl-esters in pectin and changing pectin's susceptibility to subsequent (non-)enzymatic conversions and gel formation.
As a consequence, depending on the product at hand, PME stimulation or inactivation can be pursued. By using processing tools like conventional thermal or emerging hydrostatic pressure treatments, PME-induced pectin conversions can be tailored (based on the enzyme's activity and stability in the *p,T* domain), hence controlling pectin-related functional features of plant-derived food products (i.e., texture, rheology and cloud stability).
Besides inactivation due to processing, enzyme inhibition may be an alternative approach to control endogenous PME activity. In this context, the discovery of the proteinaceous PMEI in kiwi fruit was a key step. Based on the strong PME-PMEI interaction, the use of kiwi PMEI as an adjuvant to inhibit undesired PME activity in food applications has been postulated (for example, to obtain cloud-stable juices). In addition, the discovery of this PMEI offers possibilities for the development of an innovative (microscopic) technique based on labelled PMEI to localise endogenous PME *in situ* and, hence, to improve the insight in the relationship between enzymatic pectin conversions and related macroscopic

properties (such as firmness and viscosity), both in model systems and in structured, real food matrices.

Over the past years, knowledge on the kiwi PMEI primary and 3D structure, its specificity, mode of action and role *in vivo* has been growing, as illustrated in Section 1.3. However, progress concerning the PME inhibitor in a food technological context has been limited. Profound knowledge on the PME-PMEI interaction as influenced by both intrinsic product factors (such as pH and ionic strength) and extrinsic process factors (such as high temperature and high pressure), required for application of PMEI in either PME inhibition or detection, for instance, is lacking.

In the current work, this improved insight is aimed at, following methodologically different strategies to monitor the PME-PMEI interaction, including enzyme inhibition measurements (**Chapter 2**), interaction analysis by surface plasmon resonance (**Chapter 3**) and complex formation through size exclusion chromatography (**Chapter 4**). In a final chapter (**Chapter 5**), the potential of PME as a molecular probe for detection of PME *in situ*, also in the context of food processing, is evaluated.

2

PLANT PME AND KIWI PMEI: STUDY OF ACTIVITY, STABILITY AND INHIBITION[1]

2.1 INTRODUCTION

Efficient application of kiwi PMEI to control or to detect plant PME requires a profound knowledge on the PME-PMEI interaction. This first research chapter aims at a better insight in the PME-PMEI complex as influenced by intrinsic product factors (pH and ionic strength) and extrinsic process factors (temperature and hydrostatic pressure), based on enzyme inhibition measurements. Both the effects of pH and NaCl concentration and of a temperature- or pressure-induced denaturation of PMEI on its inhibitory capacity are studied. Furthermore, the way the PME-PMEI complex behaves at elevated temperature or pressure in the presence of the pectin substrate is assessed. Given the intrinsic value and the essentiality for a reliable interpretation of the inhibition data, control experiments using PME alone were also conducted in parallel, investigating the effect of pH, NaCl and processing on plant PME in absence of PMEI.

In the current chapter, carrot PME, considered to be a representative plant PME, is selected as object of study. Like in many other plants, endogenous carrot PME activity can affect positively or negatively the quality of derived foods. For instance, stimulation of PME activity before cooking of carrots has been demonstrated to enhance the texture of the final product (Ng and Waldron, 1997; Sila *et al.*, 2004), whereas PME-catalysed pectin hydrolysis can cause undesired cloud loss in carrot juice (Sims *et al.*, 1993). Hence, carrot PME activity control is a major point of interest in the quest of obtaining high-quality products. In this context, the effects of high temperature and high pressure on the stability and catalytic activity of carrot PME have been documented, in model as well as in

[1] This chapter is based on the following paper:
Jolie, R.P., Duvetter, T., Houben, K., Clynen, E., Sila, D.N., Van Loey, A.M., Hendrickx, M.E. (2009). Carrot pectin methylesterase and its inhibitor from kiwi fruit: Study of activity, stability and inhibition. *Innovative Food Science and Emerging Technologies*, 10(4), 601-609.

food systems (Tijskens *et al.*, 1997; Vora *et al.*, 1999; Ly-Nguyen *et al.*, 2003; Balogh *et al.*, 2004; Sila *et al.*, 2007a), but neither PME inhibition by means of PMEI nor *in situ* detection of the carrot enzyme have been investigated yet.
Additionally, this chapter provides a more elaborate description of the extraction, purification and characterisation procedures and results for plant PME and kiwi PMEI, also employed in the following chapters.

2.2 MATERIALS AND METHODS

2.2.1 Materials

Young Holland red carrots (*Daucus carota* cv. Nerac) and green kiwi fruits (*Actinidia deliciosa* cv. Hayward) were purchased from a local supermarket. Apple pectin (degree of methyl-esterification: 70 - 75%) was obtained from Fluka (Buchs, Switzerland). NHS (*N*-hydroxysuccinimide)-activated Sepharose 4 Fast Flow was from GE Healthcare Bio-Sciences AB (Uppsala, Sweden) and CNBr-activated Sepharose 4B from Sigma (Darmstadt, Germany). All other chemicals were of analytical grade.

2.2.2 Extraction and purification of carrot PME

Extraction and purification of carrot PME were based on the method of Ly-Nguyen *et al.* (2002). Carrot roots (1 kg) were peeled and homogenised in water (2:1 w/v). The pellet was collected by filtration using a cheesecloth and mixed by end-over-end rotation overnight at 4 °C with 0.2 M Tris-HCl pH 8.0 (Tris = tris(hydroxymethyl)aminomethane) containing 1.0 M NaCl (1:1.3 w/v) for the extraction of cell-wall-bound PME. Afterwards, the salt extract was separated by filtration and subjected to ammonium sulphate precipitation. The fraction precipitating between 30% and 80% ammonium sulphate saturation was isolated by centrifugation (18000 × *g*, 15 min, 4 °C) and dissolved in 20 mM Tris-HCl pH 7.0. This crude PME extract was stored frozen at -80 °C until further purification by affinity chromatography.
To purify carrot PME, previously purified kiwi PMEI (as described in Section 2.2.3) was covalently coupled to a NHS-activated Sepharose 4 Fast Flow matrix. The resin was swollen in 1 mM HCl and mixed end-over-end with the purified kiwi PMEI in 0.1 M Na_2CO_3 pH 8.3 containing 0.5 M NaCl. Unoccupied sites were deactivated with 0.1 M Tris-HCl pH 8.0. Once the kiwi PMEI – NHS-activated Sepharose matrix was prepared, it was allowed to mix with the crude carrot PME for at least 2 h. Subsequently, the PME – PMEI – NHS-Sepharose gel was rinsed with water and packed onto a column (XK16, GE Healthcare). The column was first washed with 2 mM KH_2PO_4 pH 6.0 containing 0.5 M NaCl, prior to PME recovery by elution with 50 mM Na_2CO_3 pH 9.85 containing 1.0 M NaCl at a flow rate of 0.1 mL/min. Hereto, an ÄKTAprime™ system was used (GE Healthcare). After elution, fractions possessing PME activity were pooled and desalted using Vivaspin 20 centrifugal filters (10 kDa MWCO, Sartorius, Goettingen, Germany). The purified carrot PME concentrate in 10 mM Na-phosphate pH 6.5 was quickly frozen in liquid N_2 and stored at -80 °C.

2.2.3 Extraction and purification of kiwi PMEI

Extraction and purification of kiwi PMEI were based on the method of Giovane *et al.* (1995). About 1 kg of ripe kiwi fruits was peeled and homogenised (1:1 w/v) in a suspension of polyvinylpolypyrrolidone (PVPP, 7.5%) in water at 4 °C. The supernatant, containing the PMEI, was separated from the pellet by centrifugation at 20000 × g for 20 min (4 °C). The pH was adjusted to 6.0 and the supernatant was filtered to remove seeds and other small particles.
To purify PMEI, PME was first extracted and purified from oranges according to the methods of Section 2.2.2 and Van den Broeck *et al.* (1999), and then chemically immobilised on a CNBr-Sepharose 4B resin, analogously to the immobilisation of kiwi PMEI on a NHS-Sepharose 4 Fast Flow gel, as described in the previous section. The kiwi juice, containing PMEI, was mixed end-over-end with the orange PME – CNBr-Sepharose matrix for at least 2 h. Afterwards, the PMEI – PME – CNBr-Sepharose gel was packed onto a column (XK16) and washed with 75 mL of 2 mM KH_2PO_4 pH 6.0 containing 0.5 M NaCl. PMEI was recovered by eluting with 20 mM Na_2CO_3 pH 9.85 containing 1.0 M NaCl at a flow rate of 0.1 mL/min, on an ÄKTAprime™ system. After elution, fractions possessing PMEI activity were pooled and desalted using Vivaspin 20 centrifugal filters (5 kDa MWCO). The purified kiwi PMEI concentrate in 10 mM Na-phosphate pH 6.5 was quickly frozen in liquid N_2 and stored at -80 °C.

2.2.4 PME activity and PMEI inhibitory capacity assays

PME activity was measured by the continuous titration of carboxyl groups formed during the PME-catalysed pectin de-esterification, using an automatic pH-stat titrator (Metrohm, Herisau, Switzerland) with 0.01 M NaOH (Ly-Nguyen *et al.*, 2002). Routine assays were performed at pH 6.5 and 22 °C, using 30 mL of a 0.35% (w/v) pectin solution containing 0.117 M NaCl. One unit (U) of PME activity is defined as the amount of enzyme catalysing the hydrolysis of 1 µmol of methyl-ester bonds per min under aforementioned conditions.
PMEI inhibitory capacity was determined as the ability to block PME activity in a titrimetric assay (Ly-Nguyen *et al.*, 2004). It was calculated as the difference between the PME activity of a blank sample (i.e., without PMEI) and the remaining PME activity after 15 min of preincubation with a PMEI sample (more precisely, an amount maximally inhibiting ~75% of the total initial PME activity), routinely at 22 °C and pH 6.5. One unit of inhibition (UI) is defined as the amount of PMEI blocking 1 U of PME under the assay conditions described above.
To measure the PME activity or PMEI inhibitory capacity at various pH values and NaCl concentrations, either set pH (4.0 to 10.0, by addition of NaOH) or NaCl concentration (0.0 to 1.0 M) of the pectin solution (and of the preincubation, if appropriate) was adjusted, keeping all other conditions constant. The measured activity value was corrected for pectin autohydrolysis in the alkaline region (pH ≥ 7.0) by subtraction of the acid production in a pectin solution without PME and for incomplete dissociation of demethoxylated carboxyl groups in the acidic region (pH ≤ 5.0) by multiplication with a correction factor (Christgau *et al.*, 1996).

2.2.5 Protein content

The protein content of PME and PMEI samples was determined using the bicinchoninic acid (BCA) kit according to Sigma procedure TPRO-562 (Sigma). This method is based on the reduction of Cu^{2+} to Cu^{+} by proteins in an alkaline environment. BCA forms a coloured complex with Cu^{+}, quantified spectrophotometrically at 562 nm and 25 °C (Ultrospec 2100 pro, GE Healthcare). The protein concentration (mg/mL) was calculated by comparison with a standard curve of bovine serum albumin.

2.2.6 Gel electrophoresis

Sodium dodecyl sulphate polyacrylamide gel electrophoresis (SDS-PAGE) and isoelectric focusing (IEF) were performed on a PhastSystem™ (GE Healthcare Bio-Sciences AB) for molar mass and isoelectric pH (pI) estimations, respectively. Gel staining was carried out by the silver staining technique according to Heukeshoven and Dernick (1985).
For SDS-PAGE, Phastgel homogeneous 20% and PhastGel tricine-Tris-SDS buffer strips were used. Protein samples, dissolved in a buffer containing 2.5% SDS and 5% β-mercaptoethanol, were heated in boiling water for 5 min before application on the gel. The molar mass was estimated by comparing the migration distance with those of standard protein markers (Low Molecular Weight SDS Marker Kit, ranging from 14.4 to 97.0 kDa) using IMAGEMASTER 1D software.
For IEF, PhastGel IEF 3-9 media, i.e., precast homogeneous polyacrylamide gels containing 2 - 6% Pharmalyte as carrier ampholyte and a pI separation range from 3 to 9, were employed. The pI was estimated by comparison of the migration distance of the protein bands with those of standard protein markers (IEF Calibration Kit Broad pI, ranging from pH 3.5 to 9.3).

2.2.7 MALDI-TOF mass spectrometry[2]

Matrix-assisted laser desorption/ionisation time-of-flight mass spectrometry (MALDI-TOF MS) was performed on a Reflex IV (Bruker Daltonics, Bremen, Germany), equipped with a N_2-laser and pulsed ion-extraction accessory. One µL of protein sample, dissolved in ultrapure water, was transferred to a steel target, mixed with 1 µL of a saturated solution of either sinapic acid in 50% acetonitrile with 0.1% trifluoroacetic acid (20 - 200 kDa) or α-cyano-4-hydroxycinnamic acid in acetone (0.5 - 20 kDa) and air dried. The instrument was calibrated using standard peptide and protein mixtures (Bruker Daltonics). Positive ion spectra were recorded in the reflectron mode (0.5 - 3 kDa) and in the linear mode (3 - 20 kDa and 20 - 200 kDa).

[2] MALDI-TOF MS analyses were carried out in cooperation with the Research Group Functional Genomics and Proteomics, K.U.Leuven.

2.2.8 PME and PMEI stability study

2.2.8.1 Thermal and high-pressure treatments

Thermal inactivation experiments of purified carrot PME and kiwi PMEI were performed in a temperature-controlled water bath. Protein solutions (in 10 mM Na-phosphate buffer pH 6.5, a buffer with a small $\Delta pK_a/\Delta T$) were enclosed in 200 µL glass capillaries (Brand, Wertheim, Germany) to ensure isothermal heating. After preset time intervals, samples were withdrawn from the water bath and immediately cooled in an ice water bath. Residual PME activity or PMEI inhibitory capacity were measured within 2 h. During storage in ice water, no reactivation of PME or PMEI was observed.
Isobaric-isothermal inactivation experiments were conducted in a laboratory-scale high-pressure equipment (Resato, Roden, The Netherlands) with eight reactors, each surrounded by a thermostatted mantle connected to a cryostat. The pressure medium was a propylene glycol - water mixture (PG fluid, Resato). Flexible microtubes (0.3 mL, Carl Roth, Karlsruhe, Germany) were filled with either purified carrot PME in 10 mM Na-phosphate buffer pH 6.5 or kiwi PMEI in 10 mM MES-NaOH pH 6.5 (MES = 2-(*N*-morpholino)ethanesulfonic acid) and enclosed in the pressure reactors, already equilibrated to 25 °C. MES buffer was chosen because of its putative pressure stability, i.e., the ability to maintain the set pH upon pressurisation (Bruins *et al.*, 2007), in contrast to Na-phosphate buffer (Neuman *et al.*, 1973). Pressure was built up slowly (100 MPa/min) to minimise temperature increase due to compression heating. After pressure build-up, an equilibration period of 2 min was taken into account to allow temperature and pressure to evolve to the desired value. After preset time intervals, counted after equilibration, the individual reactors were depressurised instantaneously and samples were cooled in an ice water bath. Residual PME activity or PMEI inhibitory capacity were measured within 2 h. During storage in ice water, reactivation of neither PME nor PMEI was observed.

2.2.8.2 Kinetic data-analysis

Despite being complex processes involving several events (cf. Sections 1.4.3 and 1.4.4), thermal and high-pressure inactivation of enzymes are often described by a first-order kinetic model (Lencki *et al.*, 1992; Van Loey *et al.*, 2003):

$$A = A_0 \exp(-kt) \qquad 2.1$$

where A_0 is the initial activity, A is the residual activity after treatment time t (min) and k is the inactivation rate constant (min^{-1}).
When several enzyme fractions with different processing stability (i.e., a labile and a stable fraction) are present, both inactivating according to a first-order model, a biphasic kinetic model can be applied:

$$A = A_L \exp(-k_L t) + A_S \exp(-k_S t) \qquad 2.2$$

where subscripts L and S refer to the labile and the stable fraction, respectively.
When only the labile fraction inactivates, whereas the stable fraction is not affected under the processing conditions applied (i.e., if $k_S = 0$), a fractional-conversion kinetic model can be used:

$$A = A_\infty + (A_0 - A_\infty)\exp(-k_L t) \quad 2.3$$

with A_∞ the non-zero residual activity after prolonged thermal or high-pressure treatment.

In the case of a succession of (two) irreversible (first-order) reaction steps, i.e., the conversion of the native protein to an intermediate with lower specific activity and the subsequent conversion of the intermediate to an inactive form, a consecutive-step model can be appropriate, mathematically expressed as:

$$A = \left[A_1 - A_2\left(\frac{k_1}{k_1 - k_2}\right)\right]\exp(-k_1 t) + A_2\left(\frac{k_1}{k_1 - k_2}\right)\exp(-k_2 t) \quad 2.4$$

with k_1 and A_1 referring to step 1, and k_2 and A_2 referring to step 2. When, in a particular case, the second step would not occur (i.e., k_2 = 0), this model is simplified to:

$$A = A_2 + (A_1 - A_2)\exp(-k_1 t) \quad 2.5$$

In practice, by plotting activity (A) against time during isothermal and isobaric treatment, the different kinetic parameters of the respective models were estimated by nonlinear regression analysis (SAS Statistical Software version 9.1, Cary, North Carolina).

The temperature dependence (at constant pressure) of the inactivation rate constants, expressed in terms of activation energy (E_a), can be estimated using the Arrhenius equation:

$$k = k_{ref}\exp\left[\frac{E_a}{R_T}\left(\frac{1}{T_{ref}} - \frac{1}{T}\right)\right] \quad 2.6$$

where k_{ref} is the inactivation rate constant at reference temperature T_{ref} (K), E_a the activation energy (J/mol) and R_T the universal gas constant. As a measure for the pressure dependence (at constant temperature) of the enzyme inactivation, the activation volume (V_a) can be estimated using the Eyring relationship:

$$k = k_{ref}\exp\left[\frac{V_a}{R_p T}(p_{ref} - p)\right] \quad 2.7$$

where k_{ref} is the inactivation rate constant at reference pressure p_{ref} (MPa), V_a the activation volume (cm^3/mol) and R_p the universal gas constant. Practically, E_a and V_a were estimated by nonlinear regression analysis of the k-values versus absolute T or p, respectively (SAS Statistical Software version 9.1).

As a measure for the quality of model fitting for nonlinear regression analysis, the corrected R^2 (Corr R^2) was considered:

$$\text{Corr } R^2 = \left[1 - \frac{(m-1)\left(1 - \frac{\text{SSQ}_{\text{regression}}}{\text{SSQ}_{\text{total}}}\right)}{(m-j)}\right] \quad 2.8$$

where m is the number of observations, j is the number of model parameters and SSQ is the sum of squares (Neter *et al.*, 1996).

2.2.9 PME activity study in absence and presence of PMEI

The carrot PME catalytic activity at elevated temperature or pressure in absence and presence of kiwi PMEI was determined by measuring the amount of methanol released during PME-catalysed pectin hydrolysis as a function of treatment time.

2.2.9.1 Methanol content

Methanol was quantified according to the method of Klavons and Bennett (1986), in which methanol is oxidised to formaldehyde by alcohol oxidase (EC 1.1.3.13, Sigma) followed by a condensation with 0.02 M 2,4-pentadione in 2.0 M ammonium acetate and 0.05 M acetic acid to form 3,5-diacetyl-1,4-dihydro-2,6-dimethylpyridine. The coloured compound produced was measured spectrophotometrically at 412 nm and 25 °C.

2.2.9.2 Thermal and high-pressure treatments

Starting from a 0.35% pectin solution in 0.1 M Na-phosphate buffer pH 6.5 containing 0.117 M NaCl, three stock samples were prepared: *(1)* a pectin blank, for correcting the amount of methanol formed due to autohydrolysis; *(2)* pectin (5 mL) mixed with PME (1 U); and *(3)* pectin (5 mL) mixed with PME (1 U) and PMEI (0.5 UI). For the latter stock sample, PME and PMEI were first preincubated for 15 min at 25 °C. Within 4 min, six flexible microtubes (0.4 mL, Carl Roth) were filled with each of the three stock solutions (so, 18 in total). For isothermal experiments at atmospheric pressure, all microtubes were then placed in a temperature-controlled water bath. After 1 min of equilibration and after preset time intervals (up to 10 min), a triad of microtubes (i.e., a pectin blank, a pectin-PME mixture and a pectin-PME-PMEI mixture) was withdrawn from the water bath and immediately heat-quenched at 85 °C for 2 min. Subsequently, samples were cooled in an ice bath and methanol was quantified as described in the previous section. The experiment was done in duplicate.
For high-pressure experiments, analogously, three sets of stock samples were prepared: *(1)* a pectin blank; *(2)* pectin (5 mL) mixed with PME (0.5 U); and *(3)* pectin (5 mL) mixed with PME (0.5 U) and PMEI (0.35 UI). However, the pressure-sensitive Na-phosphate buffer was substituted by a pressure-stable imidazole-HCl buffer (0.1 M, pH 6.5) (Kitamura and Itoh, 1987). After 4 min of sample preparation and microtube filling, 2 additional minutes were taken to introduce the samples in a multi-reactor high-pressure equipment (identical to the device described in Section 2.2.8.1 but with six reactors), equilibrated to 25 °C. Pressure was built up manually to the desired level (at 100 MPa/min). After an equilibration period of 2 min and after preset time intervals at isothermal-isobaric conditions (up to 10 min), individual reactors were decompressed instantaneously and a triad of microtubes (i.e., a pectin blank, a pectin-PME mixture and a pectin-PME-PMEI mixture) was withdrawn. Samples were heat-quenched at 85 °C for 2 min prior to cooling in an ice bath. The amount of methanol was determined colourimetrically. The experiment was carried out in duplicate.

2.2.9.3 Data-analysis

The reaction rate constant V_0 (in µmol methanol/(mL·min)) of the PME-catalysed hydrolysis of pectin, in the presence or absence of PMEI, was estimated from the initial, linear part of the curve obtained by plotting the amount of methanol (µmol/mL) produced by PME versus isothermal-isobaric treatment time (min). This net methanol production due to enzymatic hydrolysis was calculated by subtracting the amount of methanol produced in the blank samples from the amount of methanol produced in the pectin-PME(-PMEI) mixtures. The temperature and pressure dependence of the reaction rate constant, expressed in terms of activation energy E_a and activation volume V_a respectively, were estimated for selected temperature and pressure regions using the Arrhenius (Equation 2.6) and Eyring equation (Equation 2.7).

2.3 RESULTS AND DISCUSSION

2.3.1 Extraction and purification of carrot PME

Cell-wall-bound carrot PME was extracted from raw carrot roots by use of a high ionic strength buffer. To remove contaminating proteins, the crude extract was subjected to ammonium sulphate precipitation. A crude yield of about 5000 PME units per kg of raw material was obtained. By using a single-step affinity chromatography method on a kiwi PMEI – NHS-activated Sepharose matrix, PME was selectively isolated. Loosely bound proteins were washed out, prior to elution of pure PME with a high ionic strength and high pH buffer. **Figure 2.1** illustrates a successful recovery with two unresolved peaks of PME activity. PME fractions eluting before appearance of the second elution peak were pooled, containing the main, most abundant carrot PME isoform. As separation of the PME on the PMEI affinity column indicates different binding behaviour to kiwi PMEI, the second elution peak was excluded not to hamper the interpretation of inhibition

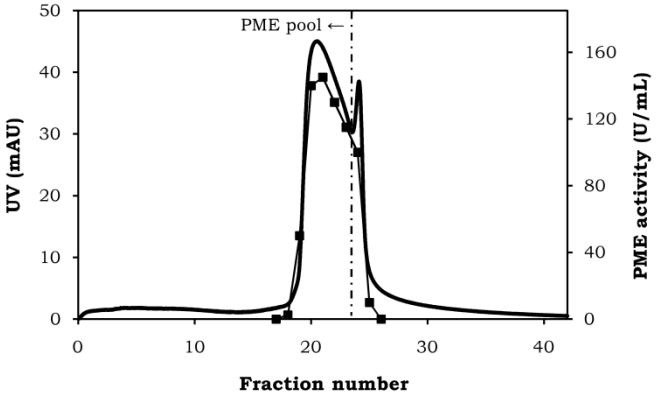

Figure 2.1. Affinity chromatography elution profile of carrot PME on an activated Sepharose column, illustrating UV absorbance at 280 nm (—) and PME activity in the different fractions (■). Fractions eluting before appearance of the second elution peak were pooled.

experiments. The specific activity of the purified carrot PME pool was estimated at 485 U/mg protein, about a tenfold higher than the specific activity of the crude extract after ammonium sulphate precipitation, indicating a purification factor of 10.

SDS-PAGE and MALDI-TOF MS were carried out to check the extract purity and to estimate the molar mass of the main carrot PME isoform. SDS-PAGE (**Figure 2.2**) showed a single band around 34 kDa and the mass spectrum (**Figure 2.3A**) revealed one major ion peak at 34.045 kDa. These results are in close agreement with the theoretical molar mass of 34.237 kDa as calculated from the amino acid sequence (Markovic *et al.*, 2002) and with other SDS-PAGE estimations (Markovic *et al.*, 2002; Ly-Nguyen *et al.*, 2002; Sila *et al.*, 2007a). The absence of other mass signals confirmed that the carrot PME sample after affinity chromatography was

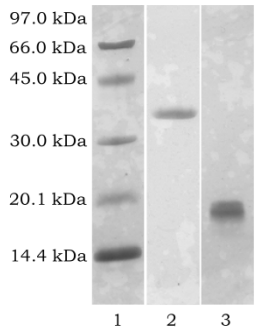

Figure 2.2. SDS-PAGE of carrot PME (lane 2) and kiwi PMEI (lane 3) after affinity chromatography. Standard proteins with respective molar masses are shown in lane 1.

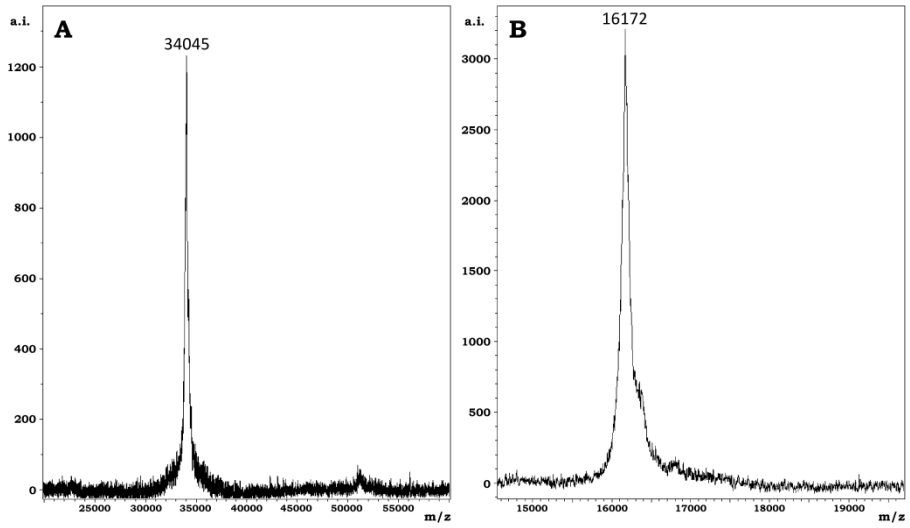

Figure 2.3. MALDI-TOF mass spectra of carrot PME (A) and kiwi PMEI (B) after affinity chromatography (m/z is mass-to-charge ratio; a.i. is absolute intensity)

free from contaminating proteins. Isoelectric focusing also revealed a single PME band with a pI greater than 9.3 (results not shown), confirming former pI estimations of carrot PME (Markovic *et al.*, 2002; Ly-Nguyen *et al.*, 2002; Alonso *et al.*, 2003; Sila *et al.*, 2007a).

2.3.2 Extraction and purification of kiwi PMEI

The proteinaceous PME inhibitor (PMEI) was extracted from ripe kiwi fruits by homogenisation in 7.5% PVPP and centrifugation. PMEI was further purified from the crude kiwi juice by a single-step affinity chromatography method on an orange PME – CNBr-activated Sepharose matrix. Loosely bound proteins were removed, prior to elution of pure PMEI with a high ionic strength and high pH buffer. Single sharp peaks of proteins (i.e., UV) and PMEI activity were obtained, as shown in **Figure 2.4**. Fractions containing inhibitory capacity towards plant PME were collected.

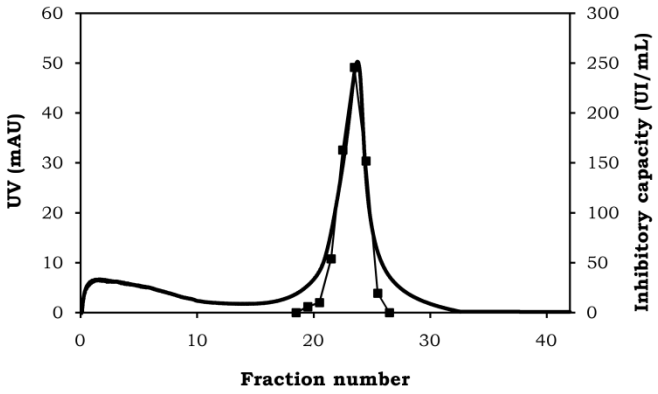

Figure 2.4. Affinity chromatography elution profile of kiwi PMEI on an activated Sepharose column, illustrating UV absorbance at 280 nm (—) and PMEI inhibitory capacity in the different fractions (■).

An extract purity check and molar mass estimation of kiwi PMEI were performed by means of SDS-PAGE and MALDI-TOF MS. SDS-PAGE (**Figure 2.2**) displayed a single but broad protein band around 17 kDa, and the mass spectrum (**Figure 2.3B**) exhibited one major ion peak at 16.172 kDa. The molar mass results are in accordance with the theoretical value of 16.277 kDa reported by Camardella *et al.* (2000) and with former estimations by SDS-PAGE, ranging from 16 to 18 kDa (Giovane *et al.*, 1995; Camardella *et al.*, 2003; Ly-Nguyen *et al.*, 2004). The singularity of the protein band/ion peak confirms the absence of contaminating proteins in the kiwi PMEI sample after affinity chromatography. The broadness of both SDS-PAGE band and ion peak, however, suggests the presence of several PMEI isoforms with minor molar mass differences. The latter hypothesis is in line with observed heterogeneities in the primary structure and cDNA of kiwi PMEI (cf. Section 1.3.2.1).

In literature, reported estimations for the pI of kiwi PMEI vary from < 3.5 to 4.8 (Balestrieri *et al.*, 1990; Marquis and Bucheli, 1994; Camardella *et al.*, 2000;

Camardella *et al.*, 2003; Ly-Nguyen *et al.*, 2004; Ciardiello *et al.*, 2008). IEF experiments performed during the current study did not allow refining this broad range, since no single, consistent estimation was obtained (results not shown). Nevertheless, different researchers do agree on the highly acidic nature of the kiwi PMEI.

2.3.3 Effect of pH and NaCl concentration on carrot PME activity and kiwi PMEI inhibitory capacity

2.3.3.1 Effect of pH

The effect of pH on the catalytic activity of carrot PME and the inhibitory capacity of kiwi PMEI, obtained via the titrimetric PME and PMEI assays at various pH values in the range of 4.0 to 10.0, is represented in **Figure 2.5**. Changes in pH had a significant effect on the PME activity, attributable to alteration of the ionisation of charged amino acids, influencing substrate binding and/or catalytic action. The enzyme was active in the pH range from 5.0 to 10.0 with an optimum at pH 9.0. At pH 4.0, no PME activity was observed. These observations are in agreement with the studies of Ly-Nguyen *et al.* (2004) and Sila *et al.* (2007a).

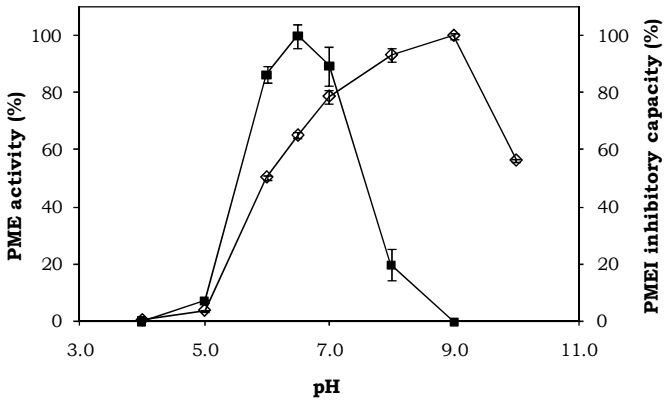

Figure 2.5. Effect of pH on the activity of purified carrot PME (◊) and on the inhibitory capacity of purified kiwi PMEI towards carrot PME (■) at 22 °C. The molar ratio of PME to PMEI is approx. 1:0.7. Activity is expressed as a percentage of the activity at optimal pH. Each point represents the mean of repeated measurements (n = 2, ± standard error).

The pH value also profoundly affected the inhibitory capacity of kiwi PMEI towards carrot PME. Strong enzyme inhibition was observed at pH 6.0 to 7.0, with an optimum at pH 6.5. At pH 9.0 and higher, no inhibition of carrot PME occurred. In the acidic pH range (≤ 5.0), reliable inhibition measurements were impossible due to the low PME activity. The strong pH dependence of the kiwi PMEI inhibition capacity towards carrot PME is not really surprising, as a high number of ionisable groups, the charge of which is affected by their chemical environment, are suggested to be involved in the tomato PME - kiwi PMEI complex formation (Di Matteo *et al.*, 2005) (cf. Section 1.3.3.2). The reduced inhibition capacity at alkaline pH may be explained by the concomitant decrease

in net positive charge on carrot PME (having a pI ≥ 9.3) (e.g., due to deprotonation of specific amino acid residues), while the acidic kiwi PMEI bears a net negative charge in nearly the entire pH domain tested. Hence, electrostatic repulsion can be generated and the complex destabilised.

2.3.3.2 Effect of NaCl concentration

Carrot PME activity and kiwi PMEI inhibitory capacity were also measured as a function of NaCl concentration by means of the titrimetric PME and PMEI assays at pH 6.5 and 22 °C (**Figure 2.6**). The results confirmed NaCl to be a prerequisite for carrot PME activity (Rexova-Benkova and Markovic, 1976). Optimal enzyme activity was observed at 0.25 M NaCl, which lies within the optimum range of 0.13 to 0.33 M reported by Alonso *et al.* (2003). At higher concentrations, gradually lower activities were measured (e.g., only 20% of the maximal activity at 1.0 M NaCl), attributable to the Na^+-induced blocking of the free carboxylic acid groups, required for enzymatic activity.
The kiwi PMEI inhibitory capacity showed a similar trend as a function of NaCl concentration. Strong enzyme inhibition was established at 0.125 M and particularly at 0.25 M, whereas no reliable results could be obtained at 0.0 M due to the absence of PME activity. High salt concentrations resulted in reduced inhibition (e.g., hardly inhibition at 1.0 M NaCl), probably caused by a shielding of charged groups, involved in complex formation.

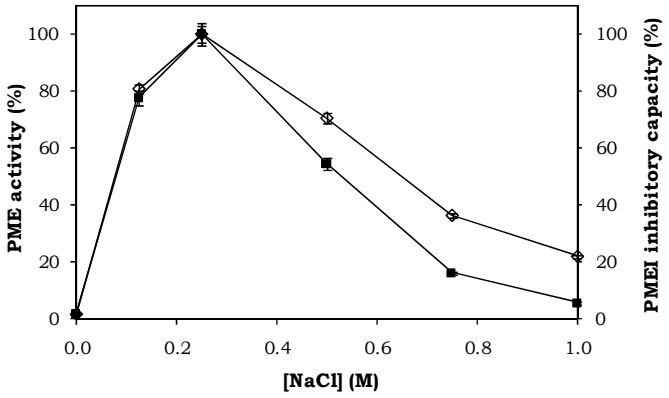

Figure 2.6. Effect of NaCl concentration on the activity of purified carrot PME (◊) and on the inhibitory capacity of purified kiwi PMEI towards carrot PME (■) at 22 °C. The molar ratio of PME to PMEI is approx. 1:0.7. Activity is expressed as a percentage of the activity at optimal [NaCl]. Each point represents the mean of repeated measurements (n = 2, ± standard error).

2.3.4 Effect of thermal or high-pressure denaturation of carrot PME on its catalytic activity

The effect of a high-temperature- or high-pressure-induced denaturation of carrot PME on its catalytic activity was investigated. Hereto, purified carrot PME (in 10 mM Na-phosphate pH 6.5) was treated for different times at isothermal-isobaric conditions and residual enzyme activity was measured.

2.3.4.1 Thermal inactivation of carrot PME

In the temperature range from 52.5 to 65 °C, isothermal inactivation of carrot PME could adequately be described by a first-order model (**Figure 2.7**). For all temperature levels, inactivation rate constants (k) were estimated by nonlinear regression analysis. As an expression for the temperature dependence of the inactivation rate constant in the temperature range studied, the activation energy (E_a) was estimated. **Table 2.1** summarizes the results of the two-step regression approach. The current study confirms earlier observations that the main carrot PME is rather thermosensitive as compared to other plant PMEs (Ly-Nguyen *et al.*, 2002; Alonso *et al.*, 2003; Duvetter *et al.*, 2009). Treatment of a few minutes at temperatures above 60 °C is sufficient to reduce its activity below detectable levels.

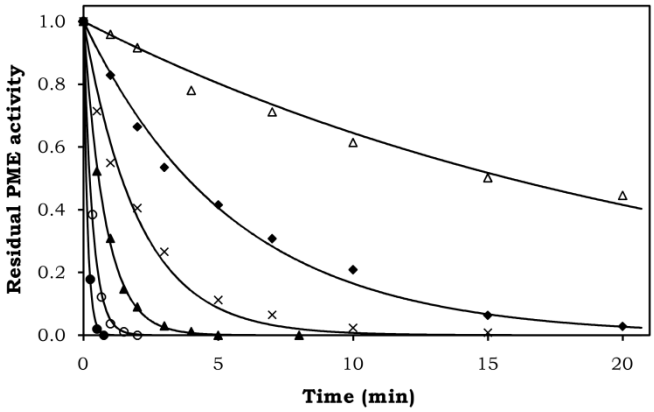

Figure 2.7. Effect of thermal denaturation of purified carrot PME (in 10 mM Na-phosphate pH 6.5) on its catalytic activity, modelled by nonlinear two-step regression of the first-order model (△ 52.5 °C, ♦ 55 °C, × 57.5 °C, ▲ 60 °C, ○ 62.5 °C and ● 65 °C). Residual activity values relative to the activity of an untreated sample are represented.

Table 2.1. Kinetic parameter estimates for first-order thermal inactivation of carrot PME (in 10 mM Na-phosphate pH 6.5), modelled by nonlinear two-step regression.

T (°C)	k (min^{-1})	Corr R^2
52.5	0.044 ± 0.002[a]	0.998
55	0.180 ± 0.006	0.998
57.5	0.489 ± 0.030	0.994
60	1.234 ± 0.020	0.999
62.5	3.006 ± 0.062	0.999
65	6.991 ± 0.154	0.999
E_a (kJ/mol)	323.3 ± 3.2[a]	
Corr R^2	0.999	

[a] Standard error of regression.

2.3.4.2 High-pressure inactivation of carrot PME

Only pressure levels of 700 MPa and higher were able to induce carrot PME inactivation at 25 °C within a reasonable time frame. In the pressure range from 700 to 800 MPa, pressure inactivation of purified carrot PME at 25 °C followed a first-order decay (**Figure 2.8**). Inactivation rate constants (k) and their pressure dependence, expressed in terms of activation volume (V_a), were estimated by nonlinear two-step regression (**Table 2.2**). Carrot PME proves to be barotolerant, but yet it is more pressure-sensitive than several other PMEs (e.g., tomato, banana and *Aspergillus aculeatus* PME) (Duvetter *et al.*, 2009).
As phosphate buffers are known to be unstable under high pressure, i.e., the pH decreases upon pressure increase (~ -0.3 units per 100 MPa) due to pressure-induced dissociation of weak acids (Neuman *et al.*, 1973), experiments were also performed in a pressure-stable imidazole-HCl buffer. High similarity between both sets of kinetic parameter estimates (results not shown) indicated that pressure inactivation of carrot PME is not controlled by pressure-induced pH changes.

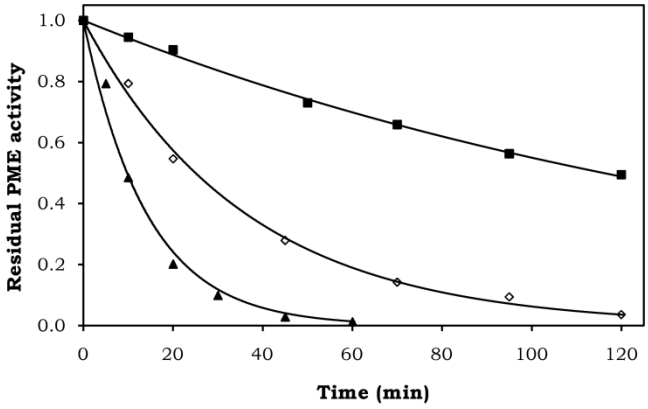

Figure 2.8. Effect of high-pressure denaturation (at 25 °C) of purified carrot PME (in 10 mM Na-phosphate pH 6.5) on its catalytic activity, modelled by nonlinear two-step regression of the first-order model (■ 700 MPa, ◊ 750 MPa and ▲ 800 MPa). Time 0 min represents the start of isothermal-isobaric conditions. Residual activity values relative to the activity of the 0 min blank are depicted.

Table 2.2. Kinetic parameter estimates for first-order high-pressure inactivation (at 25 °C) of purified carrot PME (in 10 mM Na-phosphate pH 6.5), modelled by nonlinear two-step regression.

***p* (MPa)**	***k* (min^{-1})**	**Corr R^2**
700	0.006 ± 0.0001[a]	0.999
750	0.028 ± 0.001	0.999
800	0.071 ± 0.005	0.994
V_a (cm^3/mol)	-51.1 ± 6.5[a]	
Corr R^2	0.997	

[a] Standard error of regression.

2.3.5 Effect of thermal or high-pressure denaturation of kiwi PMEI on its inhibitory capacity

The effect of a high-temperature or high-pressure denaturation of kiwi PMEI on its inhibitory capacity was investigated by treating purified kiwi PMEI at isothermal-isobaric conditions for different time intervals and measuring the residual inhibitory capacity towards carrot PME.

2.3.5.1 Model selection

Both sets of inactivation data (**Figure 2.9** and **2.10**) demonstrate the existence of a non-zero inhibitory capacity after prolonged treatment time. Mechanistically, this can be explained in two ways. On the one hand, the initial presence of two (or more) inhibitor fractions with different processing stabilities may be assumed. In this case, inactivation data may be fitted to a biphasic (Equation 2.2) or a fractional-conversion (Equation 2.3) model, with the residual non-zero activity arising from the existence of a processing-stable fraction, only affected by severe temperature or pressure conditions. On the other hand, it may be hypothesised that only one inhibitor fraction is initially present and that temperature and pressure induce the formation of an intermediate state of the inhibitor with a reduced specific inhibitory capacity. In the latter instance, a consecutive-step model (Equation 2.4 and 2.5) may apply, in which the residual inhibitory capacity after prolonged treatments originates from the PMEI intermediate created during the first step of the inactivation process.

In enzyme inactivation studies, several fractions with different processing stabilities are often associated with the existence of isoforms having differing protein characteristics (e.g., molar mass, pI etc.) (Ludikhuyze *et al.*, 2003; Plaza *et al.*, 2007). For kiwi PMEI, primary structure determination (Camardella *et al.*, 2000) and analysis of the kiwi fruit cDNA library (Irifune *et al.*, 2004) indicated the occurrence of several (> 2) isoforms (cf. Section 1.3.2.1), also suggested by the results of SDS-PAGE and MALDI-TOF MS in the current study (cf. Section 2.3.2). It seems reasonable to assume that these isoforms form the basis for two (or more) PMEI families with distinct processing stabilities, and the inactivation data were therefore primarily modelled (and represented in the following sections) according to this assumption.

However, given the lack of insight in the actual inactivation mechanism (at molecular level) and of decisive arguments supporting the existence of different initial PMEI families or rejecting the occurrence of an intermediate PMEI state, the consecutive-step approach was also examined. Compared to the biphasic/fractional-conversion approach, only minor differences in kinetic parameter estimates were observed (results not shown). This is not surprising, as both approaches mathematically coincide when the rate constant of the second step of the inactivation is very small or even negligible (as would be the case here). Only the origin of the non-zero residual inhibitory capacity (either A_2 or A_S/A_∞) differs, being a processing-induced PMEI intermediate on the one hand and an initially present processing-stable PMEI fraction on the other hand.

2.3.5.2 Thermal inactivation of kiwi PMEI

Thermal inactivation of kiwi PMEI in the temperature range from 55 °C to 95 °C, modelled according to the biphasic/fractional-conversion approach, is represented in **Figure 2.9**. At temperature values ≤ 75 °C, the fractional-conversion model (Equation 2.3) applied best, interpretable by the presence of a thermostable fraction of the inhibitor that is not inactivated in the mild temperature range even after prolonged treatments. From 85 °C on, however, PMEI inactivation was better described by a biphasic model (Equation 2.2), indicating that both the thermolabile and the thermostable fraction are affected under these conditions.

For all temperature levels studied, inactivation rate constants (k_L and, if appropriate, k_S) and percentages of the thermostable (A_∞ or A_S) and thermolabile fraction (A_L, only if $T \geq 85$ °C) were estimated by nonlinear regression analysis. As an expression for the temperature dependence of the rate constant of the

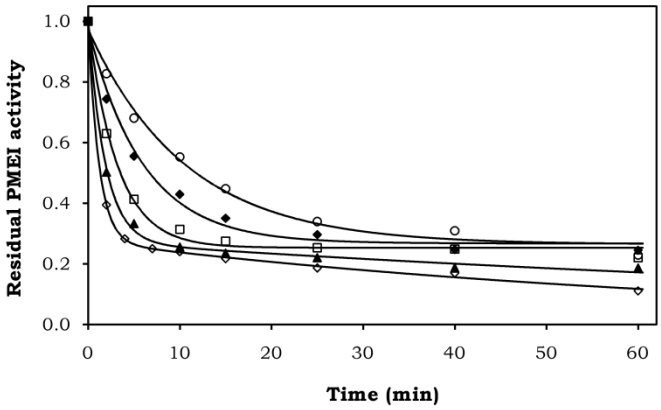

Figure 2.9. Effect of thermal denaturation of purified kiwi PMEI (in 10 mM Na-phosphate pH 6.5) on its inhibitory capacity, modelled by nonlinear two-step regression of the fractional-conversion (○ 55 °C, ♦ 65 °C and □ 75 °C) or biphasic model (▲ 85 °C and ◊ 95 °C). Residual activity values relative to the activity of an untreated sample are represented.

Table 2.3. Kinetic parameter estimates for thermal inactivation of purified kiwi PMEI (in 10 mM Na-phosphate pH 6.5), modelled by nonlinear two-step regression of the fractional-conversion (55 - 75 °C) or biphasic model (85 - 95°C).

T (°C)	k_L (min^{-1})	k_S (min^{-1})	A_L (%)	A_∞ or A_S (%)	Corr R^2
55	0.101 ± 0.001[a]	n/a[b]	n/a	26.4 ± 2.3	0.998
65	0.176 ± 0.016	n/a	n/a	27.0 ± 1.7	0.997
75	0.317 ± 0.021	n/a	n/a	25.4 ± 1.1	0.998
85	0.542 ± 0.042	0.008 ± 0.002	72.5 ± 2.3	26.9 ± 1.5	0.999
95	0.865 ± 0.037	0.014 ± 0.001	72.6 ± 1.0	26.9 ± 0.6	0.999
E_a (kJ/mol)	54.8 ± 1.3[a]				
Corr R^2	0.999				

[a] Standard error of regression. [b] n/a: not appropriate.

thermolabile PMEI fraction, the activation energy (E_a) was estimated. **Table 2.3** summarises the results of a two-step regression approach. The thermostable PMEI fraction contributed approximately a quarter of all inhibitory capacity and was only lost slowly at temperatures above 75 °C. In comparison with carrot PME, thermal inactivation of kiwi PMEI shows a limited temperature dependence, as judged by the respective E_a values.

2.3.5.3 High-pressure inactivation of kiwi PMEI

The kinetics of high-pressure inactivation of purified kiwi PMEI in the range of 500 to 800 MPa are represented in **Figure 2.10**. Notably, a substantial part of the PMEI inhibition capacity is already lost during the dynamic phase of the high-pressure process (i.e., pressure build-up and equilibration time), presumably due to the temperature rise caused by adiabatic heating. For the pressure range studied, PMEI inactivation could satisfactorily be described by the fractional-conversion model (Equation 2.3), explainable by the putative presence of a pressure-stable inhibitor fraction, which is not inactivated at the processing conditions applied. So, even prolonged pressurisation did not entirely obliterate the kiwi PMEI inhibition capacity.

Based on a two-step nonlinear regression approach, inactivation rate constants k_L and percentages of the non-inactivated inhibitory capacity A_∞ were estimated, as well as the pressure dependence V_a (**Table 2.4**). Depending on the pressure level, the pressure-stable fraction accounted for approximately 44 to 26% of the total PMEI inhibitory capacity. Not surprisingly, a negative V_a value was obtained, demonstrating that PMEI inactivation is accompanied by a volume decrease and, consequently, is favoured by an elevated pressure. The observation that the contribution of the pressure-stable fraction varies with the pressure-level applied may be attributed to a lack of data points at prolonged treatment times (i.e., > 60 min). Besides, however, it may be hypothesised that, dependent on the

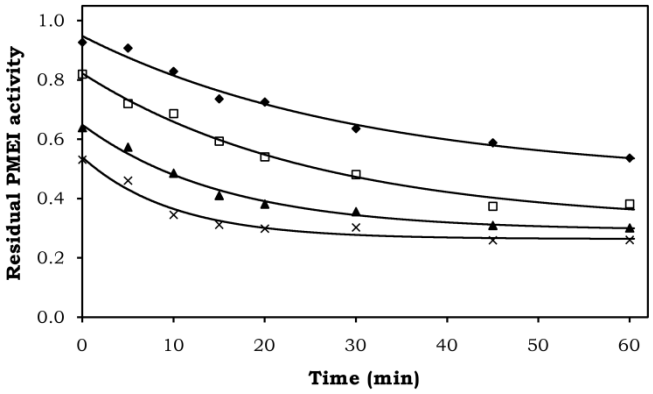

Figure 2.10. Effect of high-pressure denaturation (at 25 °C) of purified kiwi PMEI (in 10 mM MES-NaOH pH 6.5) on its inhibitory capacity, modelled by nonlinear two-step regression of the fractional-conversion model (♦ 500 MPa, □ 600 MPa, ▲ 700 MPa and × 800 MPa). Time 0 min represents the start of isothermal-isobaric conditions. Residual activity values relative to the activity of an untreated sample are depicted.

Table 2.4. Kinetic parameter estimates for high-pressure inactivation (at 25 °C) of purified kiwi PMEI (in 10 mM MES-NaOH pH 6.5), modelled by nonlinear two-step regression of the fractional-conversion model.

***p* (MPa)**	**k_L (min^{-1})**	**A_∞ (%)**	**Corr R^2**
500	0.027 ± 0.006[a]	43.9 ± 6.4	0.999
600	0.038 ± 0.005	31.2 ± 3.2	0.999
700	0.061 ± 0.006	28.9 ± 1.4	0.999
800	0.096 ± 0.016	26.3 ± 1.3	0.997
V_a (cm^3/mol)	-10.9 ± 0.4[a]		
Corr R^2	0.999		

[a] Standard error of regression.

pressure level, the various isoforms of PMEI are distributed differently over the two (pressure-labile and pressure-stable) PMEI fractions.

In addition to the inactivation study of PMEI in the pressure-stable MES buffer at pH 6.5, preliminary experiments were also performed using a pressure-sensitive Na-phosphate buffer (10 mM, pH 6.5). Remarkably, in the latter buffer, no loss of inhibition capacity occurred, even after a treatment of 60 min at 700 MPa. Since the pH of a phosphate buffer is thought to decrease with 2 units at 700 MPa (Neuman *et al.*, 1973), it was assumed that the low pH at elevated pressure (i.e., approx 4.5) was responsible for the lack of PMEI inactivation. This assumption was confirmed by the absence of inhibition capacity loss after 60 min at 700 MPa in the (relatively) pressure-stable Na-acetate buffer pH 4.5. The putative pressure stability of kiwi PMEI at low pH values opens perspectives for its use in acidic food systems to inhibit undesired PME activity, remaining after high-pressure processing (e.g., fruit juices).

2.3.6 Effect of elevated temperature or pressure on carrot PME activity in absence and presence of kiwi PMEI

2.3.6.1 Effect of elevated temperature

The carrot PME catalytic activity V_0 at elevated temperatures both in absence and presence of kiwi PMEI was determined by measuring the amount of methanol released during PME-catalysed pectin hydrolysis as a function of treatment time (**Figure 2.11**).

In absence of inhibitor, PME activity increased with increasing temperature from 25 up to 55 °C, according to the Arrhenius law. For this temperature range, an activation energy E_a of 25.0 ± 5.6 kJ/mol (Corr R^2 = 0.984) could be estimated. At temperatures above 55 °C, PME activity gradually reduced, attributed to the simultaneous occurrence of heat inactivation of the enzyme, as depicted by the thermal inactivation kinetics of purified carrot PME (cf. Section 2.3.4.1). As a matter of fact, a comparison with these inactivation results allows concluding that PME heat inactivation is clearly retarded in the presence of its substrate pectin. Sila *et al.* (2007a) reported a temperature optimum of carrot PME activity at 50 °C and an estimated E_a of 48.9 ± 6.9 kJ/mol. Differences in experimental set-up (e.g., prolonged equilibration time of 3 min) and enzyme extract

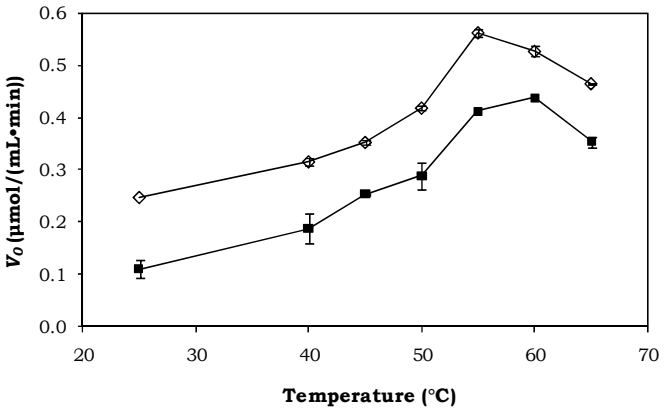

Figure 2.11. Effect of temperature on the carrot PME activity V_0 (in µmol/(mL·min)) in the absence (◊) and presence (■) of kiwi PMEI. In the latter case, the molar ratio of PME to PMEI is approx. 1:0.5. Each point represents the mean of repeated measurements (n = 2, ± standard error).

composition, used in their study, can partly explain the differences with the current results.

In the presence of kiwi PMEI, the carrot PME reaction rate constant V_0 as a function of temperature displayed a course parallel to the one without inhibitor: a gradual increase up to 55 - 60 °C, before declining (**Figure 2.11**). The distance between both curves, which is a measure for the amount of inhibited PME, was similar at all temperatures studied. These results suggest that the active, uninhibited PME has a temperature behaviour identical to PME in absence of PMEI, while the inhibited PME remains blocked during the temperature treatments. PMEI inactivation occurring at temperatures above 55 °C (as determined in the PMEI inactivation study in Section 2.3.5.2) is not accompanied by the net release of active enzyme, or by complex dissociation. Contrary to the current findings, Ly-Nguyen *et al.* (2004) interpreted a similar evolution of the PME reaction rate constant in the presence of PMEI as the occurrence of complex dissociation. However, the lack of a PME blank and the presence of an excess amount of PMEI in the latter study hamper reliable comparisons and conclusions.

2.3.6.2 Effect of elevated pressure

The reaction rate constant V_0 of the PME-catalysed demethoxylation of pectin as a function of pressure is depicted in **Figure 2.12**. In a system containing pectin and PME only, the catalytic activity increased with increasing pressure from 0.1 to 300 MPa. Based on the Eyring equation, an activation volume V_a of -7.4 ± 1.6 cm^3/mol (Corr R^2 = 0.995) was estimated. The stimulating effect of elevated pressure on PME activity at room temperature has been previously illustrated for partially purified carrot PME (Sila *et al.*, 2007a), tomato PME (Verlent *et al.*, 2004) and recombinant *A. aculeatus* PME (Duvetter *et al.*, 2006a), among others (Duvetter *et al.*, 2009). A possible explanation is that PME action is accompanied

by a volume reduction due to electrostriction, i.e., the compact alignment of water dipoles in the proximity of the charged groups created by pectin de-esterification. At pressure levels from 400 to 700 MPa, the PME-catalysed reaction was retarded and the reaction rate was even reduced below its level at atmospheric pressure. The gradual activity decrease in this pressure range could adequately be described by the Eyring equation, resulting in a positive activation volume V_a of 13.8 ± 0.4 cm^3/mol (Corr R^2 = 0.999). Since irreversible inactivation of carrot PME only occurs at very high pressure levels (≥ 700 MPa) for prolonged treatment times (as described in Section 2.3.4.2), the observed retardation of PME action at elevated pressure would rather be attributed to a reversible enzyme unfolding/inactivation or, possibly, to pressure-induced structural changes in the pectin, rendering the substrate less susceptible. Further research would be valuable to give a decisive answer.

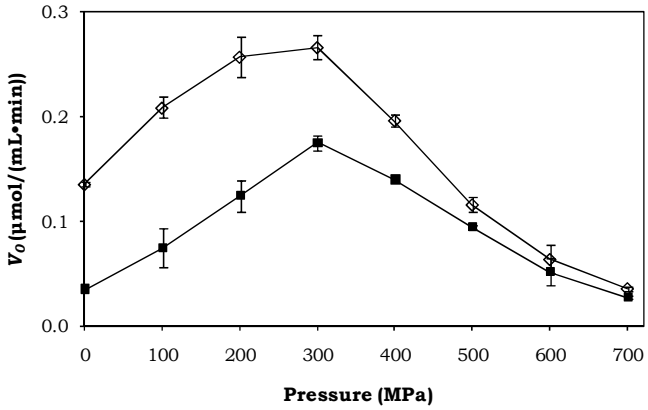

Figure 2.12. Effect of pressure on the carrot PME activity V_0 (in µmol/(mL·min)) in the absence (◊) and presence (■) of kiwi PMEI. In the latter case, the molar ratio of PME to PMEI is approx. 1:0.7. Each point represents the mean of repeated measurements (n = 2, ± standard error).

The rate of methanol formation was also followed in a system consisting of pectin, PME and PMEI (**Figure 2.12**). Two pressure domains could be distinguished. Up to 300 MPa, the PME reaction accelerated with increasing pressure, analogously to the situation without PMEI addition. The active, uninhibited PME displayed a pressure behaviour identical to PME in absence of PMEI, while the inhibited PME apparently remained blocked. There was no net release of active enzyme. Above 300 MPa, the difference in V_0 of carrot PME with and without PMEI gradually diminished, pointing to a declining amount of inhibited PME. This tendency indicates a pressure-induced dissociation of the PME-PMEI complex. While the liberated kiwi PMEI may be partly inactivated irreversibly, the liberated carrot PME behaves similarly to the other PME present, i.e., a putative reversible inactivation. Ly-Nguyen *et al.* (2004) performed similar experiments, but with an excess amount of kiwi PMEI present. From a similar course of V_0 it was concluded that the PME-PMEI complex dissociates at elevated pressures from 100 MPa on. Unfortunately, the different experimental set-up in the latter study

(e.g., excess amount of kiwi PMEI and lack of a PME blank) complicates comparison.

2.4 CONCLUSION

Carrot PME and kiwi PMEI were successfully purified from the respective plant sources by an affinity chromatography technique based on the strong PME-PMEI interaction. Using these purified protein solutions, enzyme and inhibitor activity and stability, as influenced by intrinsic product factors (pH and NaCl) and extrinsic process factors (temperature and hydrostatic pressure), were studied quantitatively. Kinetic modelling was applied where appropriate.

Carrot PME catalytic activity is markedly influenced by intrinsic factors such as pH and salt concentration. Additionally, extrinsic factors like high temperature and high pressure strongly affect the PME action: the PME-catalysed pectin hydrolysis is stimulated by intermediate temperature ($T \leq 55$ °C) or pressure ($p \leq$ 300 MPa at 25 °C) levels, whereas higher levels cause a reduced rate of product formation. However, if different processing conditions are applied, temperature and pressure can also lead to irreversible inactivation of undesired PME, although carrot PME being rather barotolerant. Consequently, both conventional thermal processing and emerging hydrostatic pressure processing prove to be valuable tools to direct the PME-catalysed pectin hydrolysis.

Besides processing, PME inhibition by kiwi PMEI can be an alternative or additional approach to control endogenous PME activity (e.g., to obtain cloud-stable juices). Based on the experimental results, it is clear that pH and salt concentration are determining factors with respect to inhibition strength. Both high temperature and high pressure induce a loss of inhibitory capacity of kiwi PMEI, but a processing-resistant fraction will remain even after prolonged processing (contrary to PME activity under the same conditions). Moreover, this study shows that the PME-PMEI complex is not dissociated by temperature ($T \leq$ 65 °C) and relatively low pressure ($p <$ 400 MPa at 25 °C) levels. These observations endorse the possibility of inhibition of undesired PME activity remaining after mild processing through pre-processing addition of PMEI. To validate these findings, extension to real food matrices is required.

3

PLANT PME AND KIWI PMEI: INTERACTION ANALYSIS BY SURFACE PLASMON RESONANCE[3]

3.1 INTRODUCTION

For efficient application of kiwi PMEI in either plant PME inhibition or its detection, insight in the PME-PMEI interaction, as influenced by intrinsic product factors and extrinsic process factors, is required. To improve this insight, the results obtained with the more common enzyme inhibition measurements, described in Chapter 2, can be extended by means of a biosensor technique based on surface plasmon resonance (SPR).

In this chapter, the development of an SPR-based interaction analysis method to study the binding between plant PME and kiwi PMEI was aimed at. SPR biosensors combined with miniaturised flow channels permit label-free and real-time quantitative monitoring of the interaction (and its kinetics) between two biomolecules (e.g., proteins), of which one is attached to a surface and the other one is free in solution. The SPR optical detection is based on the determination of changes in refractive index induced at the detector surface upon binding or dissociation (Löfas and Johnsson, 1990; Huber and Mueller, 2006). Immobilisation of both enzyme and inhibitor were intended.

Once implemented, this SPR-method was applied to analyse the binding kinetics of purified kiwi PMEI towards two plant PMEs (i.e., the main PMEs from carrot and tomato) and to investigate the effect of pH and NaCl concentration on their interaction. Moreover, the effect of a temperature- or pressure-induced denaturation of (carrot) PME on its affinity towards kiwi PMEI was studied.

---

[3] This chapter is based on the following paper:
Jolie, R.P., Duvetter, T., Houben, K., Vandevenne, E., Van Loey, A.M., Declerck, P.J., Hendrickx, M.E., Gils, A. (2010). Plant pectin methylesterase and its inhibitor from kiwi fruit: Interaction analysis by surface plasmon resonance. *Food Chemistry*, 121(1), 207-214.

3.2 MATERIALS AND METHODS

3.2.1 Materials

Young Belgian red carrots (*Daucus carota* cv. Sirena), tomatoes (*Lycopersicon esculentum* cv. Admiro) and green kiwi fruits (*Actinidia deliciosa* cv. Hayward) were purchased from a local supermarket. Apple pectin (degree of methyl-esterification: 70 - 75%) was obtained from Fluka (Buchs, Switzerland) and the EZ-Link® Micro Sulfo-NHS-LC-Biotinylation Kit from Thermo Fisher Scientific (Waltham, MA, United States). Chemicals for the SPR-based interaction analysis experiments were from GE Healthcare Bio-Sciences AB (Uppsala, Sweden). All other chemicals were of analytical grade.

3.2.2 Extraction and purification of plant PMEs and kiwi PMEI

Extraction and preparative affinity chromatography purification of carrot PME and kiwi PMEI were performed as described in Sections 2.2.2 and 2.2.3.
Tomato PME was extracted from whole ripe tomato fruits according to the method of Fachin *et al.* (2002) with some minor modifications. Tomatoes (1 kg) were homogenised in a blender (without addition of water) and centrifuged at 10000 × *g* for 30 min (4 °C). The supernatant was discarded, while the pellet was mixed end-over-end for 2 h at 4 °C with 0.2 M Tris-HCl buffer pH 8.0 containing 1.0 M NaCl (1:2.5 w/v) for the extraction of cell-wall-bound PME. Afterwards, the salt extract was collected by centrifugation (10000 × *g* for 60 min, 4 °C) and partially purified by ammonium sulphate precipitation. The fraction precipitating between 30% and 80% ammonium sulphate saturation was collected by centrifugation at 18000 × *g* (15 min, 4 °C) and dissolved in 20 mM Tris-HCl buffer pH 7.0. This crude extract, containing PME, was stored frozen at -80 °C until further purification by affinity chromatography. For the chromatography step, the same procedure as outlined previously for carrot PME (cf. Section 2.2.2) was followed.
All concentrated, purified enzyme and inhibitor solutions were quickly frozen in liquid N_2 and stored at -80 °C until use.

3.2.3 PME activity assay

PME activity was measured by the continuous titration of carboxyl groups formed during pectin de-esterification, using an automatic pH-stat titrator (Metrohm, Herisau, Switzerland) with 0.01 M NaOH. Routine assays were performed at pH 6.5 and 22 °C, using 30 mL of a 0.35% (w/v) apple pectin solution containing 0.117 M NaCl. By definition, one unit (U) of PME activity is the amount of enzyme catalysing the hydrolysis of 1 µmol of methyl-ester bonds per min under aforementioned conditions.

3.2.4 Protein content

The protein content of PME and PMEI solutions was determined using the BCA kit according to Sigma procedure TPRO-562 (Sigma, Darmstadt, Germany). The

protein concentration (mg/mL) was calculated by comparison with a standard curve of bovine serum albumin (cf. Section 2.2.5).

3.2.5 Thermal and high-pressure treatments

Purified carrot PME was thermally treated in a temperature-controlled water bath. The enzyme solution (0.07 mg/mL in 10 mM Na-phosphate buffer pH 6.5, a buffer with a small $\Delta pK_a/\Delta T$) was enclosed in 200 µL glass capillaries (Brand, Wertheim, Germany) to ensure isothermal heating. After 5 min at different temperature levels between 25 and 60 °C, samples were withdrawn from the water bath and immediately cooled in ice water.
Pressure treatment of purified carrot PME was conducted in a laboratory-scale high-pressure device (Resato, Roden, The Netherlands) with eight reactors, each surrounded by a thermostatted mantle connected to a cryostat. The pressure medium was a propylene glycol - water mixture (PG fluid, Resato). Flexible microtubes (0.3 mL, Carl Roth, Karlsruhe, Germany) were filled with the protein solution (0.07 mg/mL in 10 mM MES buffer pH 6.5) and enclosed in the pressure reactors, already equilibrated to 25 °C. MES buffer was chosen because of its putative pressure stability, in contrast to Na-phosphate buffer (cf. Section 2.2.8.1). Pressure was built up slowly to 800 MPa (100 MPa/min, to minimise temperature increase due to compression heating) and all pressure reactors were isolated. After preset time intervals (up to 60 min), individual reactors were depressurised instantaneously and samples were cooled in an ice water bath.
Part of each treated PME sample was used to measure the residual enzyme activity (within 1 h of storage in ice water). The remainder was quickly frozen with liquid N_2 and stored at -80 °C until SPR interaction analysis (as described in Section 3.2.7). Freezing and thawing caused only a minor PME activity loss.

3.2.6 SPR interaction analysis with immobilised plant PME[4]

3.2.6.1 Chip surface preparation

Real-time interaction analysis by surface plasmon resonance (SPR) with immobilised plant PME was performed on a Biacore™ 3000 analytical system (GE Healthcare Bio-Sciences AB). Amine coupling of both tomato and carrot PME on parallel flow cells of a CM5 sensor chip was carried out by injecting the proteins (8 µg/mL) in 10 mM sodium acetate pH 4.5, following activation of the carboxymethylated dextran surface using a 1:1 mixture of 0.05 M *N*-hydroxysuccinimide (NHS) and 0.2 M 1-ethyl-3-(3-dimethylaminopropyl)-carbodiimide (EDC), according to Löfas and Johnsson (1990). Throughout the immobilisation process, HBS-EP (= 0.01 M 4-(2-hydroxyethyl)-piperazine-1-ethanesulfonic acid (HEPES) pH 7.4 containing 0.15 M NaCl, 3 mM EDTA and 0.005% Surfactant P20) was used as running buffer at 5 µL/min. After immobilisation of the PMEs, excess reactive groups on the surface were deactivated by a 7-minute liquid pulse of 1.0 M ethanolamine pH 8.5. Sensor chips were coupled up to 1500 - 2000 RU of protein.

[4] All SPR interaction analyses on Biacore 3000 were performed in cooperation with the Laboratory for Pharmaceutical Biology, K.U.Leuven.

3.2.6.2 Interaction measurements

Biacore 3000 sensorgrams, plotting resonance units (RU) versus time, were recorded at a flow rate of 30 µL/min at room temperature, using different concentrations of analyte (0 - 200 nM kiwi PMEI) in a running buffer with defined pH or NaCl concentration. Association and dissociation data were both collected for 6 min. At the end of each run, the sensor chip was regenerated by a 10 µL injection of 1 mM NaOH. All binding data were referenced against a parallel microfluidic flow cell with coupled T94H3, a monoclonal antibody raised against human thrombin activatable fibrinolysis inhibitor (Gils *et al.*, 2005).
Sensorgrams were analysed using BIAEVALUATION 3.2 software. The experimental data were fitted to a single-site interaction model (1:1 Langmuir binding: A + B ↔ AB, with A the analyte and B the surface-bound ligand). Assuming pseudo first-order interaction kinetics, the rate of complex formation during sample injection is given by:

$$\frac{\mathrm{d[AB]}}{\mathrm{d}t} = k_a[\mathrm{A}][\mathrm{B}] - k_d[\mathrm{AB}] \qquad 3.1$$

which may be expressed in terms of the SPR signal as:

$$\frac{\mathrm{d}R}{\mathrm{d}t} = k_a C R_{max} - (k_a C + k_d)R \qquad 3.2$$

where $\mathrm{d}R/\mathrm{d}t$ is the rate of change of the SPR signal, C the concentration of analyte, R_{max} the maximum analyte binding capacity (in RU), and R the SPR signal at time t (in RU). Dissociation rate constants (k_d) were estimated from the data collected during the dissociation phase ($\mathrm{d}R/\mathrm{d}t = -k_dR$), while association rate constants (k_a) were derived from the above rate equation for complex formation (Equation 3.2). Numerical integration algorithms were used. From the average values of the rate constants at different analyte concentrations, the dissociation equilibrium constant (K_D) was calculated ($K_D = k_d/k_a$).

3.2.7 SPR interaction analysis with immobilised kiwi PMEI

3.2.7.1 Chip surface preparation

For real-time interaction analysis by SPR with immobilised kiwi PMEI, the same Biacore™ 3000 system was used. Prior to the immobilisation of kiwi PMEI, the protein was biotinylated by means of an EZ-Link® Micro Sulfo-NHS-LC-Biotinylation Kit. Hereto, kiwi PMEI dissolved in phosphate-buffered saline (PBS) pH 7.2 was mixed with a fivefold molar excess of a water-soluble biotin derivative (sulfo-NHS-LC-biotin) and incubated for 30 min at 25 °C. Subsequently, biotinylated kiwi PMEI was separated from unbound biotin and the sulfo-NHS leaving group on a Zeba™ Desalt Spin Column (7 kDa MWCO). By high affinity capture, biotinylated PMEI was immobilised on a SA sensor chip, upon which streptavidin had previously been coupled. A continuous flow of HBS-EP pH 7.4 at 5 µL/min was maintained during the entire immobilisation process. First, the chip surface was conditioned with 3 pulses of 5 µL of 1.0 M NaCl in 50 mM NaOH. Then, biotinylated PMEI (20 µg/mL) in 0.1 M Na-phosphate pH 7.2 containing 0.3 M NaCl was coupled until a level of 500 RU was reached.

3.2.7.2 Interaction measurements

Once the PMEI ligand was coupled, interaction measurements could be performed on the chip. Sensorgrams (RU *vs.* time) were monitored at a flow rate of 30 µL/min at room temperature by injection of different concentrations of analyte (0 - 30 nM carrot PME) in running buffer (0.15 M Na-phosphate pH 6.0). Association and dissociation data were both recorded for 6 min. After each run, chip surface regeneration was performed with 5 µL of a 5 mM NaOH solution. Binding data were referenced against an unmodified streptavidin surface. Sensorgrams were analysed with BIAEVALUATION 3.2 software. Binding curves were best fitted to a single-site interaction model (as described in Section 3.2.6.2) taking into account mass transport limitations. Association and dissociation rate constants (k_a and k_d) were estimated and used to calculate the dissociation equilibrium constant (K_D).

3.3 RESULTS AND DISCUSSION

3.3.1 Extraction and purification of plant PMEs and kiwi PMEI

Cell-wall-bound PME was extracted from raw carrot roots and tomato fruits using high salt concentration and ammonium sulphate precipitation. Crude yields of about 5000 U carrot PME and 50000 U tomato PME per kg of raw material were obtained. By use of a single-step affinity chromatography method on a kiwi PMEI – NHS-activated Sepharose matrix, PME was selectively isolated. Chromatograms of both carrot (**Figure 2.1**) and tomato PME (**Figure 3.1**) showed a double UV protein peak. As separation of the PMEs on the PMEI affinity column indicates different binding behaviour towards kiwi PMEI, all further experiments were performed with pools of merely the main, most abundant carrot PME and tomato PME isoform, eluting before the second elution peak, not to hamper the interpretation of the SPR interaction analyses.

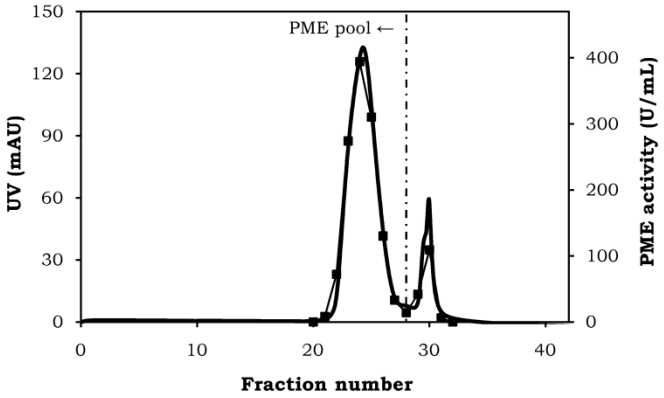

Figure 3.1. Affinity chromatography elution profile of tomato PME on an activated Sepharose column, illustrating UV absorbance at 280 nm (—) and PME activity in the different fractions (■). Fractions eluting before appearance of the second elution peak were pooled.

PMEI was extracted from ripe green kiwi fruits and purified by a single-step affinity chromatography method on an orange PME – CNBr-activated Sepharose matrix, as described elaborately in Sections 2.2.3 and 2.3.2.
Extract purity of enzymes and inhibitor was confirmed by means of MALDI-TOF MS and gel electrophoresis, according to the methods outlined in Sections 2.2.6 and 2.2.7. The results for carrot PME and kiwi PMEI were discussed in the previous chapter (Sections 2.3.1 and 2.3.2, respectively). With regard to tomato PME, the reader is referred to the work of Vandevenne *et al.* (2009). In the latter study, the same tomato PME extract (named t1PME) displayed a single ion peak of 34.5 kDa on the MALDI-TOF mass spectrum, and was identified as the major isoform of PME in tomato fruit by N-terminal sequencing, peptide mass fingerprinting and LC-MS/MS.
Specific enzyme activities of carrot PME and tomato PME were estimated at 450 U/mg and 600 U/mg, respectively. Carrot and tomato were selected because of their food technological relevance and the expected differences in affinity of their PMEs towards kiwi PMEI, as indicated by the work of Ly-Nguyen *et al.* (2004).

3.3.2 SPR interaction analysis with immobilised plant PME: method development

3.3.2.1 Surface preparation

An SPR-based interaction analysis method was implemented to study kinetics of the binding between plant PME and its proteinaceous inhibitor from kiwi fruit on a Biacore™ 3000 analytical system. Hereto, plant PME was covalently immobilised on the surface of a sensor chip. Random amine coupling was selected to be the preferential ligand immobilisation chemistry. In this coupling reaction, a stable amide bond is spontaneously formed between available amino groups on the protein (at Lys side chains or at the N-terminus) and the reactive succinimide esters, introduced on the carboxymethylated dextran surface of the chip (CM5) by treatment with a mixture of *N*-hydroxysuccinimide and carbodiimide. A coupling buffer with a low ionic strength and a pH between 3.5 and the pI of the ligand (i.e., > 9 for tomato and carrot PME) was chosen to promote electrostatic preconcentration of the positively charged ligand on the negatively charged dextran surface. This preconcentration enabled efficient immobilisation from a dilute ligand solution (i.e., 8 µg/mL). Immobilisation was continued until a coupling degree of 1500 - 2000 RU was reached, corresponding to approximately 1500 - 2000 pg of bound protein per mm^2. This coupling level allowed reliable quantitative kinetic experiments. Unoccupied reactive esters were deactivated by means of a low molar mass amine in a high ionic strength solution (i.e., 1.0 M ethanolamine-HCl pH 8.5), at the same time removing noncovalently bound material from the surface.

3.3.2.2 Interaction measurements

After surface preparation, the actual interaction measurements could be executed. During the association phase, analyte (i.e., kiwi PMEI) in an appropriate running buffer was injected over the PME-coated surface at a flow rate of 30 µL/min. A range of analyte concentrations (i.e., 0 - 200 nM) was

applied to allow accurate determination of rate constants. During the dissociation phase, sample injection was replaced by a buffer flow, due to which analyte was partly washed away from the surface. As kiwi PMEI and plant PMEs have been shown to form a 1:1 complex (Giovane *et al.*, 1995), the experimental sensorgrams were fitted to a single-site interaction model (Equations 3.1 and 3.2) and association and dissociation rate constants were estimated. Prior to the modelling, acquired binding data were corrected for changes in the bulk refractive index (and so, in the SPR response), e.g., due to small mismatches between running buffer and analyte solutions. Hereto, a parallel flow cell was coated with a non-reactive protein (i.e., MA-T94H3) not showing affinity towards the analyte, and the SPR response of this blank flow cell was subtracted from the response of the binding flow cell. The blank flow cell also allowed detection of (certain cases of) unspecific binding. Representative real-time binding sensorgrams of the interaction of kiwi PMEI and immobilised tomato and carrot PME are shown in **Figure 3.2** (A and B, respectively). At all analyte concentrations, the required curvature in the association phase and decay in the dissociation phase are perceptible.

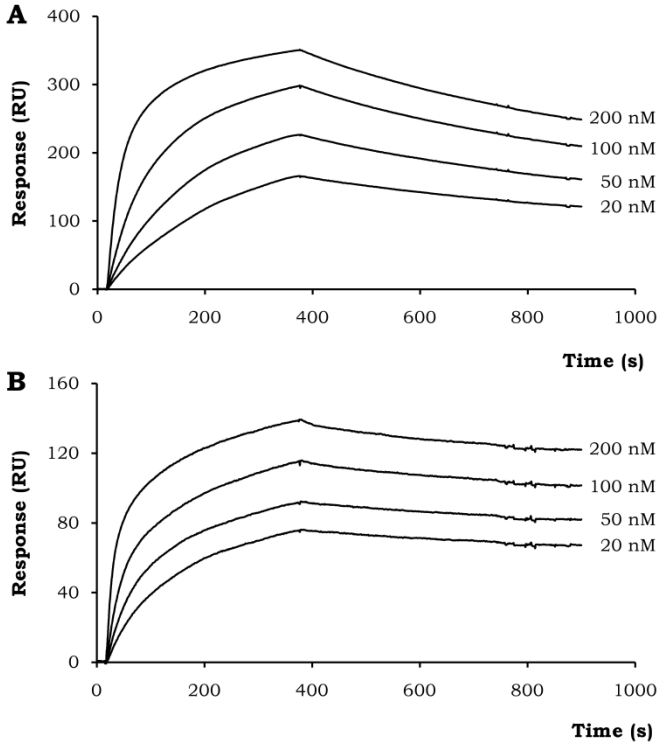

Figure 3.2. Representative binding sensorgrams obtained from SPR analysis showing the interaction of (A) kiwi PMEI and immobilised tomato PME, and (B) kiwi PMEI and immobilised carrot PME. Varying analyte concentrations were injected over the surface, as indicated on the sensorgrams. Measurements were performed at room temperature in 0.15 M Na-phosphate pH 6.0.

To enable reuse of the same PME-coated chip, the surface was regenerated after each run. A 10 µL injection of 1 mM sodium hydroxide was selected to adequately remove all bound material from the chip without significantly affecting the binding capacity of the surface.
To exclude the occurrence of mass transport limitations in the experimental setup described above, preliminary experiments were performed both with reduced degree of coupling (ca. 500 RU of carrot PME) and varying flow rate (10 - 50 µL/min) during association (with 0.15 M Na-phosphate pH 6.0 as running buffer). Sensorgrams coincided and parameter estimates did not differ significantly for the various conditions tested, indicating that it was not the transport of the analyte to the surface but its binding to the ligand that was the rate-limiting factor, determining the rate constant estimation.

3.3.3 Effect of pH on the PME-PMEI binding by SPR interaction analysis

The effect of pH on the interaction between kiwi PMEI (with pI ~ 3.5 - 4.8) and two plant PMEs (i.e., the main isoforms of tomato and carrot PME, both with pI > 9) was investigated by SPR interaction analysis with immobilised plant PME, according to the method expounded in Section 3.3.2. To span the pH range from 3.0 to 9.0, 0.15 M Na-acetate (pH 3.0 to 7.0) and 0.15 M Na-phosphate (pH 5.0 to 9.0) were selected as running buffers. Since the choice of buffer was found not to influence the relative trends in the experimental data at pH 5.0 to 7.0 but only slightly to affect the absolute values of the parameter estimates, only results for Na-phosphate as running buffer are presented. **Table 3.1** summarises the binding parameter estimates at various pH values for both tomato and carrot PME.
Reliable binding parameters could only be estimated in the pH range from 5.0 to 7.0. At higher pH values (≥ 8.0) no binding was detected, whereas at lower pH values (≤ 4.0) experimental limitations occurred, i.e., unspecific adsorption of analyte on all flow cells at pH 4.0 and irreversible chip damage at pH 3.0 due to PME denaturation (confirmed by means of enzyme activity measurements after incubation of PME at pH 3.0). Within the intermediate pH range, similar trends were observed for PMEI binding to tomato and carrot PME: a pH increase resulted in a rise of K_D, indicating a weaker binding. This tendency could mainly be attributed to a faster dissociation (i.e., larger k_d), while the association rate (k_a) did not alter significantly. Representative sensorgrams for the interaction of kiwi PMEI (at one selected concentration, i.e., 100 nM) with tomato and carrot PME at various pH values are represented in **Figure 3.3**. These sensorgrams demonstrate that, in addition to a higher dissociation rate, a pH increase was also accompanied by a reduced amount of bound analyte.
Although the global pH effect on the PMEI binding to tomato PME and carrot PME was largely similar, the actual K_D estimates revealed marked differences between the PMEs of both plant sources. In the pH range from 6.0 to 7.0, the interaction strength with tomato PME was notably lower, whereas K_D values were comparable at pH 5.0. Existing differences could be mainly explained in terms of dissociation rates. Once formed, the kiwi PMEI - carrot PME complex separated more slowly than the complex with tomato PME, except at pH 5.0.

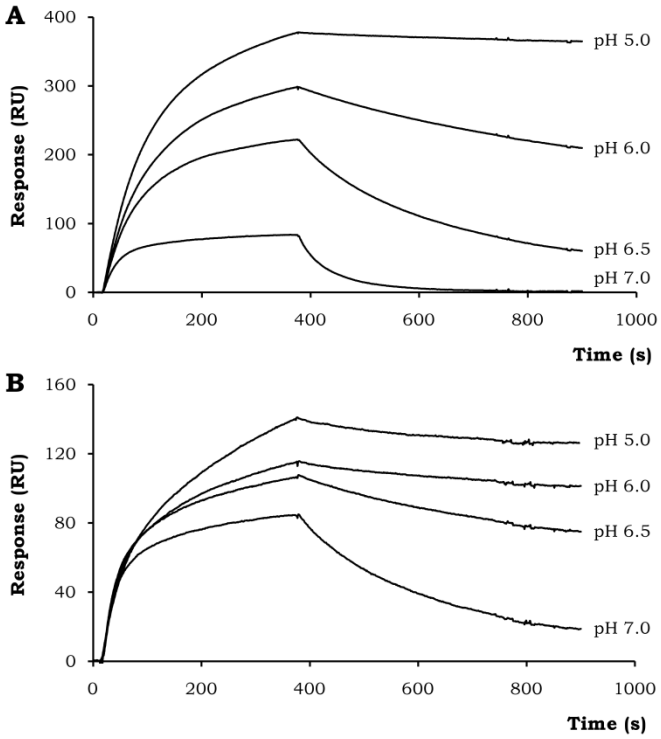

Figure 3.3. Binding sensorgrams obtained from SPR analysis showing the effect of pH on the interaction of (A) kiwi PMEI and immobilised tomato PME, and (B) kiwi PMEI and immobilised carrot PME. Kiwi PMEI (100 nM) was injected over the surface in running buffers with various pH values, as indicated on the sensorgrams. Measurements were performed at room temperature in 0.15 M Na-phosphate.

An initial, small-scale study on the binding of kiwi PMEI to tomato PME with SPR interaction analysis on a Biacore X system was already conducted by Mattei *et al.* (2002). Dissociation constants of 5.0 nM at pH 6.0 and 53 nM at pH 7.0 were reported, quite in line with the current results. The small difference with the K_D at pH 7.0 in the present study can be ascribed to the less accurate estimations of k_d at that pH (in both studies), as they are close to the measuring limit of the Biacore systems. Based on fluorescence quenching and gel filtration experiments with tomato PME and kiwi PMEI, D'Avino *et al.* (2003) observed good complex formation at pH 6.5 (K_D = 5 nM) and 7.0 (K_D = 50 nM), but decreasing complex stability at higher pH values (K_D = 350 nM at pH 7.5) and even no complex formation at pH 8.5. Both former studies are in accordance with the current observation that the complex of kiwi PMEI with tomato PME, like with carrot PME, is strongly pH-dependent, the affinity decreasing as the pH increases. This pronounced pH effect was also observed for the PMEI binding to kaki (persimmon) PME, whereas pH had only a limited influence on the interaction with kiwi PME (Ciardiello *et al.*, 2004; Ciardiello *et al.*, 2008). In SPR and gel filtration experiments, the kiwi PME-PMEI complex showed almost no

Table 3.1. Effect of pH on the interaction between kiwi PMEI and plant PME, expressed in terms of kinetic binding parameters derived from SPR data. Rate constants represent the average of measurements at four different PMEI concentrations (± SD). Measurements were performed at room temperature in 0.15 M Na-phosphate.

pH	Tomato PME			Carrot PME		
	k_a (10^5 M^{-1} s^{-1})	k_d (10^{-4} s^{-1})	K_D (nM)	k_a (10^5 M^{-1} s^{-1})	k_d (10^{-4} s^{-1})	K_D (nM)
9.0	No binding			No binding		
8.0	No binding			No binding		
7.0	1.01 ± 0.22	117 ± 11.4	116 ± 27	1.71 ± 0.53	30.1 ± 1.9	17.6 ± 5.6
6.5	0.93 ± 0.18	24.7 ± 1.21	26.6 ± 5.5	1.64 ± 0.08	6.52 ± 0.59	3.98 ± 0.41
6.0	1.09 ± 0.08	6.30 ± 0.21	5.78 ± 0.45	1.55 ± 0.52	2.09 ± 0.18	1.35 ± 0.47
5.0	1.05 ± 0.17	0.60 ± 0.13	0.569 ± 0.156	1.73 ± 0.98	1.59 ± 0.30	0.919 ± 0.552
4.0	Unspecific adsorption			Unspecific adsorption		
3.0	Chip damage			Chip damage		

Table 3.2. Effect of NaCl concentration on the interaction between kiwi PMEI and plant PME, expressed in terms of kinetic binding parameters derived from SPR data. Rate constants represent the average of measurements at four different PMEI concentrations (± SD). Measurements were performed at room temperature in 0.15 M Na-acetate pH 6.0.

[NaCl] (M)	Tomato PME			Carrot PME		
	k_a (10^5 M^{-1} s^{-1})	k_d (10^{-4} s^{-1})	K_D (nM)	k_a (10^5 M^{-1} s^{-1})	k_d (10^{-4} s^{-1})	K_D (nM)
0.0	1.11 ± 0.05	7.18 ± 0.24	6.48 ± 0.38	3.10 ± 0.39	1.43 ± 0.02	0.46 ± 0.06
0.125	0.45 ± 0.15	11.9 ± 0.24	26.3 ± 8.8	1.40 ± 0.40	5.64 ± 1.32	4.03 ± 1.48
0.25	0.25 ± 0.18	15.9 ± 0.94	64.0 ± 30.0	1.22 ± 0.09	7.58 ± 1.32	6.23 ± 1.17
0.50	0.19 ± 0.11	22.3 ± 1.59	115 ± 64	0.533 ± 0.165	12.2 ± 2.6	22.9 ± 8.6
0.75	0.15 ± 0.05	27.3 ± 3.96	181 ± 61	0.385 ± 0.124	18.1 ± 3.1	46.9 ± 17.1
1.00	0.09 ± 0.02	27.4 ± 2.67	289 ± 75	0.328 ± 0.072	21.6 ± 1.5	66.0 ± 15.2

dissociation in the pH range 3.5 to 8.0 and only complete separation at pH 10.0. The dissociation rate at pH 9.5 was similar to that observed for tomato PME at pH 7.0.

In Chapter 2, inhibitory capacity measurements were applied to assess the effect of pH on the binding between kiwi PMEI and carrot PME (cf. Section 2.3.3.1). Strong enzyme inhibition was observed at pH 6.0 to 7.0, whereas weak and no inhibition occurred at pH 8.0 and pH ≥ 9.0, respectively. In the acidic pH region (≤ 5.0), however, reliable inhibition measurements were impossible due to the low PME activity. The good agreement with the results of SPR interaction analysis in the pH range above pH 5.0 confirms the reasonable supposition that PME-PMEI interaction and enzyme inhibition are closely interrelated.

Collectively, these data suggest that ionisable groups, at least in part, mediate the interaction between kiwi PMEI and tomato/carrot PME. The large interface area and the high number of direct and water-mediated hydrogen bonds, as determined for the tomato PME - kiwi PMEI complex (Di Matteo *et al.*, 2005) (cf. Section 1.3.3.2), may account for the high stability of the PME-PMEI complex at pH 5.0 to 6.5 (with K_D values in the nanomolar range). The pH-dependent dissociation of the complex, observed at neutral and alkaline pH values, was hypothetically ascribed to the presence of two proton-linked acidic residues. The electrostatic repulsion following deprotonation of the carboxylic groups at high pH may loosen the intermolecular H-bond network and destabilise the complex (Di Matteo *et al.*, 2005; Ciardiello *et al.*, 2008). Conversely, the interaction between kiwi PMEI and the PME of the same plant source appears to be further stabilised by additional salt links at pH values where tomato PME releases the inhibitor (Ciardiello *et al.*, 2008).

3.3.4 Effect of NaCl concentration on the PME-PMEI binding by SPR interaction analysis

The SPR interaction analysis method with immobilised plant PME, as outlined in Section 3.3.2, was also applied to study the effect of NaCl concentration on the interaction between kiwi PMEI and the two plant PMEs (i.e., the main tomato and carrot PME isoforms). Na-acetate (0.15 M, pH 6.0) containing 0.0 to 1.0 M NaCl was used as running buffer. Parameter estimates for the binding kinetics of both tomato and carrot PME are represented in **Table 3.2**. Irrespective of the PME source, an increasing salt concentration weakened the interaction with kiwi PMEI. Varying the NaCl concentration affected both the rate of association and dissociation: the more NaCl present, the slower the binding and the faster the separation. This behaviour differed from the effect of pH, which was mainly restricted to k_d. By way of illustration, sensorgrams for the interaction of tomato PME and kiwi PMEI at various NaCl concentrations are depicted in **Figure 3.4** (for one selected analyte concentration, i.e., 100 nM). These sensorgrams show that a higher NaCl concentration, besides a lower binding strength, also induced a reduced amount of bound analyte. At a concentration of 1.0 M NaCl hardly any binding occurred.

In the previous chapter, measuring the inhibitory capacity of kiwi PMEI towards carrot PME as a function of NaCl concentration correspondingly showed increasing salt concentrations to result in reduced inhibition (e.g., barely

inhibition at 1.0 M NaCl) (cf. Section 2.3.3.2). Strong inhibition was established at low NaCl concentrations (0.125 - 0.25 M), but no reliable results were obtained at 0.0 M NaCl due to absence of PME activity. The shielding of charged groups, involved in complex stabilisation, by salt ions is likely to cause the weakened interaction between PME and PMEI, and concomitantly, the reduced inhibition.

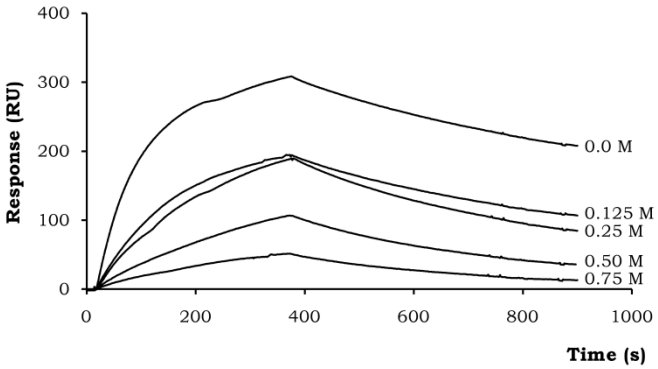

Figure 3.4. Binding sensorgrams obtained from SPR analysis showing the effect of NaCl concentration on the interaction of kiwi PMEI and immobilised tomato PME. Kiwi PMEI (100 nM) was injected over the surface in running buffers with various NaCl concentrations, as indicated on the sensorgrams. Measurements were performed at room temperature in 0.15 M Na-acetate pH 6.0.

3.3.5 SPR interaction analysis with immobilised kiwi PMEI: method development

3.3.5.1 Surface preparation

In order to study the PME-PMEI binding with varying PME samples (e.g., different degrees of denaturation), an SPR interaction analysis method was developed on a Biacore™ 3000 system with PMEI fixed on the chip surface. Contrary to plant PME, kiwi PMEI cannot be immobilised by direct covalent amino coupling, as was already experienced by Ciardiello *et al.* (2004). This failure can presumably be ascribed to the acidic nature of the inhibitor (cf. Section 2.3.2), hampering electrostatic preconcentration of the ligand at the negatively charged chip surface. Besides, available sulfhydryl groups on the PMEI molecule are lacking (established in the context of separate experiments, details not shown), not allowing direct thiol coupling chemistry. Therefore, an alternative strategy was designed through high-affinity capture of biotinylated PMEI on a sensor chip upon which streptavidin had previously been attached (SA chip). The affinity of streptavidin for biotin is extremely high, with a K_D of about 10^{-15} M, and coupling can be performed with high efficiency above the pI of the ligand, without relying on extensive electrostatic preconcentration at the chip surface.

Practically, kiwi PMEI was biotinylated with a water-soluble, amine-reactive biotin derivative (sulfo-NHS-LC-biotin), equipped with a 22.4 Å spacer arm to minimise steric hindrance and to facilitate streptavidin binding on the surface. A fivefold molar excess of the biotin derivative was selected to keep the degree of

labelling between 0.5 and 1.5. Excess biotin was removed by means of desalting spin columns. Subsequently, the SA chip surface was conditioned and biotinylated PMEI was injected at a concentration of 20 µg/mL in 0.1 M Na-phosphate pH 7.2 containing 0.3 M NaCl. The elevated ionic strength reduced electrostatic repulsion between surface and negatively charged ligand and enabled efficient ligand binding. A target coupling degree was set at 500 RU of protein, to allow reliable kinetic experiments. Deactivation of the excess of streptavidin on the chip was unnecessary.

3.3.5.2 Interaction measurements

The actual interaction measurements were carried out analogously as described in Section 3.3.2.2, with different concentrations of carrot PME (0 - 30 nM) as analyte. However, best data fitting was obtained when a single-site interaction model taking into account mass transport limitations was applied. This model enclosed a rate constant k_t for analyte transport to binding sites on the surface ($A_{bulk} \leftrightarrow A_{surface}$) and allowed kinetic information (k_a and k_d) to be derived from partially mass-transport-limited data. Injection of a 5 µL pulse of 5 mM NaOH was selected to adequately regenerate the surface without compromising the chip performance. Representative sensorgrams showing the interaction of carrot PME and immobilised kiwi PMEI are depicted in **Figure 3.5**. At all analyte concentrations, curvature in the association phase and decay in the dissociation phase are noticeable, as required. In these binding response profiles, the most apparent effect of mass transport is the fair linearity of the early portion of the association phase (Rich and Myszka, 2007).

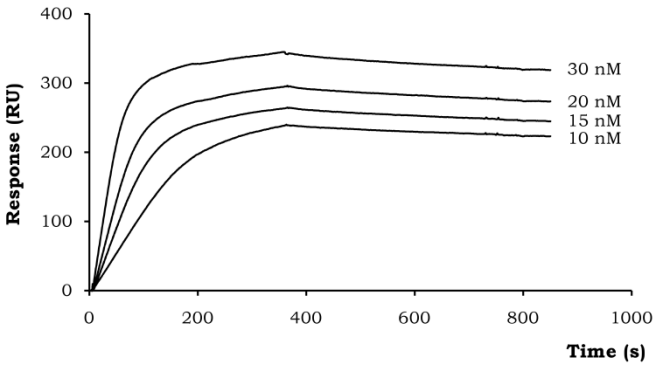

Figure 3.5. Representative binding sensorgrams obtained from SPR analysis showing the interaction of carrot PME and immobilised (biotinylated) kiwi PMEI. Varying analyte concentrations were injected over the surface, as indicated on the sensorgrams. Measurements were performed at room temperature in 0.15 M Na-phosphate pH 6.0.

3.3.6 Effect of PME denaturation on the PME-PMEI binding by SPR interaction analysis

To investigate the effect of (partial) temperature- or pressure-induced denaturation of PME on its interaction with kiwi PMEI, a series of carrot PME

samples with different degrees of residual enzyme activity was prepared and, subsequently, their remaining affinity towards kiwi PMEI was analysed. Hereto, the SPR interaction analysis method described in Section 3.3.5, with (biotinylated) PMEI attached to the chip surface, was employed.
On the one hand, purified carrot PME was thermally treated for 5 min at different temperature levels (25 to 60 °C) and the residual PME activity was quantified by pH-stat automatic titration, as a measure for the degree of irreversible PME denaturation. Increasing the intensity of the thermal treatment caused a gradual loss of enzyme activity. A set of 13 PME samples with a residual activity in the range of 100% to 0%, relative to the untreated PME sample, was obtained. Of all PME samples, kinetic binding parameters were estimated (**Table 3.3**). From 100% to ca. 50% residual PME activity, PME-PMEI interaction kinetics were hardly influenced, judging by the significantly unaltered dissociation constant K_D. Conversely, below 50% residual activity, a gradual decrease of the binding strength was noticed. At ca. 30%, K_D increased due to a slower association. At ca. 15%, the interaction with PMEI was weakened, owing to retarded association and dissociation, accompanied by a strongly impaired SPR signal, all indicating poor binding to PMEI. At a residual activity of ca. 5%, insufficient binding occurred to allow meaningful parameter estimations, while at 0 - 1% residual PME activity, no binding took place at all.

Table 3.3. Effect of thermal carrot PME denaturation on the interaction with immobilised kiwi PMEI, expressed in terms of kinetic binding parameters derived from SPR data. Rate constants represent the average of measurements at 4 different PME concentrations (± SD). Measurements were performed at room temperature in 0.15 M Na-phosphate pH 6.0.

Residual PME activity (%)	**k_a (10^6 M^{-1} s^{-1})**	**k_d (10^{-4} s^{-1})**	**K_D (nM)**
100	1.24 ± 0.69	1.23 ± 0.30	0.10 ± 0.06
99	1.25 ± 0.50	1.30 ± 0.01	0.10 ± 0.04
98	1.24 ± 0.75	1.18 ± 0.06	0.10 ± 0.06
91	1.29 ± 0.57	1.31 ± 0.35	0.10 ± 0.05
86	1.36 ± 0.59	1.29 ± 0.10	0.09 ± 0.04
76	1.13 ± 0.57	1.11 ± 0.16	0.10 ± 0.05
64	1.06 ± 0.35	1.24 ± 0.22	0.12 ± 0.04
51	1.06 ± 0.59	1.13 ± 0.11	0.11 ± 0.06
33	0.495 ± 0.149	1.22 ± 0.19	0.25 ± 0.08
17	0.0748 ± 0.0367	0.431 ± 0.101	0.58 ± 0.31
6	Insufficient binding		
1	No binding		
0	No binding		

On the other hand, purified carrot PME was pressure-treated for various time intervals at 800 MPa (25 °C) and the residual enzyme activity assayed by pH-stat automatic titration, as a measure for the degree of PME denaturation. A set of nine PME samples with residual activities between 100% and 1%, relative to the untreated PME sample, was obtained and kinetic binding parameters were estimated (**Table 3.4**). Compared to the temperature-treated samples, similar observations could be made. As long as at least 50% PME activity remained after

treatment, binding kinetics were unchanged. Below 50% residual activity, however, activity loss was accompanied by binding weakening. At ca. 40%, the interaction was impaired due to a reduced association rate. At ca. 25%, association was retarded, while dissociation was accelerated, resulting in a markedly lower binding strength. At ca. 12% residual PME activity, retardation of both association and dissociation was observed, and at ca. 1% residual activity, barely any binding to kiwi PMEI was noticed.

Table 3.4. Effect of high-pressure denaturation of carrot PME on the interaction with immobilised kiwi PMEI, expressed in terms of kinetic binding parameters derived from SPR data. Rate constants represent the average of measurements at 4 different PME concentrations (± SD). Measurements were performed at room temperature in 0.15 M Na-phosphate pH 6.0.

Residual PME activity (%)	k_a **(10^6 $M^{-1}\cdot s^{-1}$)**	k_d **(10^{-4} s^{-1})**	K_D **(nM)**
100	1.20 ± 0.28	1.60 ± 0.12	0.13 ± 0.03
87	1.12 ± 0.34	1.46 ± 0.04	0.13 ± 0.04
77	1.33 ± 0.60	1.70 ± 0.11	0.13 ± 0.06
64	1.20 ± 0.38	1.53 ± 0.03	0.13 ± 0.04
51	1.21 ± 0.76	1.57 ± 0.08	0.13 ± 0.08
41	0.698 ± 0.156	1.56 ± 0.06	0.22 ± 0.05
25	0.501 ± 0.171	3.70 ± 0.93	0.74 ± 0.31
12	0.322 ± 0.104	0.697 ± 0.219	0.22 ± 0.10
1	No binding		

So, carrot PME denaturation, both high-temperature- and high-pressure-induced, has a marked influence on its interaction with kiwi PMEI. However, a certain degree of inactivation is required before interaction kinetics as determined by SPR significantly change. Moreover, binding to the PMEI surface occurs as long as the treated PME sample possesses enzymatic activity. Unfortunately, precise interpretation of the current data is hampered by the lack of insight into the mechanism of thermal or pressure inactivation on the level of a single PME molecule. Inactivation kinetic studies are generally restricted to the population level: only the ensemble average activity is described as a function of the relevant process parameters. Insight into the distribution of the intensity of structural damage and, hence, the distribution of activity in the population is missing. Further research specifically dedicated to this particular scientific question would be helpful to interpret the SPR data and to obtain a more profound understanding of the effect of PME denaturation on the interaction with kiwi PMEI. In this context, the reader is referred to the next chapter.

Anyhow, the results reported here reveal that the PME-PMEI binding is highly associated with PME inactivation, as only completely inactivated PME does not show affinity towards PMEI anymore. This statement of a strong link between enzyme activity and susceptibility towards complexation/inhibition is endorsed by the observation that PMEI covers the putative active site cleft upon complex formation (Di Matteo *et al.*, 2005). Upon PME inactivation, the active site of the enzyme is torn apart or becomes inaccessible for both substrate and inhibitor molecules. Consequently, the intrinsically strong enzyme-inhibitor linkage is rendered completely impossible.

3.4 CONCLUSION

An SPR-based interaction analysis method was developed and proven applicable to explore the binding between plant PME and kiwi PMEI. An immobilisation strategy for both the enzyme (through direct amine coupling) and the inhibitor (through capture by streptavidin after PMEI biotinylation) to the chip surface was implemented. This biosensor method has a broad spectrum of potential applications, ranging from exploring the effect of intrinsic product factors (e.g., pH, ionic strength) or modification of kiwi PMEI or plant PME (e.g., partial denaturation, protein labelling) on the kinetics and strength of the PME-PMEI interaction, to screening for PMEI presence in various plant sources and comparing the affinity of PME from different sources towards the inhibitor from kiwi. Hence, it is a valuable addition to the common PMEI inhibitory capacity assays to examine the PME-PMEI binding event.

An improved insight in the PME-PMEI interaction, obtained with this SPR-method, is particularly valuable for the aimed use of PMEI to control undesired PME activity in food applications and for *in situ* PME detection in plant tissue, both before and after thermal/high-pressure processing. The results reported here show that kiwi PMEI and plant PME engage a strong 1:1 complex (with K_D in the nanomolar range) at pH < 7 and at low salt concentrations, whereas both pH values ≥ 8 and NaCl concentrations of around 1.0 M are effective in dissociating, clearly defining the boundaries for application. In the context of temperature (50 - 60 °C) and pressure (800 MPa, 25 °C) inactivation of PME, a notable degree of enzyme inactivation was required before interaction characteristics were significantly altered, while any incomplete inactivation of PME resulted in binding to the PMEI surface. Consequently, PMEI binding is strongly linked to residual enzymatic activity. This observation suggests that a PMEI probe will bind to endogenous PME in raw and processed plant tissue as long as the enzyme possesses activity, and hence enables detection of all endogenous PME activity. Furthermore, post-processing addition of kiwi PMEI to a food product would allow binding and, presumably, inhibiting residual undesired PME, e.g., to prevent cloud loss in fruit and vegetable juices. Further experiments to validate these findings in real foods would be valuable.

4

PLANT PME AND KIWI PMEI: COMPLEX FORMATION BY SIZE EXCLUSION CHROMATOGRAPHY[5]

4.1 INTRODUCTION

Well-reasoned use of kiwi PMEI for plant PME inhibition or detection in various potential applications demands thorough knowledge on the PME-PMEI interaction, as influenced by extrinsic process factors (such as high temperature and high pressure). Enzyme inhibition measurements (cf. Chapter 2) and SPR-based interaction analysis (cf. Chapter 3) already revealed some general tendencies, but mechanistic understanding is still limited. To further increase this understanding, a third experimental approach to study the PME-PMEI complex formation, based on high-performance size exclusion chromatography (HPSEC), was implemented.

The objective of the current research chapter was twofold. On the one hand, the effect of a temperature- or pressure-induced denaturation of plant PME on its subsequent complex formation with the proteinaceous inhibitor from kiwi fruit was investigated. On the other hand, the behaviour of a PME-PMEI mixture upon thermal or high-pressure treatment was examined. Hereto, an analytical HPSEC method was employed. As a prerequisite for reliable data interpretation, the behaviour of denatured PME on HPSEC in absence of PMEI was investigated in advance, revealing some noteworthy information on the mechanism of PME inactivation. Throughout this chapter, purified carrot PME, considered to be a representative plant PME, was selected as study vehicle.

---

[5] This chapter is based on the following paper:
Jolie, R.P., Duvetter, T., Verlinde, P.H.C.J., Van Buggenhout, S., Van Loey, A.M., Hendrickx, M.E. (2009). Size exclusion chromatography to gain insight into the complex formation of carrot pectin methylesterase and its inhibitor from kiwi fruit as influenced by thermal and high-pressure processing. *Journal of Agricultural and Food Chemistry*, 57(23), 11218-11225.

4.2 MATERIALS AND METHODS

4.2.1 Materials

Young Belgian red carrots (*Daucus carota* cv. Sirena) and green kiwi fruits (*Actinidia deliciosa* cv. Hayward) were purchased from a local supermarket. Carrot PME and kiwi PMEI were extracted and purified by affinity chromatography as described in Chapter 2 (cf. Section 2.2.2 and 2.2.3, respectively). For all experiments in this chapter, merely the main and most abundantly present carrot PME isoform was used. Purified enzyme and inhibitor solutions were quickly frozen in liquid N_2 and stored at -80 °C until use.
Apple pectin (degree of methyl-esterification: 70 - 75%) was obtained from Fluka (Buchs, Switzerland). Ultrapure water (organic free, 18 MΩ·cm resistance) was supplied by a Simplicity™ water purification system (Millipore, Billerica, MA, United States). All other chemicals were of analytical grade.

4.2.2 Protein content

The protein content of the purified PME and PMEI solutions was determined according to Sigma procedure TPRO-562 using the BCA kit (Sigma, Darmstadt, Germany). The protein concentration (mg/mL) was estimated by comparison with a standard curve of bovine serum albumin (cf. Section 2.2.5).

4.2.3 Thermal and high-pressure treatments

Thermal treatments of protein solutions were performed in a temperature-controlled water bath. Protein samples were enclosed in 200 µL glass capillaries (Brand, Wertheim, Germany) to ensure isothermal heating. After a treatment of 5 min at different temperature levels, samples were withdrawn from the water bath and immediately cooled in ice water until further use.
High-pressure treatments of protein solutions were conducted in a laboratory-scale high-pressure device (Resato, Roden, The Netherlands) consisting of eight cylindrical thermostatted reactors (8 mL each). A propylene glycol - water mixture (PG fluid, Resato) served as pressure-transmitting medium. Flexible microtubes (0.5 mL, Carl Roth, Karlsruhe, Germany) were filled with the protein solution and enclosed in the pressure reactors, already equilibrated to 25 °C. Pressure was built up slowly to 800 MPa (100 MPa/min, to minimise temperature increase due to compression heating) and all pressure reactors were subsequently isolated. An equilibration period of 2 min was taken into account to allow temperature and pressure to evolve to the desired value. After preset time intervals (0 - 60 min), individual reactors were depressurised instantaneously and samples were transferred to an ice water bath until analysis.

4.2.4 PME activity assay

PME activity was measured by an automatic pH-stat titration (Metrohm, Herisau, Switzerland) of the carboxyl groups formed during pectin de-esterification, using 0.01 M NaOH. Routine assays were performed at pH 6.5 and 22 °C, using 30 mL

of a 0.35% (w/v) apple pectin solution containing 0.117 M NaCl. By definition, one unit (U) of PME activity is the amount of enzyme catalysing the hydrolysis of 1 µmol of methyl-ester bonds per min under aforementioned conditions.

4.2.5 High-performance size exclusion chromatography

High-performance size exclusion chromatography (HPSEC) was performed on an Agilent 1200 Series HPLC system (Agilent Technologies, Santa Clara, CA, United States) with UV-DAD detection at 220 nm (G1315B, Agilent Technologies). Analytical HPLC was performed at 25 °C using a Superdex 75 10/300 GL column (300 × 10 mm, 13 µm average particle size, theoretical plates > 30000 m^{-1}, GE Healthcare Bio-Sciences AB, Uppsala, Sweden). Elution was executed with 50 mM Na-phosphate buffer pH 6.5 containing 150 mM NaCl at a flow rate of 0.45 mL/min for 55 min. Prior to injection (100 µL), protein samples were filtered through a syringe-driven filter unit (Millex®-HV, PVDF, 0.45 µm, Millipore).

4.2.6 Experimental set-up

Two series of experiments were carried out. On the one hand, purified carrot PME (0.1 mg/mL in 50 mM Na-phosphate buffer pH 6.5 containing 150 mM NaCl) was subjected to a thermal or high-pressure treatment. After treatment, bulk UV attenuance[6] of the enzyme solutions was measured at 280 nm and 25 °C in quartz cells of 10 mm optical path length with a spectrophotometer (Ultrospec 2100 pro, GE Healthcare). Subsequently, each sample was divided into three parts. A first part was used for measuring the residual enzyme activity by pH-stat automatic titration, within 2 h after treatment. A second part was directly employed for HPSEC (as outlined in Section 4.2.5), whereas a third part was mixed with (untreated) kiwi PMEI in a molar PME:PMEI ratio slightly below 1, prior to filtration and injection on the size exclusion column.
On the other hand, an equimolar mixture of purified carrot PME (0.1 mg/mL) and kiwi PMEI was thermally or high-pressure-treated. For thermal experiments, PME-PMEI mixtures were diluted in Na-phosphate buffer pH 6.5. High-pressure experiments were carried out both in Na-phosphate pH 6.5 and MES-NaOH pH 6.5. All buffers had a 50 mM concentration and contained 150 mM NaCl. MES buffer was selected because of its ability to maintain the set pH upon pressurisation, in contrast to Na-phosphate buffer (cf. Section 2.2.8.1). After treatment, bulk UV attenuance at 280 nm and 25 °C was measured for each sample. Subsequently, all treated PME-PMEI samples were analysed by HPSEC.
For selected conditions, experiments were done in duplicate. All parameters measured showed good reproducibility.

4.2.7 Data-analysis

Although enzyme inactivation and protein denaturation due to thermal or high-pressure processing are complex processes involving several events (cf. Sections

[6] IUPAC nomenclature, the term preferably used instead of 'absorbance' in cases where light scattering and/or reflection cannot be neglected (Verhoeven, 1996).

1.4.3 and 1.4.4), kinetics often obey a simple first-order model (Lencki *et al.*, 1992; Ludikhuyze *et al.*, 2003):

$$A = A_0 \exp(-kt) \qquad 4.1$$

with A the measured response (e.g., enzyme activity) and k the reaction rate constant (min^{-1}). The temperature sensitivity of the rate constant can be described by the Arrhenius equation and is expressed in terms of activation energy (E_a):

$$k = k_{ref} \exp\left[\frac{E_a}{R_T}\left(\frac{1}{T_{ref}} - \frac{1}{T}\right)\right] \qquad 4.2$$

where k_{ref} is the rate constant at reference temperature T_{ref} (K), E_a the activation energy (J/mol) and R_T the universal gas constant.
Nonlinear regression analysis was applied to estimate the kinetic parameters based on the experimental data (SAS Statistical Software version 9.1) (cf. Section 2.2.8.2). For the thermal treatments (constant treatment time at different treatment temperatures), a one-step regression approach was employed, in which the Arrhenius equation was introduced in the first-order model to describe the course of the response A as a function of treatment temperature.

4.3 RESULTS AND DISCUSSION

4.3.1 Thermal and high-pressure denaturation of carrot PME

The behaviour of denatured PME on HPSEC was investigated. Hereto, a set of PME samples with different degrees of irreversible denaturation was prepared by subjecting purified carrot PME solutions to a thermal or high-pressure treatment. Subsequently, UV attenuance of the PME solution (at 280 nm), residual enzyme activity as well as residual peak area at 220 nm on HPSEC were determined.
On the one hand, PME samples were treated for 5 min at different temperature levels (25 - 60 °C) and atmospheric pressure. Increasing the intensity of the thermal treatment caused a gradual loss of enzyme activity (**Figure 4.1**), strictly obeying first-order kinetics, in agreement with data from the kinetic inactivation study of carrot PME reported in Chapter 2 (cf. Section 2.3.4.1). A series of 13 PME samples with a residual activity in the range of 100% to 0%, relative to the untreated PME sample (25 °C), was obtained. Along with the decrease in enzyme activity, the relative attenuance of the protein solutions at 280 nm increased (**Figure 4.1**). When plotting residual enzyme activity versus relative bulk attenuance, a straight line with a slope of -1.001 and R^2 of 0.997 was obtained (not shown), revealing a markedly high correlation between both parameters. In addition, size exclusion chromatography was performed for all thermally treated PME samples. **Figure 4.2** presents an overlay of a selected number of chromatograms. In all cases (blank and treated samples), a single peak (retention time = 26.77 ± 0.01 min) was observed in the entire elution period. The area of this PME peak was calculated and plotted relative to the untreated PME (**Figure 4.1**). The residual peak area decreased with rising treatment temperature, obeying first-order kinetics. By means of nonlinear one-step regression analysis

(Corr R^2 = 0.999), the rate constant at a T_{ref} of 55 °C ($k_{55°C}$ = 0.114 ± 0.002 min^{-1}) and the activation energy (E_a = 424.4 ± 9.8 kJ/mol) were estimated. A particularly high correlation (slope = 1.003; R^2 = 0.999) between residual enzyme activity and residual peak area was obtained.

Analogously, for high-pressure inactivation, a set of nine carrot PME samples with residual enzymatic activities between 100% and 1%, relative to the untreated PME sample, was produced by treating the enzyme solutions for

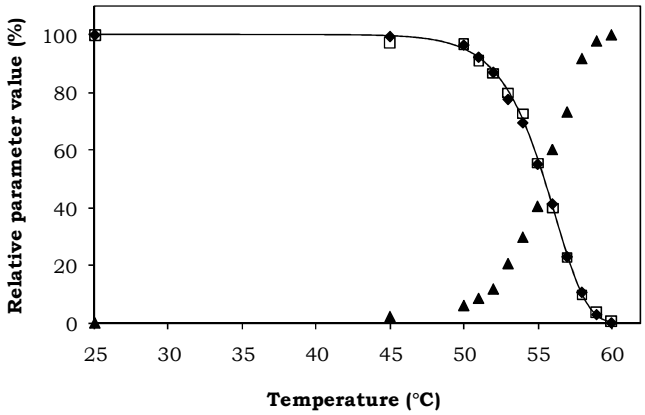

Figure 4.1. Effect of a thermal treatment (5 min at different temperatures) of purified carrot PME on the residual PME activity (♦), UV attenuance at 280 nm (▲) and residual peak area on HPSEC (□). Values relative to the maximal parameter value are depicted. The full line represents the fit of the residual PME peak area to the first-order model.

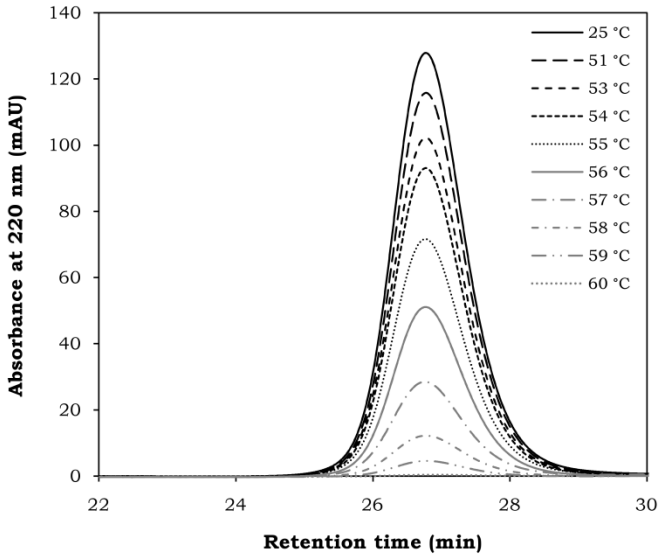

Figure 4.2. Size exclusion chromatograms of purified carrot PME after thermal treatment (5 min at different temperature levels).

different time intervals (0 - 60 min) at 800 MPa and 25 °C (**Figure 4.3**). In accordance with former data, a first-order decay was followed (cf. Section 2.3.4.2). Compared to the temperature-treated samples, similar observations could be made. A single peak of PME (retention time = 26.78 ± 0.02 min) was

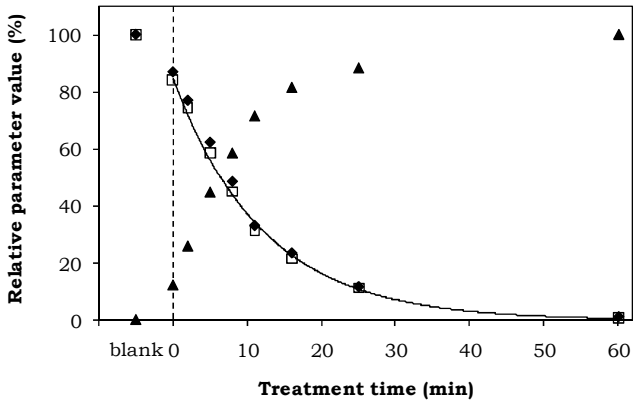

Figure 4.3. Effect of a high-pressure treatment (different time intervals at 800 MPa and 25 °C) of purified carrot PME on the residual PME activity (♦), UV attenuance at 280 nm (▲) and residual peak area on HPSEC (□). Values relative to the maximal parameter value are depicted. The full line represents the best fit of the residual PME peak area to the first-order model. Time 0 min (dashed line) refers to the start of isothermal-isobaric conditions of the high-pressure treatment.

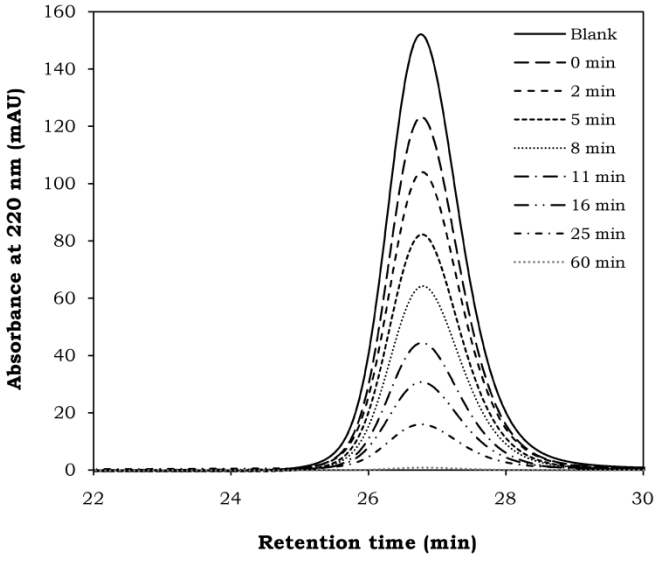

Figure 4.4. Size exclusion chromatograms of purified carrot PME after high-pressure treatment (different time intervals at 800 MPa and 25 °C). "Blank" refers to the untreated sample and "0 min" to the start of the isothermal-isobaric conditions of the high-pressure treatment.

detected on the size exclusion chromatograms (**Figure 4.4**). Residual enzyme activity was inversely correlated with relative bulk attenuance at 280 nm (slope = -1.011; R^2 = 0.993), whereas it was directly correlated with the PME peak area on HPSEC (slope = 1.012; R^2 = 0.998) (**Figure 4.3**). The first-order rate constant for the reduction in PME peak area was estimated at $k_{800\ MPa}$ = 0.082 ± 0.002 min^{-1} (Corr R^2 = 0.999).

In order to elucidate the perceived increase in bulk UV attenuance of the PME solutions after treatment, optical transmittance spectra (%T in the 200 - 900 nm range) of selected samples were recorded before and after centrifugation (10 min at 15000 × *g*). Spectra for a number of thermally treated enzyme samples are presented in **Figure 4.5**. Comparable results were obtained for pressure-treated PME (not shown). In contrast to the overall decrease in %T for the non-centrifuged samples (i.e., throughout the spectrum), an increase in %T was observed in the samples after centrifugation, mainly in the 200 - 280 nm region of the spectrum (i.e., the part of the spectrum where peptide bonds and aromatic amino acids absorb light). This observation can be explained by the processing-induced formation of protein aggregates, which cause light scattering and an increase in UV attenuance to take place (Mahler *et al.*, 2009) but can be removed by centrifugation, without loss of enzyme activity or decrease of the PME peak area on HPSEC. This aggregation tendency is usually attributed to the intermolecular interaction of hydrophobic sites, previously buried in the protein interior, as an answer to their thermodynamically unfavourable exposure to the aqueous surrounding medium upon conversion of the native to the denatured protein form (Klibanov, 1983) (cf. Section 1.4.3.1). Temperature-induced aggregation following unfolding was also demonstrated for recombinant *Aspergillus aculeatus* PME by means of Fourier transform infrared (FTIR) spectroscopy, however at a markedly higher protein concentration (20 mg/mL in D_2O) (Dirix *et al.*, 2005; Plaza *et al.*, 2008).

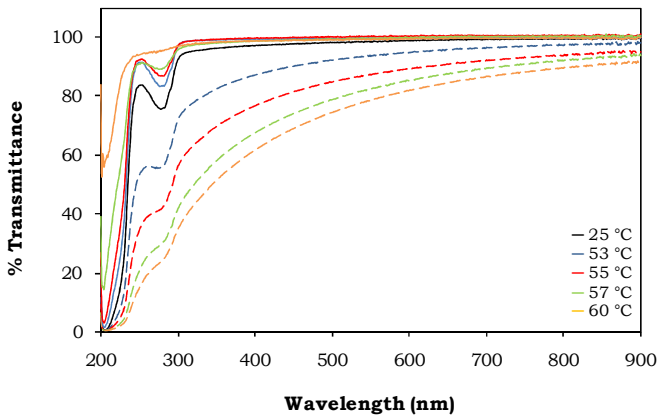

Figure 4.5. Effect of a thermal treatment of purified carrot PME (5 min at different temperature levels, as indicated on the graph) on the optical transmittance spectrum of the enzyme solution, recorded before and after centrifugation (dashed and solid lines, respectively).

Since the presence of NaCl may promote chemical and physical protein aggregation due to a decreased intermolecular repulsion (Vardhanabhuti and Foegeding, 2008), aggregation behaviour accompanying irreversible inactivation of PME was followed spectrophotometrically in presence and absence of 150 mM NaCl. No significant differences in optical transmittance and residual enzyme activity were observed, ruling out a major influence of NaCl on the inactivation process of the purified carrot PME studied here.

The above results bear the evidence for the occurrence of processing-induced formation of PME aggregates. Nevertheless, no high molar mass components were detected by size exclusion chromatography on the Superdex 75 column, neither in protein samples that underwent filtration or centrifugation prior to injection, nor in samples without preceding clearance step. In an additional experiment it was shown that sample filtration and sample centrifugation resulted in the same residual PME peak areas (R^2 > 0.997 for both thermal and high-pressure inactivation) and that sample clearance was not accompanied by loss of enzyme activity. The fact that the aggregates can be removed by filtration through a 0.45 µm filter and that they are excluded from the size exclusion column in case of omission of the preparatory clearance step suggests a high molar mass of the protein assemblies (> dimer or trimer).

All foregoing results reveal that a partly, irreversibly denatured PME sample, either thermally or high-pressure-treated, basically exists of two distinct subpopulations. One PME subpopulation is eluting from the size exclusion column and has a peak area which is highly correlated to the enzymatic activity of the sample, indicating that this subpopulation is associated with the active (i.e., non-inactivated) PME fraction. A second subpopulation, however, does not appear in the chromatogram. This subpopulation does not account for any residual PME activity, and hence can be considered the inactive, irreversibly denatured enzyme fraction. As described above, this inactive PME fraction consists of enzyme aggregates and is mainly removed during the routine filtration step prior to sample application on the HPLC column.

Remarkably, the present study shows little difference in the results for thermal and high-pressure inactivation, despite the substantial differences in the denaturation mechanisms (cf. Sections 1.4.3 and 1.4.4). Although it is observed that aggregation results less frequently from pressure than from heat treatment, which may possibly be explained by the fact that in the latter case unfolding is the first step in the denaturation process, prior to water penetration (Balny *et al.*, 2002), irreversible high-pressure inactivation of PME appears also to be accompanied by aggregate formation, even at the relatively low protein concentration used here (i.e., 0.1 mg/mL). However, since pressure-induced protein gels have been reported to possess characteristics different from the temperature-induced ones (Meersman *et al.*, 2006), it seems intuitively plausible that the pressure-induced aggregate is different from that induced thermally at 0.1 MPa. Whether or not differing, none of both types of aggregation appears to invade the independent behaviour of the non-inactivated PME population with regard to enzyme activity and size exclusion separation.

Inactivation kinetic studies of enzymes are traditionally restricted to the population level (for examples on PME, see Duvetter *et al.*, 2009). Only the ensemble average activity is described as a function of the relevant process

parameters. The same holds true for monitoring modifications of the protein conformation by FTIR spectroscopy. Insight in the distribution of the intensity of structural damage and, hence, the distribution of activity in the population is lacking. In this context, the current results give indirect proof that, post-factum, a partly and irreversibly denatured bulk PME sample is basically inhomogeneous, consisting of enzymes in either a fully active or a fully inactive state. So, when inactivating a bulk enzyme solution irreversibly, certain individual enzyme molecules will unfold (and presumably aggregate) whereas others will preserve their native, catalytically active state. To extract information on the pathway followed by an individual enzyme molecule to finally reach the irreversibly inactivated state, recent techniques such as single-molecule fluorescence spectroscopy may be appropriate (De Cremer *et al.*, 2007).

4.3.2 Effect of PME denaturation on PME-PMEI complex formation

The complex formation between carrot PME and kiwi PMEI, and more precisely the way the interaction is influenced by a preceding temperature- or pressure-induced irreversible denaturation of PME, was investigated by means of HPSEC. A broad set of partially denatured PME samples with residual enzyme activities, ranging from 100% to 0%, was prepared by thermal or high-pressure treatment, analogously to Section 4.3.1. Subsequently, these samples were incubated with a fixed amount of purified kiwi PMEI, corresponding to a minor molar excess of the inhibitor, prior to sample filtration and application on the size exclusion column. Based on the results of Chapters 2 and 3, good complex formation at the pH (i.e., 6.5) and NaCl concentration (i.e., 150 mM) of the elution buffer used for HPSEC analysis could be expected (cf. Sections 2.3.3, 3.3.3 and 3.3.4).

Chromatograms were recorded for both thermally (**Figure 4.6**) and high-pressure- (**Figure 4.7**) treated enzyme solutions. In all cases, two separate peaks with retention times of 24.45 ± 0.02 min and 27.82 ± 0.02 min were obtained, originating from the PME-PMEI complex and free PMEI, respectively. As expected, based on the respective molar masses, the retention time of free PME (26.77 min, cf. Section 4.3.1) was intermediate to the ones of PME-PMEI complex and free PMEI. Increasing the treatment intensity (i.e., treatment temperature or pressurisation time) caused the complex peak to reduce, while the PMEI peak enlarged. Remarkably, the decline in complex peak area was highly correlated with the decrease in residual enzyme activity (slope = 1.011 and R^2 = 0.999 for thermally treated PME; slope = 1.018 and R^2 = 0.996 for pressure-treated PME), as was the increase in PMEI peak area. The chromatogram of a mixture of PMEI and fully temperature- or pressure-inactivated PME coincided with the one of a mixture of PMEI and buffer ("only PMEI").

The amount of complex that can be formed between PME and PMEI after a (partial) denaturation of PME proves to be strongly associated with the residual activity of the enzyme sample. Moreover, all PMEI that is mixed with the PME sample and applied on the column is afterwards retrieved in the effluent. Although, during sample preparation, PMEI comes into contact with the entire PME population after processing, assumed to consist of individual active and aggregated inactive PME molecules (cf. previous section), all PMEI molecules

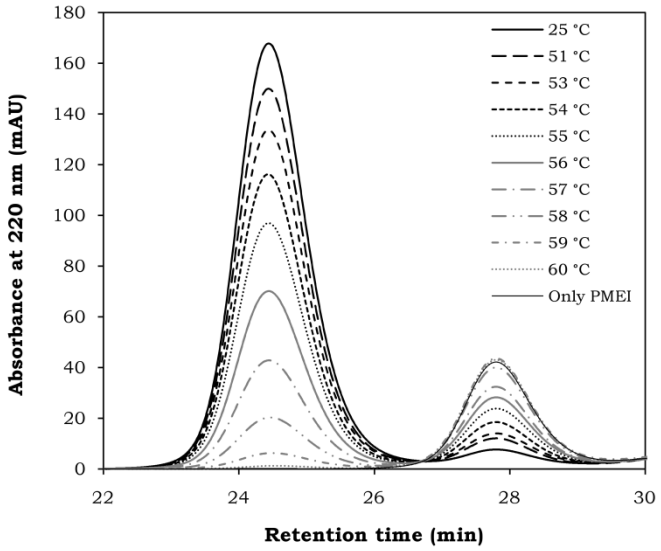

Figure 4.6. Size exclusion chromatograms of the mixture of a fixed amount of untreated kiwi PMEI with purified carrot PME that underwent a thermal treatment (5 min at different temperature levels). "Only PMEI" refers to the chromatogram of a PMEI sample without PME.

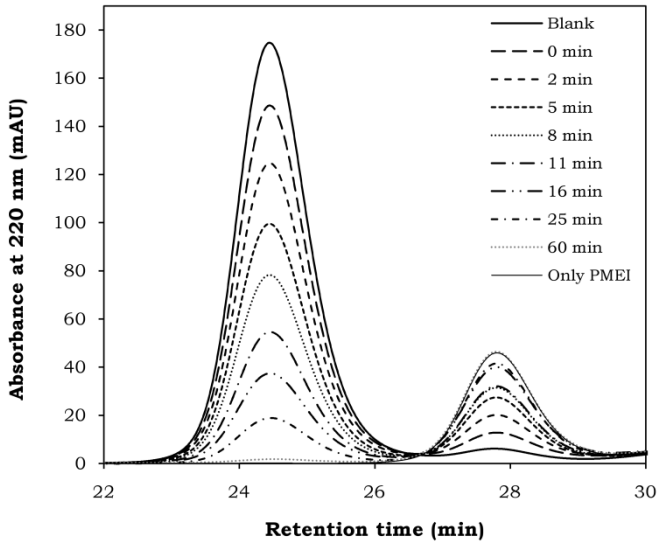

Figure 4.7. Size exclusion chromatograms of the mixture of a fixed amount of untreated kiwi PMEI with purified carrot PME that underwent a high-pressure treatment (different time intervals at 800 MPa and 25 °C, as indicated on the chromatogram). "Only PMEI" refers to the chromatogram of a PMEI sample without PME, "blank" to the untreated sample and "0 min" to the start of the isothermal-isobaric conditions of the high-pressure treatment.

elute from the column in the company of the active PME fraction. Thereby, a part of the PMEI is bound to PME, another part is not, the ratio depending on the amount of PME available for complex formation, determined by the degree of enzyme inactivation. None of the inhibitor is associated with the aggregated inactive enzyme fraction and, hence, removed by filtration prior to injection.
The whole of these observations unequivocally demonstrates that complex formation with kiwi PMEI is limited to the active (i.e., non-inactivated) PME fraction, whereas the inactivated (and aggregated) PME fraction does not bind PMEI anymore. Hence, the PME-PMEI binding is highly associated with irreversible PME inactivation. This statement of a strong link between (the potential for) enzyme activity and susceptibility towards complexation (and inhibition) is reinforced by the finding that the inhibitor covers the putative active site cleft upon PME-PMEI complex formation (Di Matteo *et al.*, 2005), and is in agreement with the conclusion drawn from the SPR interaction analysis study with denatured PME, outlined in Chapter 3 (cf. Section 3.3.6). Meanwhile, the improved insight into the distribution of residual activity in the partially denatured PME samples (i.e., PME being either fully active or fully inactive), gained with the HPSEC method, sheds a new light on the interpretation of these SPR results. Presumably, inactivated PME passes by the PMEI-coated chip surface without interacting, while the non-inactivated PME is binding to the immobilised PMEI, giving rise to the SPR response. Only when the concentration of the non-inactivated PME fraction drops below a certain limit, binding kinetics are affected and an -apparently- weaker binding is registered.

4.3.3 Effect of thermal treatment on the PME-PMEI complex

To examine the behaviour of the PME-PMEI complex upon thermal processing, an equimolar mixture of carrot PME and kiwi PMEI (in Na-phosphate buffer pH 6.5) was treated for 5 min at temperature levels between 25 and 65 °C. Afterwards, bulk UV attenuance of the protein solution (at 280 nm) was measured and size exclusion chromatograms (**Figure 4.8**) were recorded. A major peak at retention time 24.42 ± 0.02 min and a minor peak around 27.78 ± 0.04 min could be distinguished, corresponding to the PME-PMEI complex and to free PMEI, respectively. Increasing the treatment temperature caused a reduction in the complex peak area, while the PMEI peak remained negligible compared to the peak of PMEI without PME ("only PMEI"). Simultaneously, UV attenuance of the protein solutions at 280 nm increased with rising temperature (inversely correlated with the complex peak area with slope = -1.084 and R^2 = 0.996), indicating aggregation taking place. Notably, the decline in complex peak area could adequately be described by a first-order model. Nonlinear one-step regression analysis (Corr R^2 = 0.999) allowed estimation of the rate constant (at a T_{ref} of 61 °C: $k_{61°C}$ = 0.112 ± 0.002 min^{-1}) and the activation energy (E_a = 487.7 ± 12.9 kJ/mol).
The above results favour the hypothesis that, upon heat treatment of the PME-PMEI complex, enzyme and inhibitor are not driven apart. Neither separate PME nor separate PMEI are retrieved post-factum. Yet, the complex is presumably denatured (and aggregated) as a single entity, following first-order kinetics. In comparison with the thermal denaturation of carrot PME in absence of kiwi PMEI

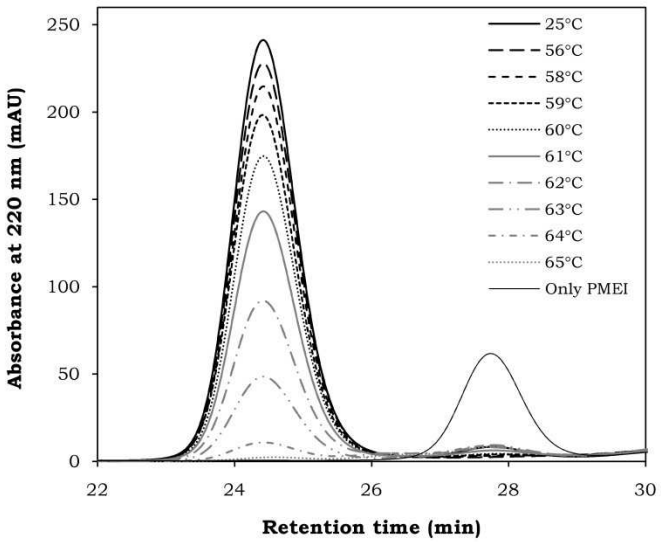

Figure 4.8. Size exclusion chromatograms of an equimolar mixture of carrot PME and kiwi PMEI after thermal treatment (5 min at different temperature levels). "Only PMEI" refers to the chromatogram of untreated PMEI without PME.

(cf. Section 4.3.1), denaturation of the PME-PMEI complex is only initiated at higher temperature levels (a difference of 6 °C to obtain a comparable *k*-value). The temperature sensitivity, however, is similar, judging by E_a values in the same order of magnitude. The presence of PMEI, like the presence of the pectin substrate (cf. Section 2.3.6.1), seems to have a slight protective effect on PME with regard to thermal denaturation. The finding that the PME-PMEI complex does not undergo thermal dissociation in the temperature range from 25 to 65 °C confirms the strong indication in that direction based on PME activity measurements in the presence of PMEI at elevated temperatures, following the rate of methanol formation as a function of treatment time (cf. Section 2.3.6.1).

4.3.4 Effect of high-pressure treatment on the PME-PMEI complex

To address the scientific question how the PME-PMEI complex behaves at elevated pressure, an equimolar mixture of carrot PME and kiwi PMEI was subjected to a pressure level of 800 MPa for different times (0 - 60 min) at 25 °C. Subsequently, bulk UV attenuance (at 280 nm) was measured and samples were analysed by HPSEC. Experiments were performed both in Na-phosphate buffer pH 6.5 and MES buffer pH 6.5. MES buffer will maintain its preset pH value of 6.5 even at elevated pressure levels ("pressure-stable") (Bruins *et al.*, 2007), whereas pressurisation will cause a pH drop in the ("pressure-labile") phosphate buffer (~ -0.3 units per 100 MPa) due to pressure-induced ionisation of weak acids (Neuman *et al.*, 1973).

Figure 4.9 represents the chromatograms of the PME-PMEI complex after high-pressure treatment in the pressure-labile Na-phosphate buffer. Peaks of PME-PMEI complex (24.39 ± 0.01 min) and peaks of free PMEI (27.73 ± 0.01 min) were registered. The evolution of the integrated areas of both peak types with treatment time, relative to the peak areas of untreated samples, is depicted in **Figure 4.10**. With prolonging treatment time, the residual complex peak area showed a first-order decrease ($k_{800\ MPa}$ = 0.081 ± 0.001 min^{-1}, Corr R^2 = 0.999). Meanwhile, the free PMEI peak area steadily augmented until an area even slightly larger than the one of untreated PMEI ("only PMEI") was reached. A concomitant increase in bulk UV attenuance of the treated PME-PMEI mixtures (data not shown) pointed to the occurrence of a pressure-induced formation of protein aggregates.

High-pressure processing of the PME-PMEI mixture in a pressure-labile buffer causes the amount of enzyme-inhibitor complex to diminish with treatment time. Remarkably, the rate of this decline is in strong accordance with the rate at which the PME peak decreases when PME alone undergoes a similar high-pressure treatment (cf. Section 4.3.1). This agreement indicates that the residual amount of PME-PMEI complex most likely is governed by the inactivation of the PME, since only non-activated PME molecules can bind to the inhibitor (as stated in Section 4.3.2). Moreover, coincidence of the chromatogram of the maximally treated PME-PMEI mixture with the one of untreated PMEI demonstrates that all PMEI initially present in the protein mixture also elutes from the column. The following hypothesis can be put forward to explain the whole of the observations. During pressurisation, the enzyme-inhibitor complexes present in the PME-PMEI

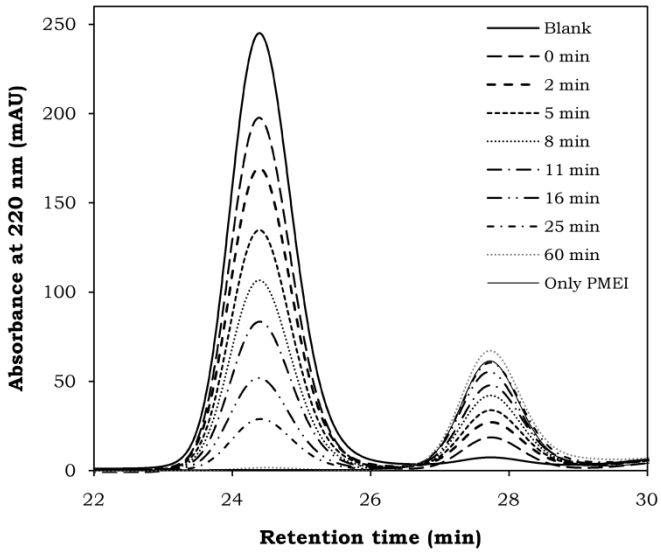

Figure 4.9. Size exclusion chromatograms of an equimolar mixture of carrot PME and kiwi PMEI after high-pressure treatment (at 800 MPa and 25 °C for different treatment times) in Na-phosphate buffer pH 6.5. "Only PMEI" refers to the chromatogram of untreated PMEI without PME.

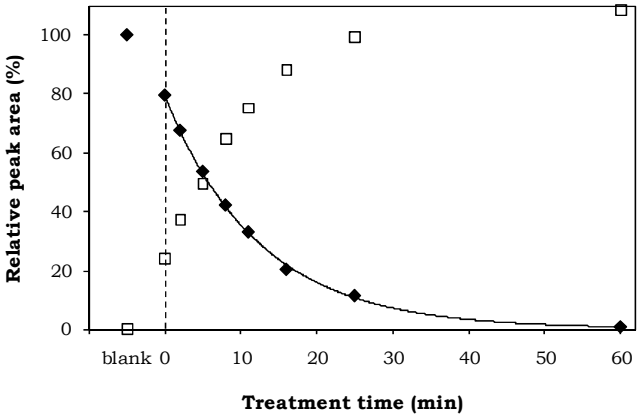

Figure 4.10. Effect of a high-pressure treatment (different time intervals at 800 MPa and 25 °C) of an equimolar mixture of carrot PME and kiwi PMEI in Na-phosphate buffer pH 6.5 on the HPSEC peak areas of the PME-PMEI complex (♦) and of free PMEI (□). Peak areas relative to those of untreated complex and untreated PMEI, respectively, are depicted. The full line represents the best fit of the residual complex peak area to the first-order model. Time 0 min (dashed line) refers to the start of isothermal-isobaric conditions.

mixture dissociate. Subsequently, PME undergoes first-order inactivation in line with its behaviour in the absence of PMEI. Conversely, PMEI is not obliterated by a pressure level of 800 MPa when dissolved in a pressure-labile phosphate buffer. The latter statement was successfully confirmed by HPSEC analysis of pressure-treated PMEI samples (data not shown), and is in conformity with the findings based on measuring residual PMEI inhibitory capacity after high-pressure treatment (cf. Section 2.3.5.3). Upon decompression, PME-PMEI complexes are formed again to a maximal extent, depending on the residual amount of active PME. In all cases (i.e., for all treatment times), an excess of PMEI is generated in the pressure-treated samples.

In order to assess whether observations are governed by pressure-induced pH changes in the protein solution, chromatograms of the PME-PMEI complex after high-pressure treatment in the pressure-stable MES buffer were recorded likewise (**Figure 4.11**). Peaks of PME-PMEI complex (24.39 ± 0.02 min) and peaks of free PMEI (27.70 ± 0.02 min) were detected and the course of their integrated areas was plotted versus treatment time, relative to untreated samples (**Figure 4.12**). The longer the treatment lasted, the lower the residual complex peak area was (first-order decay with $k_{800\ MPa}$ = 0.130 ± 0.002 min^{-1}, Corr R^2 = 0.999). Besides, the PMEI peak area gradually expanded until a plateau level was attained (~40% of the untreated "only PMEI" peak). These changes in the proportions of peak areas were accompanied by an increase in bulk UV attenuance of the samples (data not shown), indicative of light scattering by protein aggregates.

As for the pressure-labile buffer system, the amount of PME-PMEI complex retrieved after processing in the pressure-stable MES buffer decreases and a pressure-induced dissociation of the enzyme-inhibitor complexes can be assumed. Upon decompression, residual non-inactivated PME engages with

residual PMEI to form as many complexes as possible. Since the amount of complex follows first-order kinetics as a function of treatment time, as does the residual PME peak area (i.e., without PMEI) under similar conditions (cf. Section

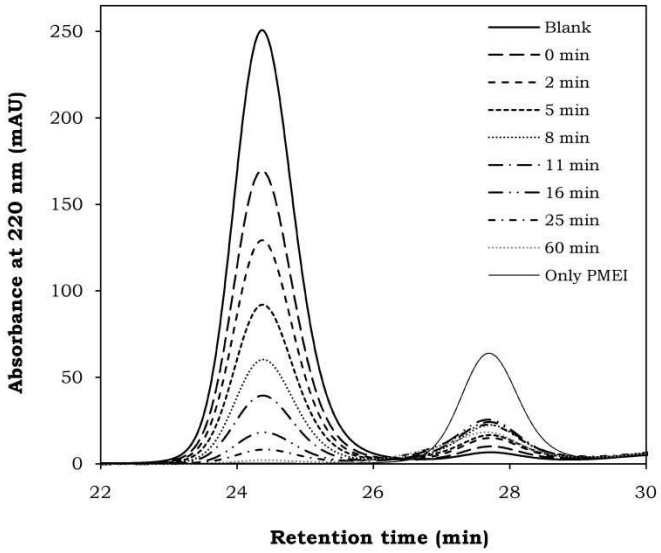

Figure 4.11. Size exclusion chromatograms of an equimolar mixture of carrot PME and kiwi PMEI after high-pressure treatment (at 800 MPa and 25 °C for different treatment times) in MES-NaOH buffer pH 6.5. "Only PMEI" refers to the chromatogram of untreated PMEI without PME.

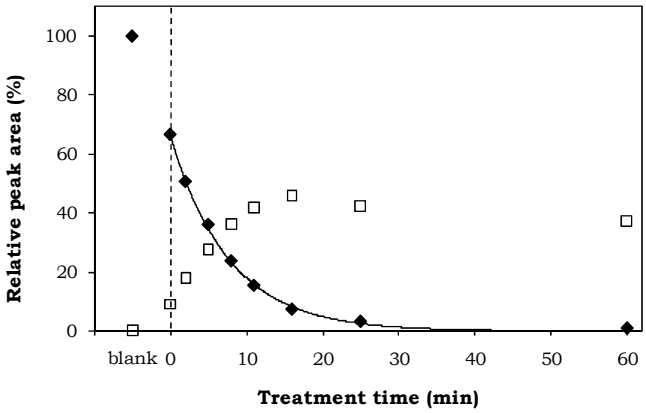

Figure 4.12. Effect of a high-pressure treatment (different time intervals at 800 MPa and 25 °C) of an equimolar mixture of carrot PME and kiwi PMEI in MES-NaOH buffer pH 6.5 on the HPSEC peak areas of the PME-PMEI complex (♦) and of free PMEI (□). Peak areas relative to those of untreated complex and untreated PMEI, respectively, are depicted. The full line represents the best fit of the residual complex peak area to the first-order model. Time 0 min (dashed line) refers to the start of isothermal-isobaric conditions.

4.3.1), the amount of native PME most likely is the limiting factor. However, the rate at which the complex peak area is reduced is higher than the degradation rate of pure PME (i.e., PME in absence of PMEI), subjected to a comparable pressure treatment. Consequently, in one way or another, the presence of PMEI seems to promote the pressure denaturation of PME. Furthermore, in all samples, an excess amount of PMEI is detected, but not all of the initially present PMEI can be retrieved in the chromatogram. This indicates that, in contrast to the results in the pressure-labile buffer, PMEI is not fully stable in the MES buffer. A plateau level of approximately 40% of the initial amount is reached after extended treatment times, suggesting the existence of a processing-stable PMEI fraction. This finding is in accordance with the results on the high-pressure stability of kiwi PMEI (in MES buffer), based on inhibitory capacity measurements (cf. Section 2.3.5.3).
In conclusion, the results discussed in this section make it clear that pH (in the test range from approx. 4 to 6.5) significantly affects the high-pressure behaviour of a PME-PMEI mixture, principally owing to a pH-dependent effect of pressure on the PME inhibitor. Nevertheless, irrespective of the buffer system used, there is marked evidence for a dissociation of the PME-PMEI complex upon high-pressure application, and high-pressure treatment of an equimolar mixture of PME and PMEI (at the conditions studied here) will anyhow give cause for a residual excess amount of PMEI.

4.4 CONCLUSION

Size exclusion chromatography was successfully implemented to study the plant PME - kiwi PMEI binding event in general, and the effect of processing on the interaction in particular. Its use allowed sound confirmation of former results, collected by using other analytical techniques (cf. Chapter 2 and 3), besides acquisition of new findings and more profound (mechanistic) understanding.
HPSEC of (partially) denatured carrot PME indicated that, post-factum, two distinct subpopulations of PME molecules are present in thermally (50 - 60 °C) or high-pressure- (800 MPa, 25 °C) treated enzyme solutions: a catalytically active (i.e., non-inactivated) population, eluting from the size exclusion column, and an inactivated population, excluded from the column. Temperature- as well as pressure-inactivated PME tends to form aggregates, which are removable by filtration or centrifugation. Complex formation with the kiwi PMEI was restricted to the non-inactivated PME subpopulation. This observation suggests that a PMEI probe will bind to endogenous PME in plant tissue, both before and after processing, as long as the enzyme possesses activity, hence enabling selective detection of all endogenous PME activity. Furthermore, post-processing addition of kiwi PMEI to a food product may allow binding and, presumably, inhibiting residual undesired PME remaining after (mild) processing, e.g., to obtain cloud-stable fruit and vegetable juices.
Besides, size exclusion chromatography was also applied to study the behaviour of the PME-PMEI complex at elevated temperature (55 - 65 °C) or pressure (800 MPa, 25 °C) levels. Evidence was gained that heat treatment does not dissociate the complex, but rather denatures the complex as a single entity. By contrast, high-pressure treatment induces disunion of enzyme and inhibitor, followed by

gradual inactivation of PME and PMEI, the latter showing pH-dependent inactivation characteristics. At pH 6.5, approximately 40% of the initial PMEI is retained after prolonged pressurisation, whereas, at lower pH values (around pH 4), PMEI is not obliterated at all. These findings especially open perspectives for pre-processing addition of kiwi PMEI to food systems in combination with high-pressure processing, particularly in (high) acid foods (e.g., fruit juices). However, further experiments are required to confirm whether these *in vitro* conclusions are transferable to real food matrices.

5

A PMEI-BASED MOLECULAR PROBE FOR DETECTION OF PLANT PME[7]

5.1 INTRODUCTION

To gain in-depth insight in the relation between enzymatic pectin conversions and allied food functional properties (such as firmness and viscosity), identification of the locations of endogenous PME activity in plant-based, complex, structured food matrices (i.e., *in situ*), both on macroscopic (e.g., by means of tissue printing) and microscopic level (fluorescence and/or electron microscopy) would be extremely helpful, in addition to investigating how food processing affects these locations (e.g., through enzyme inactivation or tissue damage). To date, several authors have reported on the production of (polyclonal and monoclonal) antibodies raised against plant PMEs for immunolocalisation (Mareck *et al.*, 1995; Quentin *et al.*, 1997; Christensen *et al.*, 1998; Morvan *et al.*, 1998; Blumer *et al.*, 2000; Li *et al.*, 2002; Vandevenne *et al.*, 2009). However, these probes have not yet been applied for the food technological purposes proposed here.

Next to anti-PME antibodies, an alternative strategy towards a molecular probe for plant PME detection could be hypothetically based on the proteinaceous PME inhibitor. The strong enzyme-inhibitor interaction opens perspectives for the development of an innovative technique based on labelled PMEI to localise PME *in situ*. However, efficient use of PMEI, either in PME inhibition or detection, requires a profound knowledge on the PME-PMEI interaction, as influenced by intrinsic product factors (such as pH and ionic strength) and extrinsic process factors (such as high temperature and high pressure). Necessary information was collected in the previous chapters, using inhibition capacity measurements

[7] This chapter is based on the following paper:
Jolie, R.P., Duvetter, T., Vandevenne, E., Van Buggenhout, S., Van Loey, A.M., Hendrickx, M.E. (2010). A pectin-methylesterase-inhibitor-based molecular probe for *in situ* detection of plant pectin methylesterase activity. *Journal of Agricultural and Food Chemistry*, 58(9), 5449-5456.

(Chapter 2), surface plasmon resonance interaction analysis (Chapter 3), and size exclusion chromatography for complex formation monitoring (Chapter 4). With these data at hand, bridging the gap towards the actual application of PMEI can be aimed.
In this last research chapter, the development of a molecular probe, based on kiwi PMEI, and the assessment of its potential as a tool to detect PME *in situ* was intended. First, focus was on the labelling of PMEI and characterisation of the conjugate. Once the labelling was implemented, the probe's ability to detect PME was tested in dot-blot binding assays and plant tissue printing. For the sake of comparison, blots were also probed with recently reported anti-PME monoclonal antibodies (Vandevenne *et al.*, 2009).

5.2 MATERIALS AND METHODS

5.2.1 Plant materials

Red carrots (*Daucus carota*), broccolis (*Brassica oleracea*), red ripe Roma tomatoes (*Lycopersicon esculentum*) and green kiwi fruits (*Actinidia deliciosa* cv. Hayward) were purchased from a local supermarket.
The proteinaceous PME inhibitor was extracted from ripe kiwi fruits and purified by preparative affinity chromatography according to the method outlined in Chapter 2 (cf. Sections 2.2.3). Extraction and purification of cell-wall-bound PME from both carrot roots and broccoli stems for HPSEC and/or dot-blot analysis (cf. infra) were carried out following the procedures described for carrot PME in Chapter 2 (cf. Section 2.2.2). Purified enzyme and inhibitor solutions were quickly frozen in liquid N_2 and stored at -80 °C until use.

5.2.2 PME activity and PMEI inhibitory capacity assays

PME activity was measured by the continuous titration of carboxyl groups formed during pectin de-esterification, using an automatic pH-stat titrator (Metrohm, Herisau, Switzerland) with 0.01 M NaOH. Routine assays were performed at pH 6.5 and 22 °C, using 30 mL of a 0.35% (w/v) apple pectin solution (degree of methyl-esterification: 70 - 75%, Fluka, Buchs, Switzerland) containing 0.117 M NaCl. One unit (U) of PME activity is defined as the amount of enzyme catalysing the hydrolysis of 1 µmol of methyl-ester bonds per min under aforementioned conditions.
PMEI inhibitory capacity was determined as the ability to block PME activity in a titrimetric assay. It was calculated as the difference between the PME activity of a blank sample (i.e., without PMEI) and the residual PME activity after 15 min of preincubation with a PMEI sample, routinely at pH 6.5 and 22 °C. One unit of inhibition (UI) is defined as the amount of PMEI that blocks 1 U of PME under the assay conditions described above.

5.2.3 Protein content

The protein content of enzyme and inhibitor solutions was determined according to Sigma procedure TPRO-562 using the BCA kit (Sigma, Darmstadt, Germany).

The protein concentration (mg/mL) was estimated by comparison with a standard curve of bovine serum albumin (cf. Section 2.2.5).

5.2.4 PMEI biotinylation

Kiwi PMEI was biotinylated by means of an EZ-Link® Micro Sulfo-NHS-LC-Biotinylation Kit (Thermo Fisher Scientific, Waltham, MA, United States). Hereto, PMEI was dissolved in PBS pH 7.2 (0.1 M Na-phosphate containing 0.15 M NaCl) at a 1 mg/mL concentration, mixed with a 25-fold molar excess of a water-soluble biotin derivative (sulfo-NHS-LC-biotin), and incubated for 60 min at 25 °C. Subsequently, biotinylated PMEI (bPMEI) was separated from unbound biotin and the sulfo-NHS leaving group on a Zeba™ Desalt Spin Column (7 kDa MWCO). The protein conjugates were stored in small aliquots at -80 °C until further use.
The degree of biotinylation was determined with the FluoReporter® Biotin Quantitation Assay Kit (Invitrogen, Paisley, United Kingdom). This fluorometric assay is based on the displacement of a ligand tagged with a quencher dye from the biotin binding sites of Biotective™ Green reagent. To expose any biotin groups in a possibly multiply labelled PMEI that are sterically restricted and inaccessible to the Biotective Green reagent, the inhibitor was first digested with protease (overnight at 37 °C). Biotinylated lysine was used as a standard for the assay. The resulting fluorescence was measured in a microplate reader using excitation/emission maxima of 485/530 nm.

5.2.5 High-performance size exclusion chromatography

High-performance size exclusion chromatography (HPSEC) was carried out on an Agilent 1200 Series HPLC system (Agilent Technologies, Santa Clara, CA, United States) with UV-DAD detection at 220 and 495 nm (G1315B, Agilent Technologies). Analytical HPLC was performed at 25 °C using a Superdex 75 10/300 GL column (300 × 10 mm, 13 µm average particle size, theoretical plates > 30000 m^{-1}, GE Healthcare Bio-Sciences AB, Uppsala, Sweden). Elution was executed with 50 mM Na-phosphate buffer pH 6.5 containing 150 mM NaCl at a flow rate of 0.45 mL/min for 55 min. Prior to injection (100 µL), protein samples were filtered through a syringe-driven filter unit (Millex®-HV, PVDF, 0.45 µm, Millipore, Billerica, MA, United States). Ultrapure water (organic free, 18 MΩ·cm resistance) was supplied by a Simplicity™ water purification system (Millipore).

5.2.6 Thermal and high-pressure treatments

Thermal treatments of PME solutions and raw plant material were performed in a temperature-controlled water bath. Enzyme samples (0.1 mg/mL in 50 mM Na-phosphate pH 6.5 containing 150 mM NaCl) were enclosed in 200 µL glass capillaries (Brand, Wertheim, Germany) and heated at 65 °C for 5 min. Carrot roots (ca. 3 cm in diameter and 10 cm in length) were vacuum-packed in a plastic bag and immersed in the water bath (85 °C for a preset time from 0 to 15 min). After treatment, samples were immediately cooled in an ice water bath. For tissue prints (cf. Section 5.2.8), transverse sections were made of the middle part of the (raw or treated) carrot root. The remainder of the plant material was cut into

small pieces, quickly frozen in liquid N_2 and stored at -80 °C until PME extraction (as described in Section 5.2.9).
High-pressure treatment of PME solutions was conducted in a laboratory-scale high-pressure device (Resato, Roden, The Netherlands) with 8-mL cylindrical thermostatted reactors and a propylene glycol - water mixture as pressure-transmitting medium (PG fluid, Resato). Flexible microtubes (0.3 mL, Carl Roth, Karlsruhe, Germany) were filled with the PME solution (0.1 mg/mL in 50 mM Na-phosphate pH 6.5 containing 150 mM NaCl) and enclosed in the pressure reactors, equilibrated to 25 °C. Pressure was built up slowly to 800 MPa and the pressure reactors were all isolated. After 60 min, the reactors were depressurised instantaneously and samples were cooled in ice water until analysis.

5.2.7 Dot-blot assays

PME samples were spotted onto pre-wet nitrocellulose (HyBond ECL, 0.45 µm pore size, GE Healthcare) in 2 µL aliquots. After air-drying for at least 30 min, irrelevant protein binding sites on the nitrocellulose were blocked overnight at 4 °C with 5% nonfat dried milk in PBS-T (i.e., 50 mM Na-phosphate pH 6.5 containing 150 mM NaCl and 0.1% Tween-20, for the membranes to be labelled with bPMEI) or TBS-T (i.e., 20 mM Tris-HCl pH 7.6 containing 137 mM NaCl and 0.1% Tween-20, for the membranes to be labelled with monoclonal antibodies). Subsequently, the primary probe in PBS-T or TBS-T, containing 1% nonfat dried milk, was added (1.5 h at room temperature). As primary probes, bPMEI (2.9 µg/mL) as well as MA-TOM2-38A11 (25 µg/mL), a mouse monoclonal antibody raised against one of the isoforms of tomato PME and with shown cross-reactivity towards carrot PME (Vandevenne *et al.*, 2009), were used. After extensive washing in PBS-T or TBS-T, blots were incubated in the secondary probe solution, i.e., ExtrAvidin-peroxidase (Sigma, diluted 1/2000 in PBS-T with 1% milk) or Goat-Anti-Mouse-HRP (Bio-Rad, Hercules, CA, United States, diluted 1/2000 in TBS-T with 1% milk), for 1 h at room temperature. After further washing with PBS-T or TBS-T, blots were developed using the ECL method with luminol enhancer and peroxide solutions from Pierce (Thermo Fisher Scientific) for chemiluminescent signal detection. All blots were performed at least in duplicate.

5.2.8 Tissue printing

Tissue printing was conducted in analogy with Vandevenne *et al.* (2009). Nitrocellulose membranes were first soaked for 15 min in 0.2 M Tris-HCl pH 8.0 containing 1.0 M NaCl. Subsequently, transverse sections of (raw or treated) carrot root, broccoli stem and tomato fruit were firmly pressed on the nitrocellulose membrane (ca. 30 s). The membrane was allowed to dry for 30 min and was then blocked overnight at 4 °C with 5% nonfat dried milk in PBS-T or TBS-T. After blocking, the prints were incubated for 1.5 h at room temperature with the primary probe, i.e., bPMEI (2.9 µg/mL) in PBS-T containing 1% nonfat dried milk or MA-TOM2-38A11 (25 µg/mL) in TBS-T containing 1% nonfat dried milk. A washing step with PBS-T or TBS-T was performed, followed by incubation with the secondary probe, being ExtrAvidin-peroxidase (Sigma, diluted 1/1000 in

PBS-T with 1% milk) or Goat-Anti-Mouse-HRP (Bio-Rad, diluted 1/1000 in TBS-T with 1% milk), for 1 h at room temperature. Finally, the membranes were washed and detection was carried out using the ECL method (cf. previous section). Prints developed with omission of the primary probe served as negative controls. Triplicate analyses assured reproducibility of the results.

5.2.9 PME extraction

Carrot tissue was frozen in liquid N_2 prior to homogenisation in a Grindomix GM 200 knife mill (Retsch, Haan, Germany). A known amount of homogenised material (wet weight) was mixed with 0.2 M Tris-HCl pH 8.0 containing 1.0 M NaCl for 3 h at 4 °C (1:1.5 w/v) to extract cell-wall-bound PME. The crude PME extract was obtained by filtration using a cheese cloth. PME activity was measured as described in Section 5.2.3. All extractions and activity measurements were run in duplicate.

5.3 RESULTS AND DISCUSSION

5.3.1 Biotinylation of kiwi PMEI

In search of a PMEI derivative to be used as a molecular probe for PME detection, purified kiwi PMEI was biotinylated with a water-soluble biotin reagent (sulfo-NHS-LC-biotin), equipped with a 22.4 Å spacer arm and directed towards non-protonated aliphatic amine groups, including the amine terminus of proteins and the ε-amino group of lysines. The reaction was performed at pH 7.2 to achieve a more specific labelling of the amine terminus (which has a lower pK_a than the lysine ε-amino group), because from the three-dimensional structure of the PMEI - (tomato) PME complex it is known that the N-terminal region of the inhibitor molecule is directed away from the interaction interface and seems poorly involved in the formation of the complex (Di Matteo *et al.*, 2005) (cf. Section 1.3.3.2). A 25-fold molar excess of the biotin derivative was selected in an attempt to obtain at least one biotin per PMEI molecule. Excess biotin was removed by means of desalting spin columns.
The FluoReporter Biotin Quantitation Assay Kit allowed for an estimation of the degree of biotinylation (DOB) by comparison with a standard curve of biotinylated lysine. The measured DOB of the PMEI solution was 1.01 ± 0.02. This result points to a 1:1 molar ratio of PMEI and biotin, suggesting all PMEI molecules to be equipped with exactly one biotin unit.
The specific inhibition capacity towards purified carrot PME (i.e., in UI/mg protein) was measured before and after the biotinylation reaction, and proved not to change significantly (ca. 550 UI/mg), although a certain loss of protein (ca. 10%) occurred when taken through the labelling reaction. It can be concluded that also after biotinylation the PMEI is able to inhibit carrot PME activity.

5.3.2 Characterisation of the biotinylated PMEI by HPSEC

In order to further characterise the bPMEI and to check the ability of the probe to bind to plant PME on the one hand and to an avidin species on the other hand,

HPSEC analysis was performed, in accordance with the method described in Chapter 4.

5.3.2.1 Binding to PME

An overlay of the size exclusion chromatograms of bPMEI, purified carrot PME, a PME-bPMEI mixture and the NHS-biotin reagent, all recorded at 220 nm, is represented in **Figure 5.1**. The chromatogram of bPMEI showed a major, symmetrical peak at a retention time of 27.9 min and a minor peak at 23.7 min. The retention time of 27.9 min is in close agreement with the one of native kiwi PMEI (i.e., 27.8 min), as reported in Chapter 4 (cf. Section 4.3.2), indicating that this peak contains single (biotinylated) PMEI molecules. The peak at 23.7 min, however, may originate from PMEI aggregates formed during the labelling reaction. The total absence of low molar mass peaks, as the ones observed in the chromatogram of the NHS-biotin reagent (at 38.1 and 42.0 min), confirmed the successful removal of the unbound biotin and NHS leaving group.
After mixing bPMEI with purified carrot PME, a major PME-bPMEI complex peak (retention time = 24.5 min) was obtained. The presence of a second, minor peak at 21.0 min suggested that also the putative PMEI aggregates are capable of complex formation. A molar excess of bPMEI resulted in a small peak of free, unbound bPMEI (27.9 min), while a molar excess of PME yielded an unresolved peak at ca. 26.6 min, corresponding to free, unbound PME (the latter not shown). These observations indicate that PMEI after biotinylation is still available for complex formation with PME.

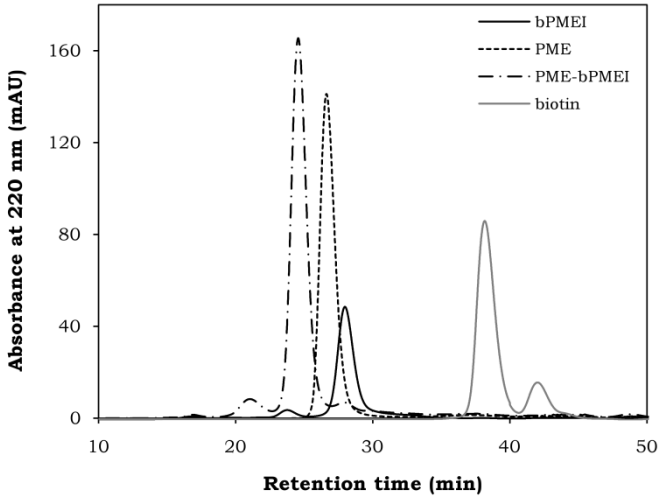

Figure 5.1. Size exclusion chromatograms of purified carrot PME, biotinylated PMEI ("bPMEI"), a PME-bPMEI mixture and the NHS-biotin reagent, all recorded at 220 nm.

5.3.2.2 Binding to avidin species

Furthermore, HPSEC analysis was applied to study complex formation between bPMEI and an avidin species. The ExtrAvidin®-FITC conjugate (Sigma,

abbreviated "ExA-FITC", FITC = fluorescein isothiocyanate), a fluorescently labelled, modified form of the egg-white avidin not exhibiting avidin's unwanted unspecific binding, was used. **Figure 5.2** shows an overlay of the chromatograms of ExA-FITC, bPMEI and a mixture of both. The elution of ExA-FITC was registered at 220 nm as well as 495 nm, the absorbance maximum of FITC. A major peak eluted at 22.5 min, a minor peak at 19.5 min. Perfect coincidence of the chromatograms at both wavelengths indicated that all ExA, be it single molecules or small aggregates, is fluorescently labelled. Upon mixing the bPMEI with the avidin species, the free bPMEI peak at 27.9 min disappeared completely and a high molar mass peak at 16.6 min was observed, the latter most likely corresponding to the bPMEI-ExA-FITC complex. In conclusion, all bPMEI can be bound by ExA-FITC if sufficient amounts of the avidin species are present.

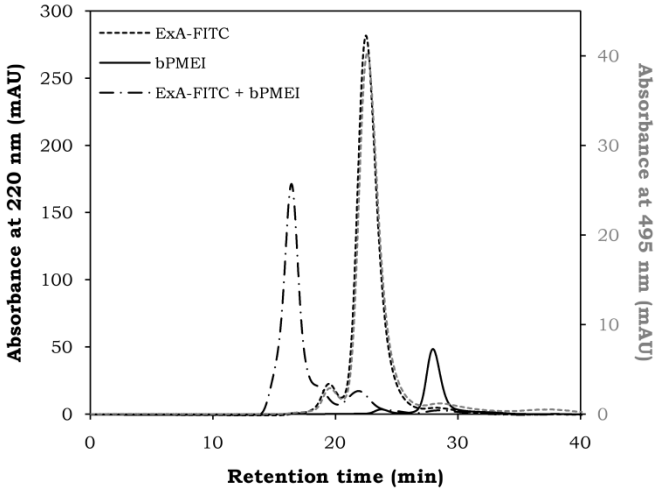

Figure 5.2. Size exclusion chromatograms of biotinylated PMEI ("bPMEI"), ExtrAvidin-FITC conjugate ("ExA-FITC") and a mixture of bPMEI and ExA-FITC, recorded at 220 nm and 495 nm (for ExA-FITC).

5.3.3 Dot-blot assays

As a preliminary step to investigate the ability of bPMEI to detect PME activity *in situ*, dot-blot binding assays with PME purified from carrot root and broccoli stem were conducted, for native as well as for high-temperature- or high-pressure-denatured enzymes. To allow for a comparison of the PME probing qualities of bPMEI with a recently reported alternative, i.e., monoclonal anti-PME antibodies, all dot blots were carried out with both bPMEI and the mouse antibody MA-TOM2-38A11 (Vandevenne *et al.*, 2009).

5.3.3.1 Native plant PMEs

The binding in dot blots of bPMEI and MA-TOM2-38A11 to coated native carrot and broccoli PMEs at various dilutions is depicted in **Figure 5.3**. bPMEI bound to carrot PME as well as to broccoli PME, with the intensity and area of the staining

depending upon the amount of PME dotted. At the highest dilution of PME (20 ng coated), hardly any staining was visible. MA-TOM2-38A11, by contrast, only recognised carrot PME. The lack of cross-reactivity towards broccoli PME of this particular anti-PME antibody, as well as of all other antibodies raised against tomato PMEs and described by Vandevenne *et al.* (2009), was confirmed by a one-side ELISA test (results not shown). These results illustrate a possible advantage of the PME inhibitor over the monoclonal antibodies as a probe for PME detection: the latter need a specific epitope on the PMEs for recognition to occur, whereas the PMEI is believed to react with all plant PMEs (Giovane *et al.*, 2004) (cf. Section 1.3.3.1).

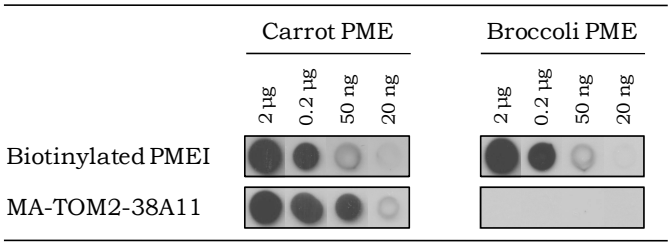

Figure 5.3. Dot-blot analysis of the binding of biotinylated PMEI and MA-TOM2-38A11 to PME purified from carrot root and broccoli stem. Dilution series of untreated, native PMEs are shown.

5.3.3.2 Treated plant PMEs

The results of the dot-blot assays of carrot and broccoli PME before and after a thermal or high-pressure treatment, probed with bPMEI and MA-TOM2-38A11, are shown in **Figure 5.4**. High-temperature and high-pressure conditions that (irreversibly) reduced the PME activity below detectable levels, as measured by automatic titration, were selected (i.e., 5 min at 65 °C/0.1 MPa and 60 min at 800 MPa/25 °C, respectively). In addition, blots of the treated PME samples after a centrifugation step for aggregate removal (5 min at 10000 × *g*, referred to as "cf") were made. In all cases, 2 µL of a 0.1 mg/mL PME starting solution were coated on the membrane.

The bPMEI probe bound to the untreated carrot and broccoli PMEs ("blank"), whereas high-temperature- and high-pressure-denatured PME samples were not recognised. MA-TOM2-38A11, conversely, was able to bind to denatured carrot PME samples, although weakened in comparison with the untreated blank. Staining disappeared upon centrifugation of the treated samples. The antibody showed no reaction with broccoli PME, neither before nor after treatment.

The complete absence of staining of the temperature- or pressure-denatured carrot and broccoli PME samples probed with bPMEI demonstrates that a temperature- or pressure-induced denaturation of plant PME renders the binding of the bPMEI probe impossible. The finding that PMEI only binds to non-inactivated PME molecules confirms the earlier observations based on interaction analysis by surface plasmon resonance (Chapter 3, Section 3.3.6) and complex formation by HPSEC (Chapter 4, Section 4.3.2) with temperature- and pressure-denatured carrot PME samples. The statement that the capacity of PME to bind PMEI is inextricably bound up with the enzyme activity is endorsed by the

observation that PMEI covers the putative active site cleft upon PME-PMEI complex formation, thus preventing substrate binding (Di Matteo *et al.*, 2005). In light of PMEI as a probe for PME activity, it is extremely valuable that the inhibitor, thanks to its specificity, can differentiate between native and inactivated PME molecules.

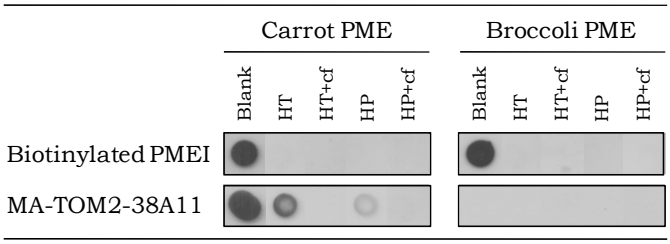

Figure 5.4. Dot-blot analysis of the binding of biotinylated PMEI and MA-TOM2-38A11 to PME purified from carrot root and broccoli stem. Untreated ("blank"), high-temperature-treated ("HT") and high-pressure-treated ("HP") PMEs, spotted before and after sample centrifugation ("cf"), are represented.

It was observed that MA-TOM2-38A11 can bind to carrot PME, even after thermal or high-pressure inactivation of the enzyme. However, the signal on the blot assay is rather weak and entirely lost when PME samples are centrifuged prior to immobilisation on the membrane. The latter observation indicates that antibody binding occurs at the aggregated state of the enzyme, the existence of which was already demonstrated in Chapter 4 (cf. Section 4.3.1), and which is removed upon centrifugation. This fact, in turn, provides a possible explanation for the low reactivity towards the non-centrifuged PME samples. On the one hand, the aggregated fraction may be less evenly spread on the membrane, due to a reduced ability to migrate before drying and attachment to the nitrocellulose. On the other hand, the epitope recognised by the antibody may still be present but less abundant and/or accessible, compared to the native state. Western Blot analysis with MA-TOM2-38A11 already demonstrated the conservation of the affinity of the antibody towards denatured (tomato) PME (Vandevenne *et al.*, 2009). However, comparison with the current results is hampered by the fact that, for Western Blotting, (thermal) denaturation is performed in presence of sodium dodecyl sulphate (SDS) and β-mercaptoethanol, rendering protein aggregation unlikely.

Taken all together, it is reasonable to conclude that PME recognition by the PMEI probe, unlike the recognition by the monoclonal anti-PME antibody, is restricted to the non-inactivated PME population, excluding the denatured enzyme subpopulation. Therefore, an additional application of the newly developed dot-blot technique with bPMEI could be its use as a rapid, sensitive tool to selectively screen for active plant PMEs (with a detection limit around 20 ng) in certain protein fractions/solutions.

5.3.4 Tissue printing for PME localisation in various plant organs

Dot-blot binding assays demonstrated that bPMEI is capable of recognising PME after coating the purified enzyme on a membrane. The usefulness of bPMEI as a probe for the *in situ* localisation of PME was further assessed by tissue printing of various plant organs, including carrot root, broccoli stem and tomato fruit. In this technique, a fresh cut surface of plant material, exposing all tissues and most cell types, is pressed onto a sheet of nitrocellulose, which is then labelled with antibodies or other molecular probes. Little or no lateral mixing or diffusion occurs and much of the spatial information regarding distribution is maintained. Hence, tissue printing can often provide a rapid overview of epitope or antigen occurrence in the context of a whole organ, as well as fine details of epitope distribution. If successful, it can be a valuable starting point for an (immuno)localisation study with fluorescence light microscopy or gold electron microscopy (in which only a part of the organ, tissue or cell can be seen), since cell-wall components can be extensively developmentally regulated within organs (Varner and Ye, 1994; Willats *et al.*, 2000).

In the current study, tissue printing for localisation of PME was carried out on nitrocellulose membranes pre-wet in a high ionic strength buffer, a strategy adjusted from Tieman and Handa (1989). This way, not only the soluble PME but also PME that is (electrostatically) bound to the cell wall was assumed to be transferred from the cut surface of the plant tissue onto the absorptive membrane, where it then was detected using bPMEI on the one hand and MA-TOM2-38A11 on the other hand. Tissue prints of raw carrot root, broccoli stem and tomato fruit, probed with bPMEI, MA-TOM2-38A11 (not for broccoli) and without primary probe, are shown in **Figure 5.5**.

On prints of carrot root, bPMEI stained both the cortex and the core, whereas recognition of PME by MA-TOM2-38A11 in the central cylinder was only limited. The latter observation is in accordance with the results of Vandevenne *et al.* (2009). The blot of carrot developed without addition of primary probe showed staining concentrated at spots in the cortex and endodermis, most likely originating from endogenous carrot peroxidase activity. The restricted staining of the carrot vascular cylinder by the antibody may hypothetically point to a differential location of various isoforms of PME in carrots (some of which would then not be recognised by the antibody) or to a too low concentration of PME in the vascular tissue of ripe carrot roots to allow for antibody detection. The latter hypothesis seems rather unlikely, given the fact that bPMEI stained the cortex successfully.

The print of the broccoli stem cut surface was labelled throughout by bPMEI. As already suggested by the outcome of the dot-blot binding assays (cf. Section 5.3.3.1), MA-TOM2-38A11 (and other monoclonal antibodies raised against tomato PME by Vandevenne *et al.* (2009)) was not able to recognise PME in prints of broccoli stem tissue (results not shown). The negative control print, developed with omission of the primary probe, did not show any staining.

Both bPMEI and MA-TOM2-38A11 stained the tissue prints of ripe tomato fruit, however with some distinct differences. In agreement with earlier results (Vandevenne *et al.*, 2009), the antibody detected PME in the pericarp and the

septa, whereas only a low signal was seen in the columella and no labelling in the placenta and locular gel. With bPMEI, conversely, strong labelling was registered throughout the fruit, except for the locular cavities. The tomato print only developed with a secondary probe was free of background staining. The bPMEI print is in good accordance with the PME activity print reported by Blumer *et al.* (2000), which shows that all regions of the tomato fruit (in the breaker stage) contain PME activity, including the jelly-like parenchyma, the radial pericarp, endoperiderm and exoperiderm.

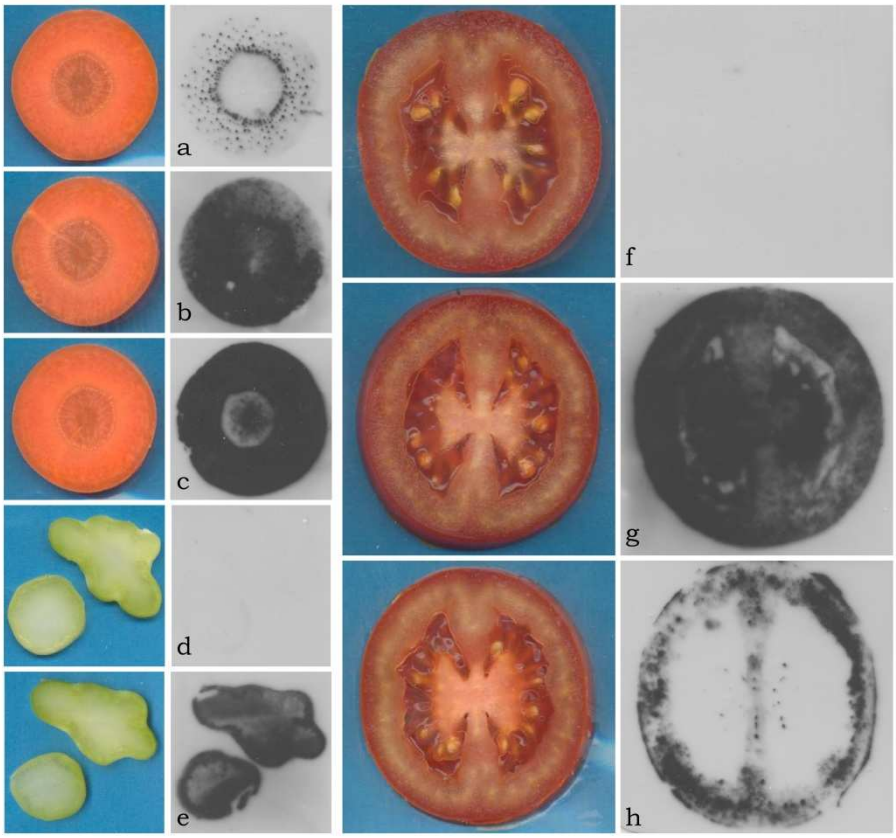

Figure 5.5. Tissue prints of raw carrot root, broccoli stem and tomato fruit, probed with biotinylated PMEI (b, e and g), MA-TOM2-38A11 (c and h) and without primary probe (a, d and f). Image scans of the respective cut surfaces are shown left of each print.

The bPMEI proves to be a versatile probe for PME, staining prints of carrot root, broccoli stem as well as tomato fruit. In its capacity as an anti-PME probe, the inhibitor may, for instance, be employable to visualise spatial or temporal changes in PME activity between different species/varieties or ripening stages of fruits and vegetables, thus far always pursued by means of antibodies (Blumer *et al.*, 2000; Nielsen and Christensen, 2002). The differences observed between bPMEI and MA-TOM2-38A11 as primary probe may indicate that the antibody, as a result of its specificity towards a defined epitope, only recognises a distinct

subset of the plant PMEs, whereas bPMEI reacts with all plant PMEs present. However, on the basis of the current results (and due to the lack of a reliable non-reactive substitute for bPMEI, as there exists for monoclonal antibodies), it cannot be excluded that bPMEI also binds, to a certain (but limited) extent, to plant components that are transferred to the membrane but differ from PME. A charge-mediated unspecific binding of PMEI is rather unlikely given the observation that a washing step with an elevated ionic strength buffer (i.e. 0.5 M NaCl) did not affect the blotting images (data not shown). Hence, in all cases (both antibodies and bPMEI), care should be taken when drawing conclusions based on localisation studies with probes.

5.3.5 Tissue printing for PME localisation after thermal treatment

The tissue-printing technique, outlined in the previous section, was applied to plant material after thermal treatment. **Figure 5.6** represents tissue prints of carrot roots after thermal treatment at 85 °C for various time intervals (0 to 15 min), probed with bPMEI, MA-TOM2-38A11 and without primary probe ("control"). The obtained picture was clearly dissimilar for the different probes.

On prints of untreated raw carrot, bPMEI stained the cortex as well as the core, while MA-TOM2-38A11 reacted strongly with the cortex but only weakly with the central cylinder. The control print merely showed staining concentrated at spots in the cortex and endodermis, probably corresponding to endogenous peroxidase activity.

After a thermal treatment of 15 min at 85 °C, a condition that reduced the PME activity in the carrot root to a level below the detection limit (measured by automatic titration after PME extraction with a high ionic strength buffer), hardly any labelling by bPMEI was observed. The antibody, however, still labelled the cortex, although somewhat weakened in comparison with the raw carrot. No background staining because of endogenous peroxidase was left.

Printing transverse sections of carrots after intermediate treatment times (i.e., 2 min and 5 min at 85 °C) and probing them with MA-TOM2-38A11 gave the same picture as for the raw carrot, i.e., intense staining of the cortex and faint staining of the core. This observation contrasted sharply with the findings for the bPMEI-probed prints. In the latter case, the dark-coloured area was reduced progressively with treatment time along the radius of the carrot disc. Besides the dark inner part of the carrot print, the outer part showed a light degree of background staining. By assuming the intensely stained shape to be circular and by manually measuring the diameter (with an accuracy of 1 mm), the residual staining area, relative to that of the untreated blank sample, could be estimated. When comparing this residual area with the residual PME activity (measured per gram of fresh weight), a good accordance was observed (**Table 5.1**). Remarkably, the control prints revealed a similar but less pronounced image compared to the bPMEI prints, i.e., a vanishing of the signal in radial direction with treatment time.

To the best of the author's knowledge, the current study is the first one to apply the technique of tissue printing on thermally treated plant tissue. Probing the prints with two kinds of molecular probes for PME recognition, i.e., a monoclonal

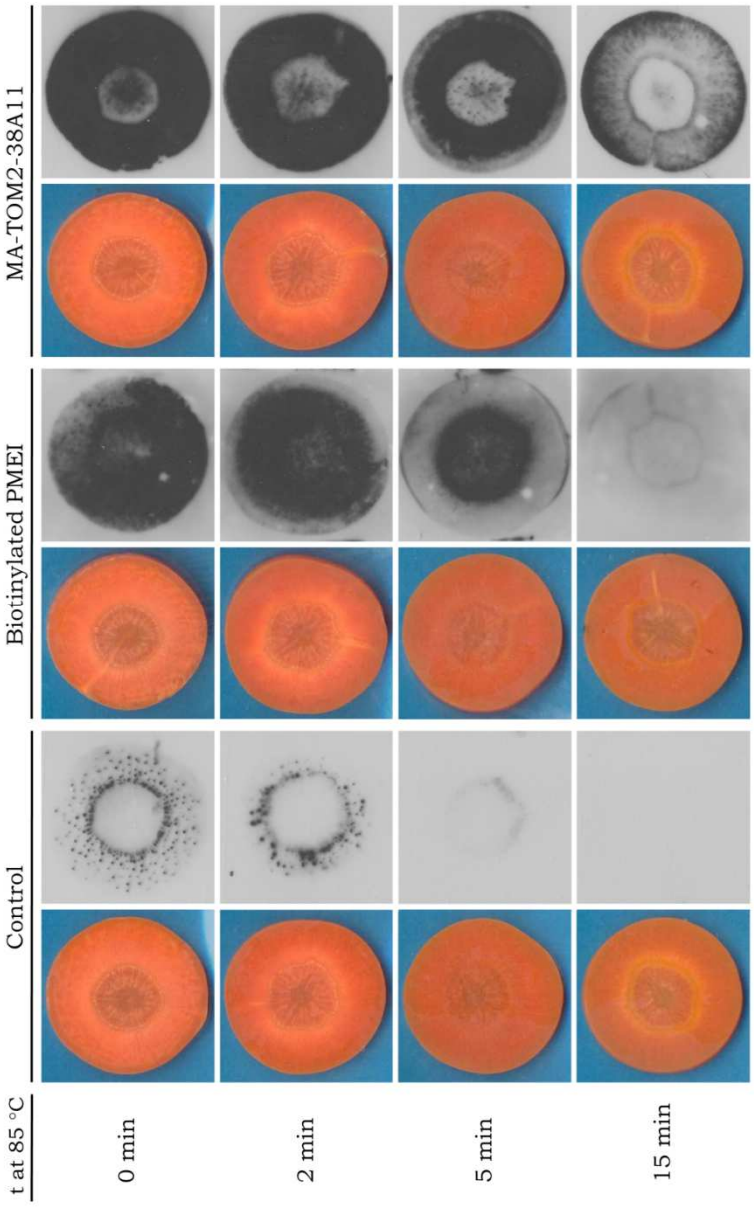

Figure 5.6. Tissue prints of carrot root after various treatment times at 85 °C, probed with biotinylated PMEI, MA-TOM2-38A11 and without primary probe ("control"). Image scans of the respective cut surfaces are shown left of each print.

Table 5.1. The residual PME activity and the residual area stained by bPMEI on tissue prints of carrot root (cf. **Figure 5.6**) after various treatment times at 85 °C, both relative to the value of the untreated blank. The residual staining area is estimated by assuming a circular staining shape and by manually measuring the diameter (with an accuracy of 1 mm).

***t* at 85 °C**	**Residual PME activity (%)**	**Residual staining area (%)**
0 min	100.0	100.0
2 min	81.6 ± 2.3	71.3 ± 1.3
5 min	41.9 ± 1.0	33.9 ± 1.8
15 min	0.0 ± 0.0	0.0 ± 0.0

antibody and a biotinylated enzyme inhibitor, provides valuable insight to both the technique of tissue printing and the qualitative distribution of the PME epitopes of the probes after thermal treatment.

The prints probed with MA-TOM2-38A11 retained most of the staining when increasing the duration of the thermal treatment. Together with the outcome of the dot-blot assays of raw and denatured purified PME (cf. Section 5.3.3.2), this observation proves that the antibody still recognises PME after thermal inactivation of the enzyme. In the mean time, it allows for the conclusion that, after thermal treatment, PME is still transferred from the carrot tissue to the absorptive surface. However, the weakened staining for the most intensively treated carrot sample may indicate a (partly) reduced extractability or recognisability of the PME.

The staining of the prints of thermally treated carrot tissue by bPMEI was obviously treatment time dependent: the longer the treatment, the smaller the labelled area. Knowing that PME is still extracted from the treated carrot tissue during printing and that bPMEI only recognises non-inactivated PME molecules in dot-blot assays, it can be assumed that the stained area corresponds to the locations where active PME is found. This hypothesis is endorsed by the fairly good correspondence between the estimated residual staining area and the residual PME activity. Furthermore, the tissue blots demonstrate that PME inactivation in an external heating medium occurs from the outside to the centre along the radius of the carrot root, caused by the intruding heat. This observation is indirectly confirmed by the control blots, which also show a progressive disappearance of the signal along the radius, attributable to gradual thermal inactivation of endogenous peroxidase. The light background colour in the bPMEI prints of 2 and 5 min, however, suggests that a certain extent of unspecific binding of the bPMEI occurs, although the presence of some residual PME activity at these locations or a certain binding of bPMEI to inactivated PME cannot be excluded.

Anyhow, the whole of the data reveals that bPMEI can be used for a reliable localisation of PME activity, e.g., remaining after treatment. By contrast, the anti-PME monoclonal antibodies studied here are not capable of distinguishing between native and inactivated enzyme molecules. Their applicability in the context of fruit and vegetable processing is therefore particularly interesting for the cases in which the complementarity of both types of probes can be played off.

5.4 CONCLUSION

In the quest of obtaining a molecular probe for *in situ* detection of pectin methylesterase, the PME inhibitor was biotinylated and the biotinylated PMEI (bPMEI) extensively characterised. Reaction conditions for single labelling of the purified PMEI with retention of its inhibitory capacity were identified. HPSEC analysis revealed that the bPMEI retained its ability to form a complex with plant PME and that it gained the capacity to strongly bind an avidin species. By means of dot-blot binding assays, the probe's ability to recognise native and high-temperature- (65 °C) or high-pressure- (800 MPa, 25 °C) denatured plant PMEs, coated on an absorptive surface, was investigated and compared with the binding characteristics of recently reported anti-PME monoclonal antibodies. Contrary to the antibodies, bPMEI only detected active (i.e., non-activated) PME molecules.
Subsequently, both types of probes were used for PME localisation in tissue-printing experiments. bPMEI proved its versatility by staining prints of carrot root, broccoli stem and tomato fruit. Applying the tissue-printing technique on carrot roots after thermal treatment demonstrated the complementarity of bPMEI and anti-PME antibodies, the former selectively detecting remaining active PME and the latter staining both native and inactivated PME molecules.
In conclusion, a PMEI-based molecular probe could be designed that successfully labels plant PMEs in dot-blot binding assays and prints of various plant tissues. No major objections were encountered that compromise the future use of PMEI as a probe in PME detection at microscopic level (in fluorescence or electron microscopy), although attention should be paid concerning a certain degree of unspecific binding of PMEI to plant tissue that may possibly occur. The observation that the PMEI probe can clearly differentiate between active and (irreversibly) inactivated PME molecules is promising in the context of PME activity localisation in plant tissue after different food processing steps, with both traditional (thermal) and nonconventional (e.g., high hydrostatic pressure, microwave and ohmic heating) processing techniques. Hence, well-considered optimisation of these processes in terms of site-specific PME stimulation or inactivation can be pursued.

GENERAL CONCLUSIONS

Based on the strong interaction between plant PME and the proteinaceous PME inhibitor found in kiwi fruit, upon which an inactive complex is formed, the use of PMEI for inhibition of undesired PME activity in specific plant-based food applications has been postulated (e.g., in the quest of obtaining juices with good cloud-stability and pastes with good consistency). Besides, the discovery of this PMEI prompts the idea for the development of a PME detection technique using a labelled PMEI derivative. Within this framework, the current thesis aimed at an improved insight in the PME-PMEI binding event, in order to evaluate the applicability of PMEI in a food technological context and to define application boundaries.

As a starting point, PME was extracted from various plant sources and PMEI from ripe kiwi fruits. Pure enzyme and inhibitor solutions, as established by gel electrophoresis and MALDI-TOF mass spectrometry, were obtained by means of a single-step affinity chromatography method. Most of the subsequent experiments were performed with the main PME isoform of carrot root, considered to be a technologically relevant and representative plant PME.

To monitor the plant PME - kiwi PMEI interaction, three methodologically different approaches were successfully implemented. Besides the more common enzyme activity/inhibition assays (based on pH-stat automatic titration or methanol quantification), complex formation experiments on an analytical size exclusion chromatograph and interaction analyses using a surface plasmon resonance biosensor method were conducted. With regard to the latter method, an immobilisation strategy for the enzyme (via direct amine coupling) as well as for the inhibitor (via capture by streptavidin after PMEI biotinylation) to the surface of a sensor chip was worked out.

By means of the above methods, the effect of intrinsic factors with relevance in food matrices, notably pH and salt concentration, on the PME-PMEI interaction was examined in model systems. The overall picture showed a marked influence of both parameters. The extent of enzyme inhibition and/or the strength of

binding (in terms of K_D) were high in the pH range from 5 to 7 and at low NaCl concentrations (0 - 0.25 M). Increasing pH and [NaCl], by contrast, weakened the interaction, with hardly any binding at pH values ≥ 8 and [NaCl] of around 1.0 M. Consequently, irrespective of the kind of application, pH and salt concentration are determining factors when a strong interaction (and hence inhibition) is strived for.

Additionally, the effect of extrinsic factors, relevant in food processing, on the interaction between plant PME and kiwi PMEI was investigated. Next to temperature, pressure was included as process parameter, because high-pressure processing is emerging in the food industry, mainly owing to an improved balance between food quality and food safety compared to conventional thermal techniques (at least for specific products). The impact of thermal and high-pressure treatments on the individual interaction partners (i.e., PME and PMEI) as well as on the PME-PMEI complex as a whole was studied.
The effect of a high-temperature- (55 - 95 °C) or high-pressure- (500 - 800 MPa at 25 °C) induced denaturation of kiwi PMEI on its interaction with plant PME was analysed by measuring residual inhibitory capacity (towards carrot PME) after treatment and estimating inactivation kinetic parameters. Remarkably, a processing-resistant PMEI fraction retained its activity even after prolonged thermal or pressure processing, contrary to PME under the same conditions. More in particular, the inhibition capacity was only minimally affected by high-pressure processing at low pH values (ca. pH 4). These findings indicate that PMEI, when added to a food system prior to preservation processing, would (at least partly) survive the treatment and remain available for inhibition of residual, unwanted PME activity.
Furthermore, SPR-based interaction analysis and size exclusion chromatography were applied to study the PME-PMEI interaction after (partial) denaturation of carrot PME induced by high temperature (50 - 60 °C) or high pressure (800 MPa, 25 °C). Both strategies revealed that the PME-PMEI binding is highly associated with PME inactivation: the PMEI selectively binds to the active (i.e., non-inactivated) PME subpopulation, whereas it does not engage a complex with the denatured enzyme fraction. From an application point of view, this observation entails that post-processing addition of kiwi PMEI to a food product may allow binding and presumably inhibiting the residual active PME, remaining after (mild) processing.
Finally, the behaviour of the PME-PMEI complex at elevated temperature or pressure levels was examined. Hereto, product formation (i.e., methanol) in a mixture of PME, PMEI and pectin as a function of treatment time was followed on the one hand, and HPSEC analysis of a PME-PMEI mixture after treatment was carried out on the other hand. The results obtained from the methanol determination suggested that the complex is not dissociated by temperature ($T \leq$ 65 °C) and relatively low pressure levels (p < 400 MPa at 25 °C), whereas exposure to higher pressures causes the complex to separate. These initial observations were confirmed by HPSEC analyses: heat treatment (55 - 65 °C) does not dissociate the complex but rather denatures the complex as a single entity; high-pressure treatment (800 MPa, 25 °C) induces disunion of enzyme and inhibitor, followed by gradual inactivation of PME and PMEI and subsequent reunion of the non-inactivated partners upon decompression. As already noticed

above, PMEI showed pH-dependent inactivation characteristics, being strikingly baroresistant at low pH values (ca. pH 4). Anyhow, independent of the pH (in the range studied here, i.e., ca. 4 to 6.5), high-pressure treatment of an equimolar mixture of PME and PMEI gave cause for an excess amount of PMEI. The whole of these data is particularly promising with regard to pre-processing addition of kiwi PMEI to food systems in combination with high-pressure processing, especially in (high) acid foods (e.g., fruit juices).

The quantitative PME-PMEI interaction study showed that only the combined use of three complementary methods gave rise to a complete and integrated picture on the PME-PMEI binding event as influenced by relevant intrinsic and extrinsic parameters, with a desired extent of mechanistic insight (e.g., with regard to the denaturation of PME and the PME-PMEI complex). Some gaps left by one of the techniques, e.g., as a result of experimental limitations, could be filled by the others. The fact that the conclusions from the different approaches are in good agreement, rather than contradictory, indicates a strong interrelation between interaction/complexation on the one hand, and enzyme inhibition on the other hand, despite the important role of the pectin substrate played in the latter.

As longed-for, the above insights in the PME-PMEI interaction allowed for a theoretical evaluation of the potential of PMEI application for PME inhibition in a food-technological context. Nevertheless, future validation experiments are required to confirm whether these *in vitro* findings are transferable to real food matrices. *In concreto*, one of the most relevant application-oriented studies to be undertaken is a cloud-stability/consistency shelf-life study on juices or purées with PMEI as technological adjuvant, on lab- and (semi-)industrial scale. Various plant raw materials with different intrinsic characteristics, e.g. in terms of pH (high-acid fruits *vs.* low-acid vegetables), and various preservation unit operations, e.g., thermal, high-pressure and combined thermal/high-pressure processing, could be evaluated. Addition of PMEI at different stages of the production process, i.e., prior to or after the preservation step, and in either a purified form (extracted or recombinantly produced) or in the form of natural kiwi fruit juice could be assessed, also taking into account economic, cost-efficient aspects.

In a final part of this work, focus was put on a second hypothetical application of PMEI, notably the *in situ* detection and localisation of plant PME in model or food systems. Hereto, a molecular probe was constructed through biotinylation of the PMEI, retaining the ability for complex formation with PME and gaining the capacity for strongly binding an avidin species. The PMEI-based probe was successfully tested in dot-blot assays and tissue prints of various plant organs (i.e., carrot root, broccoli stem and tomato fruit). In agreement with the earlier results, recognition by the probe was restricted to the non-inactivated PME.

In the current study, no major objections were encountered that compromise the future use of PMEI as a molecular probe for *in situ* PME visualisation at the microscopic level (in fluorescence or electron microscopy), the obvious follow-up step to be taken. After implementation of the microscopic technique, insight in the (spatially) heterogeneous distribution of PME, naturally present in the starting plant material but also induced by different food processing steps, can

be strived for, both in tissue systems and in plant-based food suspensions. In this context, the observation that the PMEI probe can clearly differentiate between native and inactivated PME molecules shows great promise to assess the way the locations of residual PME activity are changed by processing, e.g., through enzyme inactivation or tissue damage. Traditional thermal and nonconventional processing techniques (e.g., high hydrostatic pressure, microwave heating, ohmic heating), the former being conductive heating and the latter often showing volumetric impact, may result in differences which are detectable with the newly developed method but untraceable with the 'classical' methods, measuring the volume-averaged PME activity at product level. Consequently, well-considered optimisation of these processes in terms of site-specific PME stimulation or inactivation can be pursued (i.e., precision processing), executing (or eventually combining) these processes in such a way that PME at specific, desired locations is actually reached.

In addition, the prospective use of the PMEI probe in the co-localisation of PME and well-defined pectin structures (e.g., in terms of degree of methyl-esterification, or calcium cross-linking) by means of specific anti-pectin antibodies can provide information on how PME alters the fine structure of its substrate *in situ*, eliminating the need for extraction and the risk for concomitant artefacts (e.g., structure modifications, interaction changes etc.). Ultimately, enzyme-catalysed pectin modifications may be related to allied food functional properties (such as firmness and viscosity), identifying targets for food texture engineering.

LIST OF REFERENCES

Ackerley, J., Corredig, M., Wicker, L. (2002). Clarification of citrus juice is influenced by specific activity of thermolabile pectinmethylesterase and inactive PME-pectin complexes. *Journal of Food Science,* 67(7), 2529-2533.

Aertsen, A., Meersman, F., Hendrickx, M.E.G., Vogel, R.F., Michiels, C.W. (2009). Biotechnology under high pressure: applications and implications. *Trends in Biotechnology,* 27(7), 434-441.

Ahern, T.J., Klibanov, A.M. (1985). The mechanism of irreversible enzyme inactivation at 100 °C. *Science,* 228(4705), 1280-1284.

Albersheim, P., Darvill, A.G., O'Neill, M.A., Schols, H., Voragen, A.G.J. (1996). An hypothesis: The same six polysaccharides are components of the primary cell wall of all higher plants. In Visser, J., Voragen, A.G.J., *Pectins and Pectinases* (pp. 47-53). Amsterdam: Elsevier.

Albersheim, P., Neukom, H., Deuel, H. (1960). Splitting of pectin chain molecules in neutral solutions. *Archives of Biochemistry and Biophysics,* 90(1), 46-51.

Alkorta, I., Garbisu, C., Llama, M.J., Serra, J.L. (1998). Industrial applications of pectic enzymes: a review. *Process Biochemistry,* 33(1), 21-28.

Alonso, J., Canet, W., Howell, N., Alique, R. (2003). Purification and characterisation of carrot (Daucus carota L) pectinesterase. *Journal of the Science of Food and Agriculture,* 83(15), 1600-1606.

An, S.H., Sohn, K.H., Choi, H.W., Hwang, I.S., Lee, S.C., Hwang, B.K. (2008). Pepper pectin methylesterase inhibitor protein CaPMEI1 is required for antifungal activity, basal disease resistance and abiotic stress tolerance. *Planta,* 228(1), 61-78.

Baker, R.A., Bruemmer, J.H. (1972). Pectinase stabilization of orange juice cloud. *Journal of Agricultural and Food Chemistry,* 20(6), 1169-1173.

Baker, R.A., Cameron, R.G. (1999). Clouds of citrus juices and juice drinks. *Food Technology,* 53(1), 64-69.

Balestrieri, C., Castaldo, D., Giovane, A., Quagliuolo, L., Servillo, L. (1990). A glycoprotein inhibitor of pectin methylesterase in kiwi fruit (*Actinidia chinensis*). *European Journal of Biochemistry,* 193(1), 183-187.

Balestrieri, C., Servillo, L., Quagliuolo, L., Giovane, A., Castaldo, D. (1991). Proteic inhibitor of pectinesterase and use thereof in the preparation of fruit and vegetable juices. *United States Patent,* 5,053,232, 1-6.

Balny, C. (2004). Pressure effects on weak interactions in biological systems. *Journal of Physics-Condensed Matter,* 16(14), S1245-S1253.

Balny, C., Masson, P. (1993). Effects of high-pressure on proteins. *Food Reviews International,* 9(4), 611-628.

Balny, C., Masson, P., Heremans, K. (2002). High pressure effects on biological macromolecules: from structural changes to alteration of cellular processes. *Biochimica Et Biophysica Acta,* 1595(1-2), 3-10.

Balny, C., Mozhaev, V.V., Lange, R. (1997). Hydrostatic pressure and proteins: Basic concepts and new data. *Comparative Biochemistry and Physiology A-Physiology,* 116(4), 299-304.

Balogh, T., Smout, C., Ly Nguyen, B., Van Loey, A., Hendrickx, M.E. (2004). Thermal and high-pressure inactivation kinetics of carrot pectinmethylesterase: from model system to real foods. *Innovative Food Science and Emerging Technologies,* 5, 429-436.

BeMiller, J.N., Kumari, G.V. (1972). Beta-elimination in uronic acids - Evidence for an elcb mechanism. *Carbohydrate Research,* 25(2), 419-428.

Bellincampi, D., Camardella, L., Delcour, J.A., Desseaux, V., D'Ovidio, R., Durand, A., Elliot, G., Gebruers, K., Giovane, A., Juge, N., Sorensen, J.F., Svensson, B., Vairo, D. (2004). Potential physiological role of plant glycosidase inhibitors. *Biochimica Et Biophysica Acta-Proteins and Proteomics,* 1696(2), 265-274.

Benen, J.A.E., van Alebeek, G.J.W.M., Voragen, A.G.J., Visser, J. (2003a). Pectic esterases. In Whitaker, J.R., Voragen, A.G.J., Wong, D.W.S., *Handbook of Food Enzymology* (pp. 849-856). New York: Marcel Dekker Inc.

Benen, J.A.E., Vincken, J.P., van Alebeek, G.J. (2002). Microbial pectinases. In Seymour, G.B., Knox, J.P., *Pectins and their Manipulation* (pp. 174-221). Oxford: Blackwell Publishing, CRC Press.

Benen, J.A.E., Visser, J. (2003a). Pectate and pectin lyases. In Whitaker, J.R., Voragen, A.G.J., Wong, D.W.S., *Handbook of Food Enzymology* (pp. 1029-1041). New York: Marcel Dekker Inc.

Benen, J.A.E., Visser, J. (2003b). Polygalacturonases. In Whitaker, J.R., Voragen, A.G.J., Wong, D.W.S., *Handbook of Food Enzymology* (pp. 857-866). New York: Marcel Dekker Inc.

Benen, J.A.E., Voragen, A.G.J., Visser, J. (2003b). Pectic enzymes. In Whitaker, J.R., Voragen, A.G.J., Wong, D.W.S., *Handbook of Food Enzymology* (pp. 845-848). New York: Marcel Dekker Inc.

Beveridge, T. (2002). Opalescent and cloudy fruit juices: Formation and particle stability. *Critical Reviews in Food Science and Nutrition,* 42(4), 317-337.

Blumer, J.M., Clay, R.P., Bergmann, C.W., Albersheim, P., Darvill, A. (2000). Characterization of changes in pectin methylesterase expression and pectin esterification during tomato fruit ripening. *Canadian Journal of Botany-Revue Canadienne De Botanique,* 78(5), 607-618.

Bonnin, E., Clavurier, K., Daniel, S., Kauppinen, S., Mikkelsen, J.D.M., Thibault, J.F. (2008). Pectin acetylesterases from *Aspergillus* are able to deacetylate homogalacturonan as well as rhamnogalacturonan. *Carbohydrate Polymers,* 74(3), 411-418.

Boonyaratanakornkit, B.B., Park, C.B., Clark, D.S. (2002). Pressure effects on intra- and intermolecular interactions within proteins. *Biochimica Et Biophysica Acta-Protein Structure and Molecular Enzymology,* 1595(1-2), 235-249.

Bordenave, M. (1996). Analysis of pectin methyl esterases. In Linskens, H.F., *Plant cell wall analysis* (pp. 165-180). Berlin: Springer New York.

Bordenave, M., Goldberg, R. (1993). Purification and characterization of pectin methylesterases from mung bean hypocotyl cell-walls. *Phytochemistry,* 33(5), 999-1003.

Bosch, M., Cheung, A.Y., Hepler, P.K. (2005). Pectin methylesterase, a regulator of pollen tube growth. *Plant Physiology,* 138(3), 1334-1346.

Bosch, M., Hepler, P.K. (2005). Pectin methylesterases and pectin dynamics in pollen tubes. *Plant Cell,* 17(12), 3219-3226.

Braccini, I., Perez, S. (2001). Molecular basis of Ca2+-induced gelation in alginates and pectins: The egg-box model revisited. *Biomacromolecules,* 2(4), 1089-1096.

Brett, C.T., Waldron, K.W. (1996). *Physiology and biochemistry of plant cell walls*. London: Chapman & Hall.

Brown, J.A., Fry, S.C. (1993). Novel O-D-galacturonoyl esters in the pectic polysaccharides of suspension-cultured plant-cells. *Plant Physiology,* 103(3), 993-999.

Brownleader, M.D., Jackson, P., Mobasheri, A., Pantelides, A.T., Sumar, S., Trevan, M., Dey, P.M. (1999). Molecular aspects of cell wall modifications during fruit ripening. *Critical Reviews in Food Science and Nutrition,* 39(2), 149-164.

Bruins, M.E., Matser, A.M., Janssen, A.E.A., Boom, R.M. (2007). Buffer selection for HP treatment of biomaterials and its consequences for enzyme inactivation studies. *High Pressure Research,* 27(1), 101-107.

Brummell, D.A. (2006). Cell wall disassembly in ripening fruit. *Functional Plant Biology,* 33(2), 103-119.

Brummell, D.A., Harpster, M.H. (2001). Cell wall metabolism in fruit softening and quality and its manipulation in transgenic plants. *Plant Molecular Biology,* 47(1-2), 311-340.

Caffall, K.H., Mohnen, D. (2009). The structure, function, and biosynthesis of plant cell wall pectic polysaccharides. *Carbohydrate Research,* 344(14), 1879-1900.

Camardella, L., Carratore, V., Ciardiello, M.A., Servillo, L., Balestrieri, C., Giovane, A. (2000). Kiwi protein inhibitor of pectin methylesterase - Amino-acid sequence and structural importance of two disulfide bridges. *European Journal of Biochemistry,* 267(14), 4561-4565.

Camardella, L., Giovane, A., Servillo, L. (2003). Structure-function of a proteinaceous inhibitor of plant pectin methylesterase. In Voragen, A., Schols, H., Visser, R., *Advances in Pectin and Pectinase Research* (pp. 363-372). Dordrecht: Kluwer Academic Publishers.

Cameron, R.G., Baker, R.A., Grohmann, K. (1998). Multiple forms of pectinmethylesterase from citrus peel and their effects on juice cloud stability. *Journal of Food Science,* 63(2), 253-256.

Cantarel, B.L., Coutinho, P.M., Rancurel, C., Bernard, T., Lombard, V., Henrissat, B. (2009). The Carbohydrate-Active EnZymes database (CAZy): an expert resource for glycogenomics. *Nucleic Acids Research,* 37, D233-D238.

Castaldo, D., Laratta, B., Loiudice, R., Giovane, A., Quagliuolo, L., Servillo, L. (1997). Presence of residual pectin methylesterase activity in thermally stabilized industrial fruit preparations. *Lebensmittel-Wissenschaft Und-Technologie-Food Science and Technology,* 30(5), 479-484.

Castaldo, D., Lovoi, A., Quagliuolo, L., Servillo, L., Balestrieri, C., Giovane, A. (1991). Orange juices and concentrates stabilization by a proteic inhibitor of pectin methylesterase. *Journal of Food Science,* 56(6), 1632-1634.

Castaldo, D., Servillo, L., Loiudice, R., Balestrieri, C., Laratta, B., Quagliuolo, L., Giovane, A. (1996). The detection of residual pectin methylesterase activity in pasteurized tomato juices. *International Journal of Food Science and Technology,* 31(4), 313-318.

Catoire, L., Pierron, M., Morvan, C., du Penhoat, C.H., Goldberg, R. (1998). Investigation of the action patterns of pectinmethylesterase isoforms through kinetic analyses and NMR spectroscopy - Implications in cell wall expansion. *Journal of Biological Chemistry,* 273(50), 33150-33156.

Cheftel, J.-C. (1992). Effects of high hydrostatic pressure on food constituents: an overview. In Balny, C., Hayashi, R., Heremans, K., Masson, P., *High Pressure and Biotechnology* (pp. 195-209). London: John Libbey and Company Ltd.

Christensen, T.M.I.E., Nielsen, J.E., Kreiberg, J.D., Rasmussen, P., Mikkelsen, J.D. (1998). Pectin methyl esterase from orange fruit: characterization and localization by in-situ hybridization and immunohistochemistry. *Planta,* 206(4), 493-503.

Christgau, S., Kofod, L.V., Halkier, T., Andersen, L.N., Hockauf, M., Dorreich, K., Dalboge, H., Kauppinen, S. (1996). Pectin methyl esterase from Aspergillus aculeatus: Expression cloning in yeast and characterization of the recombinant enzyme. *Biochemical Journal,* 319, 705-712.

Ciardiello, M.A., D'Avino, R., Amoresano, A., Tuppo, L., Carpentieri, A., Carratore, V., Tamburrini, M., Giovane, A., Pucci, P., Camardella, L. (2008). The peculiar structural features of kiwi fruit pectin methylesterase: Amino acid sequence, oligosaccharides structure, and modeling of the interaction with its natural proteinaceous inhibitor. *Proteins,* 71(1), 195-206.

Ciardiello, M.A., Tamburrini, M., Tuppo, L., Carratore, V., Giovane, A., Mattei, B., Camardella, L. (2004). Pectin methylesterase from kiwi and kaki fruits: Purification, characterization, and role of pH in the enzyme regulation and interaction with the kiwi proteinaceous inhibitor. *Journal of Agricultural and Food Chemistry,* 52(25), 7700-7703.

Clausen, M.H., Willats, W.G.T., Knox, J.P. (2003). Synthetic methyl hexagalacturonate hapten inhibitors of antihomogalacturonan monoclonal antibodies LM7, JIM5 and JIM7. *Carbohydrate Research,* 338(17), 1797-1800.

Coenen, G.J., Bakx, E.J., Verhoef, R.P., Schols, H.A., Voragen, A.G.J. (2007). Identification of the connecting linkage between homo- or xylogalacturonan and rhamnogalacturonan type I. *Carbohydrate Polymers,* 70(2), 224-235.

Considine, K.M., Kelly, A.L., Fitzgerald, G.F., Hill, C., Sleator, R.D. (2008). High-pressure processing - effects on microbial food safety and food quality. *Fems Microbiology Letters,* 281(1), 1-9.

Corredig, M., Wicker, L. (2002). Juice clarification by thermostable fractions of marsh grapefruit pectinmethylesterase. *Journal of Food Science,* 67(5), 1668-1671.

Crelier, S., Robert, M.C., Claude, J., Juillerat, M.A. (2001). Tomato (*Lycopersicon esculentum*) pectin methylesterase and polygalacturonase behaviors regarding heat- and pressure-induced inactivation. *Journal of Agricultural and Food Chemistry,* 49(11), 5566-5575.

Croak, S., Corredig, M. (2006). The role of pectin in orange juice stabilization: Effect of pectin methylesterase and pectinase activity on the size of cloud particles. *Food Hydrocolloids,* 20(7), 961-965.

D'Avino, R., Camardella, L., Christensen, T.M.I.E., Giovane, A., Servillo, L. (2003). Tomato pectin methylesterase: Modeling, fluorescence, and inhibitor interaction studies - Comparison with the bacterial (*Erwinia chrysanthemi*) enzyme. *Proteins,* 53(4), 830-839.

Daniel, R.M., Danson, M.J., Eisenthal, R. (2001). The temperature optima of enzymes: a new perspective on an old phenomenon. *Trends in Biochemical Sciences,* 26(4), 223-225.

De Cremer, G., Roeffaers, M.B.J., Baruah, M., Sliwa, M., Sels, B.F., Hofkens, J., De Vos, D.E. (2007). Dynamic disorder and stepwise deactivation in a chymotrypsin catalyzed hydrolysis reaction. *Journal of the American Chemical Society,* 129(50), 15458-15459.

De Roeck, A., Duvetter, T., Fraeye, I., Van der Plancken, I., Sila, D.N., Van Loey, A., Hendrickx, M. (2009). Effect of high-pressure/high-temperature processing on chemical pectin conversions in relation to fruit and vegetable texture. *Food Chemistry,* 115(1), 207-213.

Dedeurwaerder, S., Menu-Bouaouiche, L., Mareck, A., Lerouge, P., Guerineau, F. (2009). Activity of an atypical *Arabidopsis thaliana* pectin methylesterase. *Planta,* 229(2), 311-321.

Denès, J.M., Baron, A., Drilleau, J.F. (2000a). Purification, properties and heat inactivation of pectin methylesterase from apple (cv Golden Delicious). *Journal of the Science of Food and Agriculture,* 80(10), 1503-1509.

Denès, J.M., Baron, A., Renard, C.M.G.C., Pean, C., Drilleau, J.F. (2000b). Different action patterns for apple pectin methylesterase at pH 7.0 and 4.5. *Carbohydrate Research,* 327(4), 385-393.

Di Matteo, A., Giovane, A., Raiola, A., Camardella, L., Bonivento, D., De Lorenzo, G., Cervone, F., Bellincampi, D., Tsernoglou, D. (2005). Structural basis for the interaction between pectin methylesterase and a specific inhibitor protein. *Plant Cell,* 17(3), 849-858.

Ding, J.L.C., Hsu, J.S.F., Wang, M.M.C., Tzen, J.T.C. (2002). Purification and glycosylation analysis of an acidic pectin methylesterase in jelly fig (*Ficus awkeotsang*) achenes. *Journal of Agricultural and Food Chemistry,* 50(10), 2920-2925.

Dirix, C., Duvetter, T., Van Loey, A., Hendrickx, M., Heremans, K. (2005). The in situ observation of the temperature and pressure stability of recombinant *Aspergillus aculeatus* pectin methylesterase with Fourier transform IR spectroscopy reveals an unusual pressure stability of beta-helices. *Biochemical Journal,* 392, 565-571.

Dorokhov, Y.L., Makinen, K., Frolova, O.Y., Merits, A., Saarinen, J., Kalkkinen, N., Atabekov, J.G., Saarma, M. (1999). A novel function for a ubiquitous plant enzyme pectin methylesterase: the host-cell receptor for the tobacco mosaic virus movement protein. *Febs Letters,* 461(3), 223-228.

Dorokhov, Y.L., Skurat, E.V., Frolova, O.Y., Gasanova, T.V., Ivanov, P.A., Ravin, N.V., Skryabin, K.G., Makinen, K.M., Klimyuk, V.I., Gleba, Y.Y., Atabekov, J.G. (2006). Role of the leader sequence in tobacco pectin methylesterase secretion. *Febs Letters,* 580(13), 3329-3334.

Duvetter, T., Fraeye, I., Sila, D.N., Verlent, I., Smout, C., Clynen, E., Schoofs, L., Schols, H., Hendrickx, M., Van Loey, A. (2006a). Effect of temperature and high pressure on the activity and mode of action of fungal pectin methyl esterase. *Biotechnology Progress,* 22(5), 1313-1320.

Duvetter, T., Fraeye, I., Sila, D.N., Verlent, I., Smout, C., Hendrickx, M., Van Loey, A. (2006b). Mode of de-esterification of alkaline and acidic pectin methyl esterases at different pH conditions. *Journal of Agricultural and Food Chemistry,* 54(20), 7825-7831.

Duvetter, T., Fraeye, I., Van Hoang, T., Van Buggenhout, S., Verlent, I., Smout, C., Van Loey, A., Hendrickx, M. (2005a). Effect of pectinmethylesterase infusion methods and processing techniques on strawberry firmness. *Journal of Food Science,* 70(6), S383-S388.

Duvetter, T., Sila, D.N., Van Buggenhout, S., Jolie, R., Van Loey, A., Hendrickx, M. (2009). Pectins in processed fruit and vegetables: Part I - Stability and catalytic activity of pectinases. *Comprehensive Reviews in Food Science and Food Safety,* 8(2), 75-85.

Duvetter, T., Van Loey, A., Smout, C., Verlent, I., Ly-Nguyen, B., Hendrickx, M. (2005b). *Aspergillus aculeatus* pectin methylesterase: study of the inactivation by temperature and pressure and the inhibition by pectin methylesterase inhibitor. *Enzyme and Microbial Technology,* 36(4), 385-390.

Eagerman, B.A., Rouse, A.H. (1976). Heat inactivation temperature-time relationships for pectinesterase inactivation in citrus juices. *Journal of Food Science,* 41(6), 1396-1397.

Endress, H.-U., Mattes, F., Norz, K. (2006). Pectins. In Hui, Y.H., *Handbook of Food Science, Technology and Engineering* (pp. 140-1-140-35). Boca Raton: CRC Taylor&Francis.

Fachin, D., Van Loey, A.M., Nguyen, B.L., Verlent, I., Indrawati, Hendrickx, M.E. (2002). Comparative study of the inactivation kinetics of pectinmethylesterase in tomato juice and purified form. *Biotechnology Progress,* 18(4), 739-744.

Federici, L., Caprari, C., Mattei, B., Savino, C., Di Matteo, A., De Lorenzo, G., Cervone, F., Tsernoglou, D. (2001). Structural requirements of endopolygalacturonase for the interaction with PGIP (polygalacturonase-inhibiting protein). *Proceedings of the National Academy of Sciences of the United States of America,* 98(23), 13425-13430.

Fry, S.C. (2004). Primary cell wall metabolism: tracking the careers of wall polymers in living plant cells. *New Phytologist,* 161(3), 641-675.

Gaffe, J., Tieman, D.M., Handa, A.K. (1994). Pectin methylesterase isoforms in tomato (*Lycopersicon esculentum*) tissues - Effects of expression of a pectin methylesterase antisense gene. *Plant Physiology,* 105(1), 199-203.

Gils, A., Ceresa, E., Macovei, A.M., Marx, P.F., Peeters, M., Compernolle, G., Declerck, P.J. (2005). Modulation of TAFI function through different pathways - implications for the development of TAFI inhibitors. *Journal of Thrombosis and Haemostasis,* 3(12), 2745-2753.

Giovane, A., Balestrieri, C., Quagliuolo, L., Castaldo, D., Servillo, L. (1995). A glycoprotein inhibitor of pectin methylesterase in kiwi fruit - Purification by affinity chromatography and evidence of a ripening-related precursor. *European Journal of Biochemistry,* 233(3), 926-929.

Giovane, A., Laratta, B., Loiudice, R., Quagliuolo, L., Castaldo, D., Servillo, L. (1996). Determination of residual pectin methylesterase activity in food products. *Biotechnology and Applied Biochemistry,* 23, 181-184.

Giovane, A., Quagliuolo, L., Servillo, L., Balestrieri, C., Laratta, B., Loiudice, R., Castaldo, D. (1994). Purification and characterization of 3 isozymes of pectin methylesterase from tomato fruit. *Journal of Food Biochemistry,* 17(5), 339-349.

Giovane, A., Servillo, L., Balestrieri, C., Raiola, A., D'Avino, R., Tamburrini, M., Ciardiello, M.A., Camardella, L. (2004). Pectin methylesterase inhibitor. *Biochimica Et Biophysica Acta-Proteins and Proteomics,* 1696(2), 245-252.

Goldberg, R., Pierron, M., Bordenave, M., Breton, C., Morvan, C., du Penhoat, C.H. (2001). Control of mung bean pectinmethylesterase isoform activities - Influence of pH and carboxyl group distribution along the pectic chains. *Journal of Biological Chemistry,* 276(12), 8841-8847.

Greve, L.C., Shackel, K.A., Ahmadi, H., McArdle, R.N., Gohlke, J.R., Labavitch, J.M. (1994). Impact of heating on carrot firmness - Contribution of cellular turgor. *Journal of Agricultural and Food Chemistry,* 42(12), 2896-2899.

Gross, M., Jaenicke, R. (1994). Proteins under pressure - The influence of high hydrostatic pressure on structure, function and assembly of proteins and protein complexes. *European Journal of Biochemistry,* 221(2), 617-630.

Hawley, S.A. (1971). Reversible pressure-temperature denaturation of chymotrypsinogen. *Biochemistry,* 10(13), 2436-2442.

Hendrickx, M., Ludikhuyze, L., Van den Broeck, I., Weemaes, C. (1998). Effects of high pressure on enzymes related to food quality. *Trends in Food Science & Technology,* 9(5), 197-203.

Heremans, K. (1982). High-pressure effects on proteins and other biomolecules. *Annual Review of Biophysics and Bioengineering,* 11, 1-21.

Heremans, K. (1993). The behaviour of proteins under pressure. In Winter, R., Jonas, J., *High Pressure Chemistry, Biochemistry and Materials Science* (pp. 443-469). Dordrecht: Kluwer Academic Publishers.

Heukeshoven, J., Dernick, R. (1985). Simplified method for silver staining of proteins in polyacrylamide gels and the mechanism of silver staining. *Electrophoresis,* 6(3), 103-112.

Hoover, D.G., Metrick, C., Papineau, A.M., Farkas, D.F., Knorr, D. (1989). Biological effects of high hydrostatic pressure on food microorganisms. *Food Technology,* 43(3), 99-107.

Hothorn, M., Wolf, S., Aloy, P., Greiner, S., Scheffzek, K. (2004). Structural insights into the target specificity of plant invertase and pectin methylesterase inhibitory proteins. *Plant Cell,* 16(12), 3437-3447.

Huber, W., Mueller, F. (2006). Biomolecular interaction analysis in drug discovery using surface plasmon resonance technology. *Current Pharmaceutical Design,* 12(31), 3999-4021.

Irifune, K., Nishida, T., Egawa, H., Nagatani, A. (2004). Pectin methylesterase inhibitor cDNA from kiwi fruit. *Plant Cell Reports,* 23(5), 333-338.

Ishii, T., Matsunaga, T. (2001). Pectic polysaccharide rhamnogalacturonan II is covalently linked to homogalacturonan. *Phytochemistry,* 57(6), 969-974.

Jaenicke, R. (1991). Protein stability and molecular adaptation to extreme conditions. *European Journal of Biochemistry,* 202(3), 715-728.

Jarvis, M.C., Briggs, S.P.H., Knox, J.P. (2003). Intercellular adhesion and cell separation in plants. *Plant Cell and Environment,* 26(7), 977-989.

Jauneau, A., Roy, S., Reis, D., Vian, B. (1998). Probes and microscopical methods for the localization of pectins in plant cells. *International Journal of Plant Sciences,* 159(1), 1-13.

Jayani, R.S., Saxena, S., Gupta, R. (2005). Microbial pectinolytic enzymes: A review. *Process Biochemistry,* 40(9), 2931-2944.

Jenkins, J., Mayans, O., Smith, D., Worboys, K., Pickersgill, R.W. (2001). Three-dimensional structure of *Erwinia chrysanthemi* pectin methylesterase reveals a novel esterase active site. *Journal of Molecular Biology,* 305(4), 951-960.

Jiang, C.M., Li, C.P., Chang, J.C., Chang, H.M. (2002). Characterization of pectinesterase inhibitor in jelly fig (*Ficus awkeotsang* Makino) achenes. *Journal of Agricultural and Food Chemistry,* 50(17), 4890-4894.

Johansson, K., El-Ahmad, M., Friemanna, R., Jornvall, H., Markovic, O., Eklund, H. (2002). Crystal structure of plant pectin methylesterase. *Febs Letters,* 514(2-3), 243-249.

Jones, S., Thornton, J.M. (1996). Principles of protein-protein interactions. *Proceedings of the National Academy of Sciences of the United States of America,* 93(1), 13-20.

Juge, N. (2006). Plant protein inhibitors of cell wall degrading enzymes. *Trends in Plant Science,* 11(7), 359-367.

Kashyap, D.R., Vohra, P.K., Chopra, S., Tewari, R. (2001). Applications of pectinases in the commercial sector: A review. *Bioresource Technology,* 77(3), 215-227.

Keijbets, M.J., Pilnik, W. (1974). Beta-elimination of pectin in presence of anions and cations. *Carbohydrate Research,* 33(2), 359-362.

Kim, Y., Teng, Q., Wicker, L. (2005). Action pattern of Valencia orange PME de-esterification of high methoxyl pectin and characterization of modified pectins. *Carbohydrate Research,* 340(17), 2620-2629.

Kiss, J. (1974). Beta-eliminative degradation of carbohydrates containing uronic acid residues. *Advances in Carbohydrate Chemistry and Biochemistry,* 29, 229-233.

Kitamura, Y., Itoh, T. (1987). Reaction volume of protonic ionization for buffering agents - Prediction of pressure-dependence of pH and pOH. *Journal of Solution Chemistry,* 16(9), 715-725.

Klavons, J.A., Bennett, R.D. (1986). Determination of methanol using alcohol oxidase and its application to methyl-ester content of pectins. *Journal of Agricultural and Food Chemistry,* 34(4), 597-599.

Klavons, J.A., Bennett, R.D., Vannier, S.H. (1994). Physical/chemical nature of pectin associated with commercial orange juice cloud. *Journal of Food Science,* 59(2), 399-401.

Klibanov, A.M. (1983). Stabilization of enzymes against thermal inactivation. *Advances in Applied Microbiology,* 29, 1-28.

Knorr, D., Heinz, V., Buckow, R. (2006). High pressure application for food biopolymers. *Biochimica Et Biophysica Acta-Proteins and Proteomics,* 1764(3), 619-631.

Knox, J.P. (2008). Revealing the structural and functional diversity of plant cell walls. *Current Opinion in Plant Biology,* 11(3), 308-313.

Knox, J.P., Linstead, P.J., King, J., Cooper, C., Roberts, K. (1990). Pectin esterification is spatially regulated both within cell-walls and between developing-tissues of root apices. *Planta,* 181(4), 512-521.

Krall, S.M., McFeeters, R.F. (1998). Pectin hydrolysis: Effect of temperature, degree of methylation, pH, and calcium on hydrolysis rates. *Journal of Agricultural and Food Chemistry,* 46(4), 1311-1315.

Kravtchenko, T.P., Arnould, I., Voragen, A.G.J., Pilnik, W. (1992). Improvement of the selective depolymerization of pectic substances by chemical beta-elimination in aqueous solution. *Carbohydrate Polymers,* 19(4), 237-242.

Krop, J.P.P., Pilnik, W. (1974). Effect of pectic acid and bivalent cations on cloud loss of citrus juice. *Lebensmittel-Wissenschaft Und-Technologie-Food Science and Technology,* 7, 62-63.

Laratta, B., Fasanaro, G., Desio, F., Castaldo, D., Palmieri, A., Giovane, A., Servillo, L. (1995). Thermal inactivation of pectin methylesterase in tomato puree - Implications on cloud stability. *Process Biochemistry,* 30(3), 251-259.

Laurent, F., Kotoujansky, A., Labesse, G., Bertheau, Y. (1993). Characterization and overexpression of the Pem gene encoding pectin methylesterase of *Erwinia chrysanthemi* strain-3937. *Gene,* 131(1), 17-25.

Lencki, R.W., Arul, J., Neufeld, R.J. (1992). Effect of subunit dissociation, denaturation, aggregation, coagulation, and decomposition on enzyme inactivation kinetics. 1. 1st-order behavior. *Biotechnology and Bioengineering,* 40(11), 1421-1426.

Lewis, K.C., Selzer, T., Shahar, C., Udi, Y., Tworowski, D., Sagi, I. (2008). Inhibition of pectin methyl esterase activity by green tea catechins. *Phytochemistry,* 69(14), 2586-2592.

Li, Y.Q., Mareck, A., Faleri, C., Moscatelli, A., Liu, Q., Cresti, M. (2002). Detection and localization of pectin methylesterase isoforms in pollen tubes of *Nicotiana tabacum* L. *Planta,* 214(5), 734-740.

Lietzke, S.E., Scavetta, R.D., Yoder, M.D., Jurnak, F. (1996). The refined three-dimensional structure of pectate lyase E from *Erwinia chrysanthemi* at 2.2 angstrom resolution. *Plant Physiology,* 111(1), 73-92.

Lievens, S., Goormachtig, S., Herman, S., Holsters, M. (2002). Patterns of pectin methylesterase transcripts in developing stem nodules of *Sesbania rostrata*. *Molecular Plant-Microbe Interactions,* 15(2), 164-168.

Limberg, G., Korner, R., Buchholt, H.C., Christensen, T.M.I.E., Roepstorff, P., Mikkelsen, J.D. (2000). Analysis of pectin structure part 1 - Analysis of different de-esterification mechanisms for pectin by enzymatic fingerprinting using endopectin lyase and endopolygalacturonase II from *A. niger*. *Carbohydrate Research,* 327(3), 293-307.

Liners, F., Letesson, J.J., Didembourg, C., Vancutsem, P. (1989). Monoclonal-antibodies against pectin - Recognition of a conformation induced by calcium. *Plant Physiology,* 91(4), 1419-1424.

Lionetti, V., Francocci, F., Ferrari, S., Volpi, C., Bellincampi, D., Galletti, R., D'Ovidio, R., De Lorenzo, G., Cervone, F. (2010). Engineering the cell wall by reducing de-methyl-esterified homogalacturonan improves saccharification of plant tissues for bioconversion. *Proceedings of the National Academy of Sciences of the United States of America,* 107(2), 616-621.

Lionetti, V., Raiola, A., Camardella, L., Giovane, A., Obel, N., Pauly, M., Favaron, F., Cervone, F., Bellincampi, D. (2007). Overexpression of pectin methylesterase inhibitors in *Arabidopsis* restricts fungal infection by *Botrytis cinerea*. *Plant Physiology,* 143(4), 1871-1880.

Lo Conte, L., Chothia, C., Janin, J. (1999). The atomic structure of protein-protein recognition sites. *Journal of Molecular Biology,* 285(5), 2177-2198.

Löfas, S., Johnsson, B. (1990). A novel hydrogel matrix on gold surfaces in Surface Plasmon Resonance sensors for fast and efficient covalent immobilization of ligands. *Journal of the Chemical Society-Chemical Communications,* 21, 1526-1528.

Lopez, P., Sanchez, A.C., Vercet, A., Burgos, J. (1997). Thermal resistance of tomato polygalacturonase and pectinmethylesterase at physiological pH. *Zeitschrift Fur Lebensmittel-Untersuchung Und-Forschung A-Food Research and Technology,* 204(2), 146-150.

Ludikhuyze, L., Van Loey, A., Indrawati, Smout, C., Hendrickx, M. (2003). Effects of combined pressure and temperature on enzymes related to quality of fruits and vegetables: From kinetic information to process engineering aspects. *Critical Reviews in Food Science and Nutrition,* 43(5), 527-586.

Lumry, R., Eyring, H. (1954). Conformation changes of proteins. *Journal of Physical Chemistry,* 58, 110-120.

Ly-Nguyen, B., Van Loey, A.M., Fachin, D., Verlent, I., Indrawati, Hendrickx, M.E. (2002). Partial purification, characterization, and thermal and high-pressure inactivation of pectin methylesterase from carrots (*Daucus carota* L.). *Journal of Agricultural and Food Chemistry,* 50(19), 5437-5444.

Ly-Nguyen, B., Van Loey, A.M., Smout, C., Ozcan, S.E., Fachin, D., Verlent, I., Truong, S.V., Duvetter, T., Hendrickx, M.E. (2003). Mild-heat and high-pressure inactivation of carrot pectin methylesterase: A kinetic study. *Journal of Food Science,* 68(4), 1377-1383.

Ly-Nguyen, B., Van Loey, A.M., Smout, C., Verlent, I., Duvetter, T., Hendrickx, M.E. (2004). Effect of intrinsic and extrinsic factors on the interaction of plant pectin methylesterase and its proteinaceous inhibitor from kiwi fruit. *Journal of Agricultural and Food Chemistry,* 52(26), 8144-8150.

Mahler, H.C., Friess, W., Grauschopf, U., Kiese, S. (2009). Protein aggregation: Pathways, induction factors and analysis. *Journal of Pharmaceutical Sciences,* 98(9), 2909-2934.

Mareck, A., Gaffe, J., Morvan, O., Alexandre, C., Morvan, C. (1995). Characterization of isoforms of pectin methylesterase of *Linum usitatissimum* using polyclonal antibodies. *Plant and Cell Physiology,* 36(3), 409-417.

Marin-Rodriguez, M.C., Orchard, J., Seymour, G.B. (2002). Pectate lyases, cell wall degradation and fruit softening. *Journal of Experimental Botany,* 53(377), 2115-2119.

Markovic, O., Cederlund, E., Griffiths, W.J., Lipka, T., Jornvall, H. (2002). Characterization of carrot pectin methylesterase. *Cellular and Molecular Life Sciences,* 59(3), 513-518.

Markovic, O., Janecek, S. (2004). Pectin methylesterases: Sequence-structural features and phylogenetic relationships. *Carbohydrate Research,* 339(13), 2281-2295.

Markovic, O., Jornvall, H. (1992). Disulfide bridges in tomato pectinesterase - Variations from pectinesterases of other species - Conservation of possible active-site segments. *Protein Science,* 1(10), 1288-1292.

Markovic, O., Jornvall, H. (1986). Pectinesterase - The primary structure of the tomato enzyme. *European Journal of Biochemistry,* 158(3), 455-462.

Markovic, O., Kohn, R. (1984). Mode of pectin deesterification by *Trichoderma reesei* pectinesterase. *Experientia,* 40(8), 842-843.

Marquis, H., Bucheli, P. (1994). Inhibition of tomato pectin methylesterase by partially purified kiwi pectin methylesterase inhibitor protein. *International Journal of Food Science and Technology,* 29(2), 121-128.

Masson, P. (1992). Pressure denaturation of proteins. In Balny, C., Hayashi, R., Heremans, K., Masson, P., *High pressure and biotechnology* (pp. 89-99). London: John Libbey Ltd.

Matser, A.A., Krebbers, B., van den Berg, R.W., Bartels, P.V. (2004). Advantages of high pressure sterilisation on quality of food products. *Trends in Food Science & Technology,* 15(2), 79-85.

Mattei, B., Raiola, A., Caprari, C., Federici, L., Bellincampi, D., De Lorenzo, G., Cervone, F., Giovane, A., Camardella, L. (2002). Studies on plant inhibitors of pectin modifying enzymes: Polygalacturonase-inhibiting protein (PGIP) and pectin methylesterase inhibitor (PMEI). In Teeri, T.T., Svensson, B., Gilbert, H.J., Feizi, T., *Carbohydrate Bioengineering. Interdisciplinary Approaches* (pp. 160-167). Cambridge: The Royal Society of Chemistry.

May, C.D. (1990). Industrial pectins - Sources, production and applications. *Carbohydrate Polymers,* 12(1), 79-99.

McCann, M.C., Roberts, K. (1996). Plant cell wall architecture: The role of pectins. In Visser, J., Voragen, A.G.J., *Pectins and pectinases* (pp. 91-107). Amsterdam: Elsevier.

McMillan, G.P., Perombelon, M.C.M. (1995). Purification and characterization of a high pI pectin methyl esterase isoenzyme and its inhibitor from tubers of *Solanum tuberosum* subsp Tuberosum cv Katahdin. *Physiological and Molecular Plant Pathology,* 46(5), 413-427.

Meersman, F., Nies, E., Heremans, K. (2008). On the thermal expansion of water and the phase behavior of macromolecules in aqueous solution. *Zeitschrift Fur Naturforschung Section B-A Journal of Chemical Sciences,* 63(6), 785-790.

Meersman, F., Smeller, L., Heremans, K. (2006). Protein stability and dynamics in the pressure-temperature plane. *Biochimica Et Biophysica Acta-Proteins and Proteomics,* 1764(3), 346-354.

Mei, X.H., Hao, Y.L., Zhu, H.L., Gao, H.Y., Luo, Y.B. (2007). Cloning of pectin methylesterase inhibitor from kiwi fruit and its high expression in *Pichia pastoris*. *Enzyme and Microbial Technology,* 40(5), 1001-1005.

Micheli, F. (2001). Pectin methylesterases: cell wall enzymes with important roles in plant physiology. *Trends in Plant Science,* 6(9), 414-419.

Micheli, F., Sundberg, B., Goldberg, R., Richard, L. (2000). Radial distribution pattern of pectin methylesterases across the cambial region of hybrid aspen at activity and dormancy. *Plant Physiology,* 124(1), 191-199.

Mohnen, D. (2008). Pectin structure and biosynthesis. *Current Opinion in Plant Biology,* 11(3), 266-277.

Mort, A.J. (2002). Interactions between pectins and other polymers. In Seymour, G.B., Knox, J.P., *Pectins and their Manipulation* (pp. 30-51). Oxford: Blackwell Publishing, CRC Press.

Morvan, O., Quentin, M., Jauneau, A., Mareck, A., Morvan, C. (1998). Immunogold localization of pectin methylesterases in the cortical tissues of flax hypocotyl. *Protoplasma,* 202(3-4), 175-184.

Moustacas, A.M., Nari, J., Borel, M., Noat, G., Ricard, J. (1991). Pectin methylesterase, metal-ions and plant cell wall extension - The role of metal-ions in plant cell wall extension. *Biochemical Journal,* 279, 351-354.

Mozhaev, V.V., Berezin, I.V., Martinek, K. (1988). Structure-stability relationship in proteins - Fundamental tasks and strategy for the development of stabilized enzyme catalysts for biotechnology. *Crc Critical Reviews in Biochemistry,* 23(3), 235-281.

Mozhaev, V.V., Lange, R., Kudryashova, E.V., Balny, C. (1996). Application of high hydrostatic pressure for increasing activity and stability of enzymes. *Biotechnology and Bioengineering,* 52(2), 320-331.

Mozhaev, V.V., Martinek, K. (1982). Inactivation and reactivation of proteins (enzymes). *Molecular Biology,* 16(4), 527-543.

Nari, J., Noat, G., Ricard, J. (1991). Pectin methylesterase, metal-ions and plant cell-wall extension - Hydrolysis of pectin by plant cell-wall pectin methylesterase. *Biochemical Journal,* 279, 343-350.

Neter, J., Kutner, M.H., Nachtsheim, C.J., Wasserman, W. (1996). *Applied Linear Statistical Models*. Boston: WCB/McGraw-Hill.

Neuman, Jr.R.C., Kauzmann, W., Zipp, A. (1973). Pressure dependence of weak acid ionization in aqueous buffers. *Journal of Physical Chemistry,* 77(22), 2687-2691.

Ng, A., Waldron, K.W. (1997). Effect of cooking and pre-cooking on cell-wall chemistry in relation to firmness of carrot tissues. *Journal of the Science of Food and Agriculture,* 73(4), 503-512.

Nielsen, J.E., Christensen, T.M.I.E. (2002). Distribution of pectin methyl esterase and acetylesterase in the genus Citrus visualized by tissue prints and chromatography. *Plant Science,* 162(5), 799-807.

Oey, I., Lille, M., Van Loey, A., Hendrickx, M. (2008a). Effect of high-pressure processing on colour, texture and flavour of fruit- and vegetable-based food products: a review. *Trends in Food Science & Technology,* 19(6), 320-328.

Oey, I., Van der Plancken, I., Van Loey, A., Hendrickx, M. (2008b). Does high pressure processing influence nutritional aspects of plant based food systems? *Trends in Food Science & Technology,* 19(6), 300-308.

Ogawa, H., Fukuhisa, K., Kubo, Y., Fukumoto, H. (1990). Pressure inactivation of yeasts, molds, and pectinesterase in Satsuma mandarin juice - Effects of juice concentration, pH, and organic acids, and comparison with heat sanitation. *Agricultural and Biological Chemistry,* 54(5), 1219-1225.

Ovodov, Y.S. (2009). Current views on pectin substances. *Russian Journal of Bioorganic Chemistry,* 35(3), 269-284.

Pace, C.N. (1990). Conformational stability of globular proteins. *Trends in Biochemical Sciences,* 15(1), 14-17.

Patterson, M.F. (2005). Microbiology of pressure-treated foods. *Journal of Applied Microbiology,* 98(6), 1400-1409.

Peaucelle, A., Louvet, R., Johansen, J.N., Hofte, H., Laufs, P., Pelloux, J., Mouille, G. (2008). *Arabidopsis* phyllotaxis is controlled by the methyl-esterification status of cell wall pectins. *Current Biology,* 18(24), 1943-1948.

Pelloux, J., Rusterucci, C., Mellerowicz, E.J. (2007). New insights into pectin methylesterase structure and function. *Trends in Plant Science,* 12(6), 267-277.

Pickersgill, R., Jenkins, J. (2003). The structures and active sites of pectinases. In Voragen, A., Schols, H., Visser, R., *Advances in Pectin and Pectinase Research* (pp. 267-275). Dordrecht: Kluwer Academic Publishers.

Pickersgill, R., Smith, D., Worboys, K., Jenkins, J. (1998). Crystal structure of polygalacturonase from *Erwinia carotovora* ssp. carotovora. *Journal of Biological Chemistry,* 273(38), 24660-24664.

Pina, C., Pinto, F., Feijo, J.A., Becker, J.D. (2005). Gene family analysis of the *Arabidopsis* pollen transcriptome reveals biological implications for cell growth, division control, and gene expression regulation. *Plant Physiology,* 138(2), 744-756.

Plaza, L., Duvetter, T., Monfort, S., Clynen, E., Schoofs, L., Van Loey, A.M., Hendrickx, M.E. (2007). Purification and thermal and high-pressure inactivation of pectinmethylesterase isoenzymes from tomatoes (*Lycopersicon esculentum*): A novel pressure labile isoenzyme. *Journal of Agricultural and Food Chemistry,* 55(22), 9259-9265.

Plaza, L., Duvetter, T., Van der Plancken, I., Meersman, F., Van Loey, A., Hendrickx, M. (2008). Influence of environmental conditions on thermal stability of recombinant *Aspergillus aculeatus* pectinmethylesterase. *Food Chemistry,* 111(4), 912-920.

Porretta, S. (1996). New findings on tomato products. *Fruit Processing,* 2, 58-65.

Protsenko, M.A., Buza, N.L., Krinitsyna, A.A., Bulantseva, E.A., Korableva, N.P. (2008). Polygalacturonase-inhibiting protein is a structural component of plant cell wall. *Biochemistry-Moscow,* 73(10), 1053-1062.

Quentin, M., Jauneau, A., Morvan, O., Mareck, A., Gaffe, J., Morvan, C. (1997). Immunolocalization of pectin methylesterases in the hypocotyl tissues of flax. *Plant Physiology and Biochemistry,* 35(6), 475-482.

Raiola, A., Camardella, L., Giovane, A., Mattei, B., De Lorenzo, G., Cervone, F., Bellincampi, D. (2004). Two *Arabidopsis thaliana* genes encode functional pectin methylesterase inhibitors. *Febs Letters,* 557(1-3), 199-203.

Ralet, M.C., Andre-Leroux, G., Quemener, B., Thibault, J.F. (2005). Sugar beet (*Beta vulgaris*) pectins are covalently cross-linked through diferulic bridges in the cell wall. *Phytochemistry,* 66(24), 2800-2814.

Ralet, M.C., Dronnet, V., Buchholt, H.C., Thibault, J.F. (2001). Enzymatically and chemically de-esterified lime pectins: characterisation, polyelectrolyte behaviour and calcium binding properties. *Carbohydrate Research,* 336(2), 117-125.

Rausch, T., Greiner, S. (2004). Plant protein inhibitors of invertases. *Biochimica Et Biophysica Acta-Proteins and Proteomics,* 1696(2), 253-261.

Renard, C.M.G.C., Thibault, J.-F. (1996). Pectins in mild alkaline conditions: Beta-elimination and kinetics of demethoxylation. In Visser, J., Voragen, A.G.J., *Pectins and Pectinases* (pp. 603-608). Amsterdam: Elsevier.

Rexova-Benkova, L., Markovic, O. (1976). Pectic enzymes. *Advances in Carbohydrate Chemistry and Biochemistry,* 33, 323-385.

Rich, R.L., Myszka, D.G. (2007). Survey of the year 2006 commercial optical biosensor literature. *Journal of Molecular Recognition,* 20(5), 300-366.

Ridley, B.L., O'Neill, M.A., Mohnen, D.A. (2001). Pectins: structure, biosynthesis, and oligogalacturonide-related signaling. *Phytochemistry,* 57(6), 929-967.

Röckel, N., Wolf, S., Kost, B., Rausch, T., Greiner, S. (2008). Elaborate spatial patterning of cell-wall PME and PMEI at the pollen tube tip involves PMEI endocytosis, and reflects the distribution of esterified and de-esterified pectins. *Plant Journal,* 53(1), 133-143.

Rolin, C. (2002). Commercial pectin preparations. In Seymour, G.B., Knox, J.P., *Pectins and their Manipulation* (pp. 222-241). Oxford: Blackwell Publishing, CRC Press.

Sajjaanantakul, T., Van Buren, J.P., Downing, D.L. (1989). Effect of methyl-ester content on heat degradation of chelator-soluble carrot pectin. *Journal of Food Science,* 54(5), 1272-1277.

San Martin, M.F., Barbosa-Canovas, G.V., Swanson, B.G. (2002). Food processing by high hydrostatic pressure. *Critical Reviews in Food Science and Nutrition,* 42(6), 627-645.

Savary, B.J., Hotchkiss, A.T., Fishman, M.L., Cameron, R.G., Shatters, R.G. (2003). Development of a Valencia orange pectin methylesterase for generating novel pectin products. In Voragen, A.G.J., Schols, H., Visser, R., *Advances in Pectin and Pectinase Research* (pp. 345-361). Dordrecht: Kluwer Academic Publishers.

Schols, H., Voragen, A.G.J. (1996). Complex pectins: Structure elucidation using enzymes. In Visser, J., Voragen, A.G.J., *Pectins and Pectinases* (pp. 3-19). Amsterdam: Elsevier.

Scognamiglio, M.A., Ciardiello, M.A., Tamburrini, M., Carratore, V., Rausch, T., Camardella, L. (2003). The plant invertase inhibitor shares structural properties and disulfide bridges arrangement with the pectin methylesterase inhibitor. *Journal of Protein Chemistry,* 22(4), 363-369.

Sila, D.N., Smout, C., Elliot, F., Van Loey, A., Hendrickx, M. (2006). Non-enzymatic depolymerization of carrot pectin: Toward a better understanding of carrot texture during thermal processing. *Journal of Food Science,* 71(1), E1-E9.

Sila, D.N., Smout, C., Satara, Y., Truong, V., Van Loey, A., Hendrickx, M. (2007a). Combined thermal and high pressure effect on carrot pectinmethylesterase stability and catalytic activity. *Journal of Food Engineering,* 78(3), 755-764.

Sila, D.N., Smout, C., Vu, T.S., Hendrickx, M.E. (2004). Effects of high-pressure pretreatment and calcium soaking on the texture degradation kinetics of carrots during thermal processing. *Journal of Food Science,* 69(5), 205-211.

Sila, D.N., Van Buggenhout, S., Duvetter, T., Fraeye, I., De Roeck, A., Van Loey, A., Hendrickx, M. (2009). Pectins in processed fruit and vegetables: Part II - Structure-function relationships. *Comprehensive Reviews in Food Science and Food Safety,* 8(2), 86-104.

Sila, D.N., Yue, X., Van Buggenhout, S., Smout, C., Van Loey, A., Hendrickx, M. (2007b). The relation between (bio-)chemical, morphological, and mechanical properties of thermally processed carrots as influenced by high-pressure pretreatment condition. *European Food Research and Technology,* 226(1-2), 127-135.

Silva, J.L., Foguel, D., Royer, C.A. (2001). Pressure provides new insights into protein folding, dynamics and structure. *Trends in Biochemical Sciences,* 26(10), 612-618.

Silva, J.L., Weber, G. (1993). Pressure stability of proteins. *Annual Review of Physical Chemistry,* 44, 89-113.

Sims, C.A., Balaban, M.O., Matthews, R.F. (1993). Optimization of carrot juice color and cloud stability. *Journal of Food Science,* 58(5), 1129-1131.

Smeller, L. (2002). Pressure-temperature phase diagrams of biomolecules. *Biochimica Et Biophysica Acta-Protein Structure and Molecular Enzymology,* 1595(1-2), 11-29.

Sorensen, J.F., Kragh, K.M., Sibbesen, O., Delcour, J., Goesaert, H., Svensson, B., Tahir, T.A., Brufau, J., Perez-Vendrell, A.M., Bellincampi, D., D'Ovidio, R., Camardella, L., Giovane, A., Bonnin, E., Juge, N. (2004). Potential role of glycosidase inhibitors in industrial biotechnological applications. *Biochimica Et Biophysica Acta-Proteins and Proteomics,* 1696(2), 275-287.

Stauffer, E. (1989). *Enzyme Assays for Food Scientists.* New York: Van Nostrand Reinhold.

Suzuki, K. (1960). Studies on the kinetics of protein denaturation under high pressure. *The Review of Physical Chemistry of Japan,* 29(2), 91-97.

Szczesniak, A.S. (2002). Texture is a sensory property. *Food Quality and Preference,* 13(4), 215-225.

Szczesniak, A.S. (1971). Consumer awareness of and attitudes to food texture. *Journal of Texture Studies,* 2, 280-295.

Thakur, B.R., Singh, R.K., Handa, A.K. (1997). Chemistry and uses of pectin - A review. *Critical Reviews in Food Science and Nutrition,* 37(1), 47-73.

Thibault, J.-F., Ralet, M.-C. (2003). Physico-chemical properties of pectins in the cell walls and after extraction. In Voragen, F., Schols, H., Visser, R., *Advances in Pectin and Pectinase Research* (pp. 91-105). Dordrecht: Kluwer Academic Publishers.

Thibault, J.-F., Renard, C.M.G.C., Axelos, M.A.V., Roger, P., Crepeau, M.J. (1993). Studies of the length of homogalacturonic regions in pectins by acid hydrolysis. *Carbohydrate Research,* 238, 271-286.

Tieman, D.M., Handa, A.K. (1994). Reduction in pectin methylesterase activity modifies tissue integrity and cation levels in ripening tomato (*Lycopersicon esculentum* Mill) fruits. *Plant Physiology,* 106(2), 429-436.

Tieman, D.M., Handa, A.K. (1989). Immunocytolocalization of polygalacturonase in ripening tomato fruit. *Plant Physiology,* 90(1), 17-20.

Tijskens, L.M.M., Waldron, K.W., Ng, A., Ingham, L., Van Dijk, C. (1997). The kinetics of pectin methyl esterase in potatoes and carrots during blanching. *Journal of Food Engineering,* 34(4), 371-385.

Tsou, C.L. (1986). Location of the active sites of some enzymes in limited and flexible molecular regions. *Trends in Biochemical Sciences,* 11(10), 427-429.

Tucker, G.A., Seymour, G.B. (2002). Modification and degradation of pectins. In Seymour, G.B., Knox, J.P., *Pectins and their manipulation* (pp. 150-168). Oxford: Blackwell Publishing, CRC Press.

Van Buggenhout, S., Sila, D.N., Duvetter, T., Van Loey, A., Hendrickx, M. (2009). Pectins in processed fruits and vegetables: Part III - Texture engineering. *Comprehensive Reviews in Food Science and Food Safety,* 8(2), 105-117.

Van Buren, J.P. (1979). The chemistry of texture in fruits and vegetables. *Journal of Texture Studies,* 10, 1-23.

Van den Broeck, I., Ludikhuyze, L.R., Weemaes, C.A., Van Loey, A.M., Hendrickx, M.E. (1999). Thermal inactivation kinetics of pectinesterase extracted from oranges. *Journal of Food Processing and Preservation,* 23(5), 391-406.

Van Loey, A., Indrawati, Smout, C., Hendrickx, M. (2003). Inactivation of enzymes. From experimental design to kinetic modelling. In Whitaker, J.R., Voragen, A.G.J., Wong, D.W.S., *Handbook of food enzymology* (pp. 49-58). New York: Marcel Dekker Inc.

VandenBosch, K.A., Bradley, D.J., Knox, J.P., Perotto, S., Butcher, G.W., Brewin, N.J. (1989). Common components of the infection thread matrix and the intercellular space identified by immunocytochemical analysis of pea nodules and uninfected roots. *The EMBO Journal,* 8(2), 335-341.

Vandevenne, E., Van Buggenhout, S., Duvetter, T., Brouwers, E., Declerck, P.J., Hendrickx, M.E., Van Loey, A., Gils, A. (2009). Development and evaluation of monoclonal antibodies as probes to assess the differences between two tomato pectin methylesterase isoenzymes. *Journal of Immunological Methods,* 349(1-2), 18-27.

Vardhanabhuti, B., Foegeding, E.A. (2008). Effects of dextran sulfate, NaCl, and initial protein concentration on thermal stability of beta-lactoglobulin and alpha-lactalbumin at neutral pH. *Food Hydrocolloids,* 22(5), 752-762.

Varner, J.E., Ye, Z.H. (1994). Tissue printing. *Faseb Journal,* 8(6), 378-384.

Verhertbruggen, Y., Marcus, S.E., Haeger, A., Ordaz-Ortiz, J.J., Knox, J.P. (2009). An extended set of monoclonal antibodies to pectic homogalacturonan. *Carbohydrate Research,* 344(14), 1858-1862.

Verhoeven, J.W. (1996). Glossary of terms used in photochemistry. *Pure and Applied Chemistry,* 68(12), 2223-2286.

Verlent, I., Van Loey, A., Smout, C., Duvetter, T., Ly-Nguyen, B., Hendrickx, M.E. (2004). Changes in purified tomato pectinmethyl-esterase activity during thermal and high pressure treatment. *Journal of the Science of Food and Agriculture,* 84(14), 1839-1847.

Versteeg, C., Rombouts, F.M., Spaansen, C.H., Pilnik, W. (1980). Thermostability and orange juice cloud destabilizing properties of multiple pectinesterases from orange. *Journal of Food Science,* 45(4), 969-998.

Vicente, A.R., Saladie, M., Rose, J.K.C., Labavitch, J.M. (2007). The linkage between cell wall metabolism and fruit softening: looking to the future. *Journal of the Science of Food and Agriculture,* 87(8), 1435-1448.

Vincken, J.P., Schols, H.A., Oomen, R.J.F.J., Mc Cann, M.C., Ulvskov, P., Voragen, A.G.J., Visser, R.G.F. (2003). If homogalacturonan were a side chain of rhamnogalacturonan I. Implications for cell wall architecture. *Plant Physiology,* 132(4), 1781-1789.

Vitali, J., Schick, B., Kester, H.C.M., Visser, J., Jurnak, F. (1998). The three-dimensional structure of *Aspergillus niger* pectin lyase B at 1.7-angstrom resolution. *Plant Physiology,* 116(1), 69-80.

Vora, H.M., Kyle, W.S.A., Small, D.M. (1999). Activity, localisation and thermal inactivation of deteriorative enzymes in Australian carrot (*Daucus carota* L) varieties. *Journal of the Science of Food and Agriculture,* 79(8), 1129-1135.

Voragen, A.G.J., Coenen, G.J., Verhoef, R.P., Schols, H.A. (2009). Pectin, a versatile polysaccharide present in plant cell walls. *Structural Chemistry,* 20(2), 263-275.

Wakabayashi, K., Hoson, T., Huber, D.J. (2003). Methyl de-esterification as a major factor regulating the extent of pectin depolymerization during fruit ripening: a comparison of the action of avocado (*Persea americana*) and tomato (*Lycopersicon esculentum*) polygalacturonases. *Journal of Plant Physiology,* 160(6), 667-673.

Waldron, K.W., Parker, M.L., Smith, A.C. (2003). Plant cell walls and food quality. *Comprehensive Reviews in Food Science and Food Safety,* 2, 101-119.

Waldron, K.W., Smith, A.C., Parr, A.J., Ng, A., Parker, M.L. (1997). New approaches to understanding and controlling cell separation in relation to fruit and vegetable texture. *Trends in Food Science and Technology,* 8(7), 213-221.

Warren, M.E., Kester, H., Benen, J., Colangelo, J., Visser, J., Bergmann, C., Orlando, R. (2002). Studies on the glycosylation of wild-type and mutant forms of *Aspergillus niger* pectin methylesterase. *Carbohydrate Research,* 337(9), 803-812.

Wen, F.S., Zhu, Y.M., Hawes, M.C. (1999). Effect of pectin methylesterase gene expression on pea root development. *Plant Cell,* 11(6), 1129-1140.

Willats, W.G.T., Knox, P., Mikkelsen, J.D. (2006). Pectin: New insights into an old polymer are starting to gel. *Trends in Food Science & Technology,* 17(3), 97-104.

Willats, W.G.T., McCartney, L., Mackie, W., Knox, J.P. (2001a). Pectin: cell biology and prospects for functional analysis. *Plant Molecular Biology,* 47(1-2), 9-27.

Willats, W.G.T., Orfila, C., Limberg, G., Buchholt, H.C., van Alebeek, G.J.W.M., Voragen, A.G.J., Marcus, S.E., Christensen, T.M.I.E., Mikkelsen, J.D., Murray, B.S., Knox, J.P. (2001b). Modulation of the degree and pattern of methyl-esterification of pectic homogalacturonan in plant cell walls - Implications for pectin methyl esterase action, matrix properties, and cell adhesion. *Journal of Biological Chemistry,* 276(22), 19404-19413.

Willats, W.G.T., Steele-King, C.G., McCartney, L., Orfila, C., Marcus, S.E., Knox, J.P. (2000). Making and using antibody probes to study plant cell walls. *Plant Physiology and Biochemistry,* 38(1-2), 27-36.

Wolf, S., Grsic-Rausch, S., Rausch, T., Greiner, S. (2003). Identification of pollen-expressed pectin methylesterase inhibitors in *Arabidopsis*. *Febs Letters,* 555(3), 551-555.

Wolf, S., Mouille, G., Pelloux, J. (2009). Homogalacturonan methyl-esterification and plant development. *Molecular Plant,* 2(5), 851-860.

Wu, M.C., Tseng, K.C., Huang, T.H., Chang, H.M. (2002). Pectinesterase inhibitor in rubbery banana (*Musa sapientum* L.). *Journal of Food Science,* 67(4), 1337-1340.

Yadav, S., Yadav, P.K., Yadav, D., Yadav, K.D.S. (2009). Pectin lyase: A review. *Process Biochemistry,* 44(1), 1-10.

Yamada, H. (1996). Contribution of pectins on health care. In Visser, J., Voragen, A.G.J., *Pectins and pectinases* (pp. 173-190). Amsterdam: Elsevier.

LIST OF PUBLICATIONS

Publications in international peer-reviewed journals

Rodrigo, D., Jolie, R., Van Loey, A., Hendrickx, M. (2006). Combined thermal and high pressure inactivation kinetics of tomato lipoxygenase. *European Food Research and Technology*, 222, 636–642.

Rodrigo, D., Jolie, R., Van Loey, A., Hendrickx, M. (2007). Thermal and high pressure stability of tomato lipoxygenase and hydroperoxide lyase. *Journal of Food Engineering*, 79(2), 423-429.

Duvetter, T., Sila, D.N., Van Buggenhout, S., Jolie, R., Van Loey, A., Hendrickx, M. (2009). Pectins in processed fruits and vegetables: Part I - Stability and catalytic activity of pectinases. *Comprehensive Reviews in Food Science and Food Safety*, 8, 75-85.

Jolie, R.P., Duvetter, T., Houben, K., Clynen, E., Sila, D.N., Van Loey, A.M., Hendrickx, M.E. (2009). Carrot pectin methylesterase and its inhibitor from kiwi fruit: Study of activity, stability and inhibition. *Innovative Food Science and Emerging Technologies*, 10(4), 601-609.

Jolie, R.P., Duvetter, T., Verlinde, P.H.C.J., Van Buggenhout, S., Van Loey, A.M., Hendrickx, M.E. (2009). Size exclusion chromatography to gain insight in the complex formation of carrot pectin methylesterase and its inhibitor from kiwi fruit as influenced by thermal and high-pressure processing. *Journal of Agricultural and Food Chemistry*, 57(23), 11218-11225.

Jolie, R.P., Duvetter, T., Houben, K., Vandevenne, E., Van Loey, A.M., Declerck, P.J., Hendrickx, M.E., Gils, A. (2010). Plant pectin methylesterase and its inhibitor from kiwi fruit: Interaction analysis by surface plasmon resonance. *Food Chemistry*, 121(1), 207-214.

Jolie, R.P., Duvetter, T., Vandevenne, E., Van Buggenhout, S., Van Loey, A.M., Hendrickx, M.E. (2010). A pectin-methylesterase-inhibitor-based molecular probe for *in situ* detection of plant pectin methylesterase activity. *Journal of Agricultural and Food Chemistry*, 58(9), 5449-5456.

Contributions to international meetings

Rodrigo, D., Jolie, R., Oey, I., Van Loey, A., Hendrickx, M. Combined thermal and high pressure inactivation kinetics of tomato lipoxygenase. *Poster presented at the IFT Annual Meeting, 24-28 July 2006, Orlando, Florida, United States*.

Jolie, R., Duvetter, T., Gils, A., Van Loey, A., Hendrickx, M. Real-time interaction analysis of plant pectin methylesterase and its proteinaceous inhibitor from kiwi fruit by surface plasmon resonance. *Poster presented at the 3rd International Symposium on Pectins and Pectinases, 21-23 April 2008, Wageningen, The Netherlands*.

Jolie, R., Duvetter, T., Van Loey, A., Gils, A., Hendrickx, M. Interaction of carrot pectin methylesterase and its proteinaceous inhibitor from kiwi fruit as influenced by thermal and high hydrostatic pressure processing. *Oral presentation at the IFT Annual Meeting, 6-9 June 2009, Anaheim, California, United States*.